2021

Person Identification Using Gait Biometric with Challenging Clothing and Speed Cofactors

Rokanujjaman, Md.

University of Rajshahi

PERSON IDENTIFICATION USING GAIT BIOMETRIC WITH CHALLENGING CLOTHING AND SPEED COFACTORS

In Partial Fulfillment
of the Requirements for the Degree Doctor of Philosophy

Department of Computer Science and Engineering
University of Rajshahi

February, 2021

DECLARATION

I hereby declare that the thesis is my original work and it has been written by me. I have duly acknowledged all the sources of information which have been used in the thesis.

This thesis has also not been submitted for any degree in any university previously.

Md. Rokanujjaman
Associate Professor & PhD Researcher
Department of Computer Science and Engineering
University of Rajshahi, Bangladesh
February, 2021

CERTIFICATE

It is my pleasure to certify that the thesis entitled "Person Identification using Gait Biometric with Challenging Clothing and Speed Cofactors" has been prepared by Md. Rokanujjaman, Associate Professor, Department of Computer Science & Engineering, University of Rajshahi, Bangladesh under my supervision and guidance. The entire thesis is the achievement of the candidate's own work.

I also certify that I have thoroughly gone through the final draft of the thesis and found it satisfactory for submission to University of Rajshahi, in fulfilment of the requirements for the award of the degree Doctor of Philosophy.

To the best of my knowledge this work or any of its part has not been previously submitted to any other institution for any other degree or diploma.

Md. Rezaul Islam
Supervisor and Professor
Department of Electrical & Electronic Engineering
University of Rajshahi, Bangladesh

The thesis is dedicated

To

My Respected Parents
Md. Abdur Rashid and Rabeya Khatun

ABSTRACT

Biometrics are the entire class of technologies and techniques utilized to identify the individual by using their physiological or behavioral attributes. The way of human walking, the most emergent and unique biometric signature allows automatic gait-based person identification. Gait identification task becomes more difficult due to the change of appearance by different cofactors (e.g., walking speed, shoe, surface, carrying, view, clothing and etc.). The main goal of this thesis is to develop novel methods to address the two most frequently happening covariate factors clothing and carrying condition and walking speed changes for gait recognition. These cofactors may affect some parts of gait while other parts remain unchanged and can be used for recognition. An algorithm is proposed to define which parts are more effective and which parts are less effective for cofactors like walking speed, clothing, carrying objects etc. It is found that, for clothing and carrying conditions the upper part of the body is more affected whereas for walking speed changes the lower body part is more affected.

During the process of finding the effective body parts, the whole body is divided into small segments where each segment is a single row in this work. Based on positive and negative effect of each segment in terms of recognition rate, we define the whole gait into five unequal parts for clothing and carrying conditions. Usually, the dynamic areas (e.g., legs, arms swing) are comparatively less affected than static areas (e.g. head, torso) for different cofactors in appearance-based gait representation. To give more emphasis on dynamic areas and less on static areas, frequency-domain gait entropy termed as EnDFT representation is proposed and used as gait features. Experiments are conducted on two

comprehensive benchmarking databases: The OU-ISIR Gait Database, the Treadmill dataset B with huge clothing variations and CASIA Gait Database, Dataset B with clothing and carrying conditions. The proposed method achieved the recognition rate 72.78% for OU-ISIR and 77.69% for CASIA gait database at rank-1 and presented better results in comparison with other existing gait recognition approaches.

Walking speed changes is one of the most common cofactors that affects the gait signature. The intra-class variations increase due to the changes of walking speed and the training data set fails to model the variations. In this thesis, we propose a general feature-based method to resolve the speed transition problem using the effective body parts and discarding the affected body parts. The main contribution of the proposed system is to define the body parts and create a look up table to select the most effective parts from different speed combinations of the gait and discard the redundant parts to minimize the intra-class variations. Like clothing and carrying conditions, six unequal body parts are considered for walking speed changes. The OUISIR Treadmill Database A and CASIA database C are used to show the effectiveness of the proposed method and achieve state-of- the-art performances for gait recognitions. The maximum average recognition rate at rank-1 is 96% for OUISIR gait database. In case of CASIA database, for gallery normal and slow walking speed to probe normal and slow walking speed, our proposed method ensures 100% recognition rate. On the other hand, for cross speed gait recognition highest 97% correct recognition rate is obtained in case of gallery normal to probe slow walking speed.

Finally, we proposed a general framework-based adaptive parts selection method using Zernike and Legendre moments for clothing and carrying conditions and speed

changes. The proposed method is broadly tested on variety of widely accepted gait databases. The experimental results established the robustness of the proposed methods and achieved comparatively better CCR at rank-1.

ACKNOWLEDGEMENTS

At first, I would like to give my earnest gratitude to Almighty Allah for giving me long-term patience and all the opportunities to accomplish my doctoral thesis.

I would like to extend my sincere thanks to my respected supervisor Professor Md. Rezaul Islam for his encouragement, continuous support and guidance throughout my research work. I consider it an honor to work with him.

I also wish to thank my co-supervisor Dr. M. Altab Hossain for his friendly guidance and direction throughout the research.

I wish to express my gratitude to my departmental Chairman, Professor Dr. Bimal Kumar Pramanik for his spontaneous support in all times.

I also thankful to all my colleagues including Professor Dr. A. K. M. Akhtar Hossain, Professor Dr. Somlal Das, Professor Dr. Ekramul Hamid, Md. Saiful Islam, Subrata Pramanik for their co-operative attitude during my research works.

I would like to give my special thanks to Dr. M. Iqbal Aziz Khan for his all kinds of cooperation. His enthusiastic engagement in my research and his never-ending stream of ideas have been absolutely essential for the results presented here.

I am grateful to all my family members especially to my father, Md. Abdur Rashid, for his well wishes and prayer for all times.

I greatly appreciate and acknowledge for providing me the financial support by the **Bangabandhu Science and Technology Fellowship Trust**, Ministry of Science and Technology, Bangladesh, under Science and Technology fellowship program during the early years of my research.

Last but not least, I owe my deepest gratitude to my beloved wife and my dearest daughter for their unconditional love, continuous supports, understanding and encouragement.

TABLE OF CONTENTS

LIST OF TABLES

LIST OF FIGURES

LIST OF SYMBOLS AND ABBREVIATIONS

GEI	Gait Energy Image
GEnI	Gait Entropy Image
DFT	Discrete Fourier Transform
EnDFT	Entropy-based DFT
PCA	Principal Component Analysis
LDA	Linear Discriminant Analysis
GFI	Gait Flow Image
RSM	Random Subspace Method
RWSM	Random Window Subspace Method
CNN	Convolutional Neural Network
GRF	Ground Reaction Force
DCM	Differential Composition Model
HSC	Higher-order derivative Shape Configuration
CCR	Correct Classification Rate
CMC	Cumulative Match Curve
SSGEI	Single-support GEI
GSV	Gait Silhouette Volume
NAC	Normalized Auto Correlation
SVD	Singular Value Decomposition
δ	Kronecker symbol
$L_{p,q}$	Legendre moments
$Z_{p,q}$	Zernike moments

d	Euclidian distance
N_{gait}	Number of frames in a gait Cycle
ω	Angular Frequency
x^g	Gallery sequence
x^p	Probe sequence
λ	Normalization factor

CHAPTER 1. INTRODUCTION

The ability to identify humans uniquely and to associate personal attributes like name, gender, nationality etc. with an individual has important for the human society [1]. Humans generally use physical characteristics such as face, walking style, body shape and voice along with other contextual information (e.g., clothing, time and location) to recognize each other. The characteristics associated with a person carry their personal identity. The term biometrics comes from the ancient Greek, where bios means “life” and metron is “measure”. Biometrics refers to the entire class of technologies and techniques used to identify humans utilizing their intrinsic physical or behavioral characteristics. A biometric system measures one or more physical or behavioral characteristics (see in Figure 1.1), including face, fingerprint, palm print, voice, iris, ear, retina, gait, signature, body odor, hand vein, or the DNA information of a person to identify or verify him uniquely.

High’st queen of state, Great Juno, comes; I know her by her gait. (The Tempest, Act 4, Scene 1) [2]. Gait is one of several physical and behavioral biometric signatures of a person’s that can be used for identifying him/her. Gait refers to a person’s manner of walking. Researcher's interest in the study of human gait is now active, challenging and spreads in many areas, including biometrics, biomechanics, clinical analysis, surveillance, robotics, gender discrimination, age estimation, computer game and character animation [3-10]. Gait recognition is capable of identifying person at a distance by inspecting their walking style [11, 12].

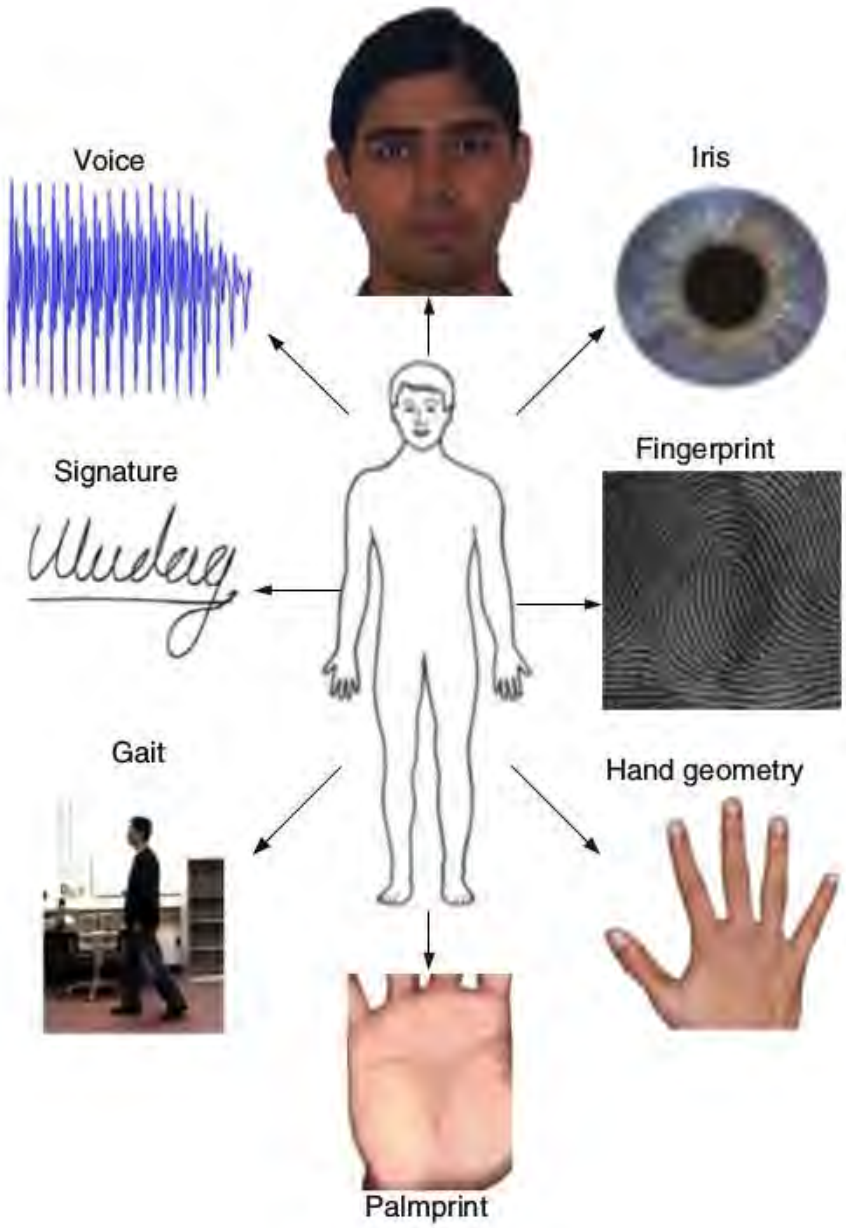

Figure 1.1 Different biometric body traits that have been used for person recognition[1]

Gait recognition is capable of identifying person at a distance by inspecting their walking style [11]. It is an interesting modality which can be performed secretively and it cannot be disguise or conceal. Gait is one of the few biometric features that can be

[1] Image source: Introduction to Biometrics [1]

measured from distance without consent, physical contact from the target, collaboration at low resolution image sequences [13-16, 17, 18]. Most often, criminals wear dark sun-glasses, bulky long coat, face masks and hand gloves to override eyes, body shape, face, and finger print that may be used for recognition. In such context, gait is the effective and useful biometric signature to identify criminals.

Thanks to the above characteristics, scopes of the gait identification are ranging from video-based wide-area surveillance [19, 20, 21] (e.g., finding terrorists or suspects in squares, stations, airports, banks, and car parking area) to criminal investigation (e.g., authenticating a criminal at a crime scene and a suspect in a street). In addition, potential application fields of the video-based gait analysis are ranging from health science (e.g., detecting the postural disorder or fallers to be) to sport science (e.g., providing the optimal technique strategies in sports training).

The human gait-based research has been made huge progress over the recent past few years. But it faces some limitations due to various factors and creates its research more challenging. So, more advanced approaches are thus desired to meet emerging application demands. In the real world, as shown in Figure 1.2, there are various factors significantly affecting human gait including clothing and carrying condition, walking speeds, shoes, elapsed time, walking surfaces, observed views, health states, etc. [3, 15] and make the gait recognition as a challenging problem. It is worth mentioning that other biometric methods also affected by different factors such as face recognition.

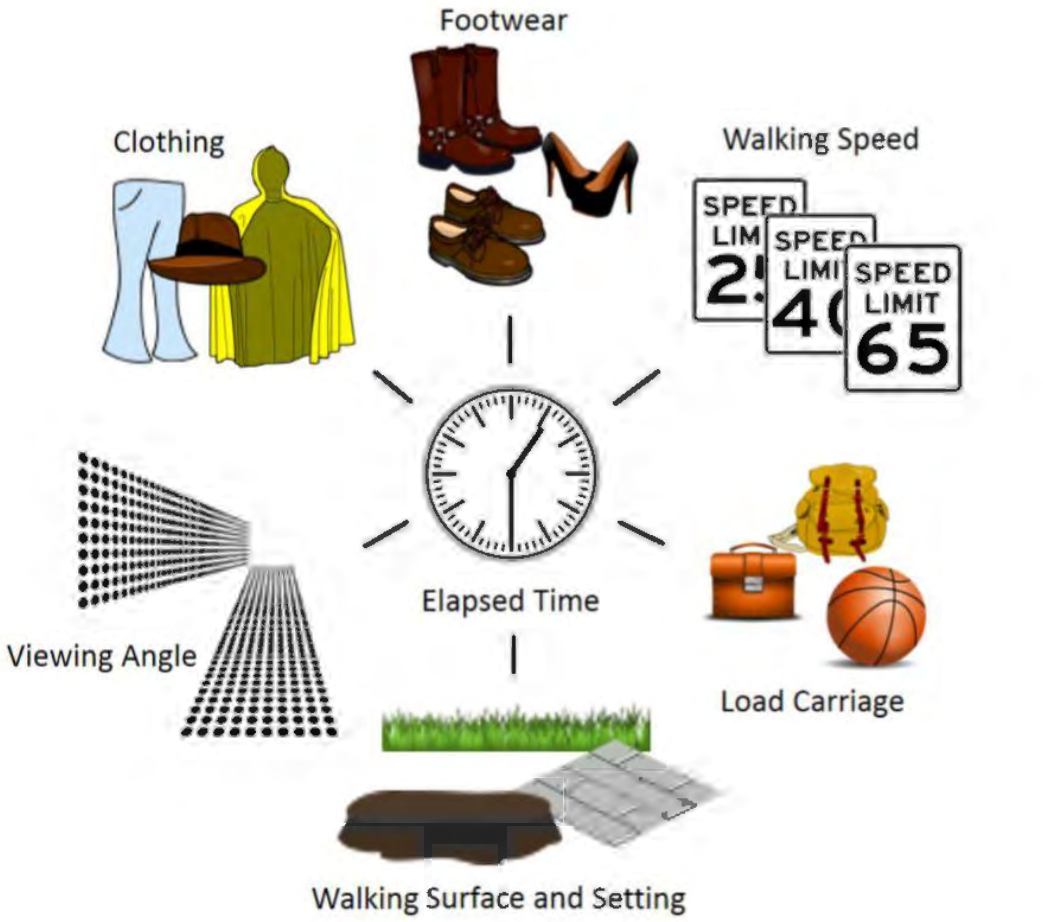

Figure 1.2 Variety of covariates significantly affect human gait[2]

During the past decade many gait recognition techniques have been proposed. However, despite the different approaches, the ability to identify an individual automatically, reliably and accurately does not meet the demands of the real-world applications. The difficulties that face many gait recognition approaches is the intra class variations caused by covariate factors that affect the gait adversely. Among the mentioned factors, clothing and carrying conditions and walking speed changes have been regarded as the most common and challenging problems for gait recognition. In our daily life it is

[2] Image Source: Biometric recognition by gait: A survey of modalities and features [2]

much common are the variations of clothing and carrying conditions. This is due to people usually wears different types of apparel in different season and festival and also carries different kinds of bags (side-bag, backpack, etc.) or other things. They do not only occlude and alter the appearance of the body shape, but also affect the dynamic pattern of body movements. This results a large intra class variation, which greatly affects the performance of gait recognition [22]. Therefore, gait recognition techniques robust against clothing and carrying status are also of great importance. Like clothing and carrying conditions, speed changes is also another most familiar and rigorous factor and frequently happens on different situation (e.g. criminals running quickly from crime place). So, speed changes alter walking patterns and produce significantly changes in appearance-based gait features which results intra class difference and degrades gait recognition performance. Thus, speed invariant gait recognition techniques are important for practical applications. In our study, the most common and frequently happening challenging factors (i) clothing and carrying conditions and (ii) walking speed changes will be addressed.

1.1 Problem Definitions, Challenges, Motivation and Contribution behind the Research

From the above discussion, the main goal of this thesis is to address the most frequently happening covariate factors clothing and carrying condition and walking speed change for gait recognition. This section will define the problems due to the covariate factors and highlight the relevant challenges. Then, our motivations and contribution to approach such problems will be explained.

1.1.1 Gait recognition under clothing and carrying condition

1.1.1.1 Problem definition

Wearing cloths and carrying bags can be found in many different forms or styles. Sample gait images under various clothing and carrying bag from the OU-ISIR treadmill gait database B [23] and CASIA gait database B [24] are shown in Figure 1.3 and Figure 1.4 respectively. As mentioned above, gaits of a person can be recorded by using different clothing or carrying conditions. Consequently, probe gait can possibly be captured under an arbitrary clothing or carry bags which does not match any of the gallery dataset. These covariate conditions obscure the body shape. Consequently, they create a confusion between the motion of the covariate factor and the gesture of the gait. Thus, it is difficult to accurately capture the style and motion of the gait under these conditions.

1.1.1.2 Challenges

Variations in clothing alter an individual's appearance, making the problem of gait identification much more difficult [23]. If the type of clothing differs between the gallery and a probe, certain parts of the gait silhouettes are occluded or distorted and the ability to discriminate subjects decreases with respect to these affected parts [25] and drastically reduce the performance of gait recognition [26].

In many situations, carrying condition is common (e.g., offices, businesses, airports, etc.) which change the gait appearance and the load may also force some body

parts to take a different pose than in natural gait [2]. Therefore, due to carrying conditions recognition rates can drop and must be taken into consideration.

Figure 1.3 Sample images of OUISIR treadmill gait database B[3]

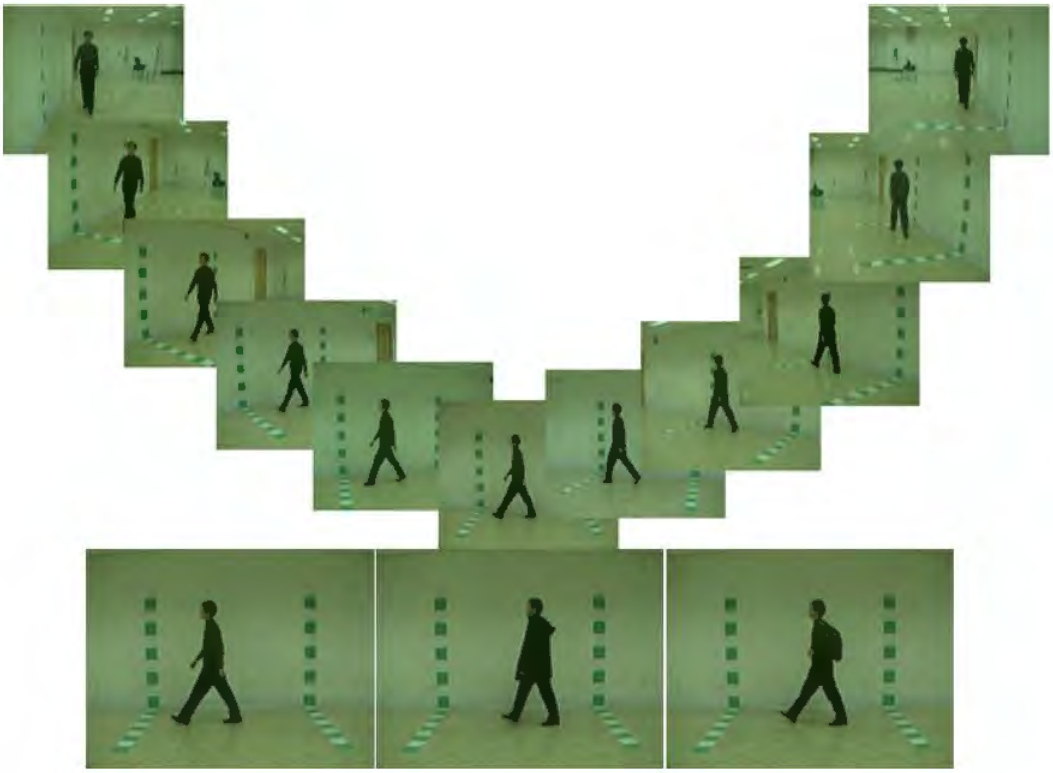

Figure 1.4 Sample images of CASIA-B data set[4]

[3]Image Source Institute of Scientific and Industrial Research (ISIR), Osaka University (OU) in [23]
[4]Image Source CASIA Gait Database, The Center for Biometrics and Security Research (CBSR) in [24]

1.1.1.3 Motivation and Contribution

Despite of wearing different types of cloths or carrying different types of bags we can recognize each other from distance. Our visual system has the capability to extract necessary information from the body shape and their walking style for the purpose of recognition. If some portion of the body shape are occluded or distorted by the cofactors, human visual system can reconstruct the full shape or discard the affected parts to determine the identity of that person.

Recently, several feature extraction and selection techniques have been introduced into gait recognition and have shown promising results. The gait signature is composed of different body parts. The effects of different cofactors (e.g., clothing, carrying objects, viewing angles, surfaces, etc.) do not change all body parts. It may alter some parts of whole gait where other parts that are useful for gait identification remained unchanged [21]. Our proposed method focuses on features which are less affected by the changes in covariate conditions and significantly distinguishable from other features to identify the person.

Generally, for the whole-based methods, significant numbers of training subjects are required for representing the variation of full-body gait features, while relatively small number of training subjects will cover such variation of part-based gait features due to its low dimensionality. With regard to the different gait representation techniques there is still a major issue to define the effective body components that influence the gait recognition under the effect of different cofactors. Although a variety of part-based techniques [17, 21, 25, 27, 28] have been proposed, the body parts are defined priory and manually in all the

studies. Therefore, they did not provide any insights into the way how to define the whole gait as parts and select the less affected parts from the whole human body under the effect of different cofactors.

From our point of view, there are two important ways to improve the recognition accuracy in case of different cofactors like clothing, carrying objects, etc.:

1. Gait features should be represented with the most discriminating information.
2. For selecting the appropriate parts, more affected and less affected body parts should be considered.

From these observations, for giving more emphasis on dynamic areas and less on static areas, the discrete Fourier transformation (DFT) based entropy (EnDFT) gait representation is computed from frequency domain gait representation is proposed. Then, a robust technique is proposed to define which parts are less affected by cofactors or more effective, and which parts are mostly affected or less effective. Based on the experimental result, we define the whole gait into five unequal parts. Among the five parts, we select three body parts as most effective and two are less effective based on recognition rate. We use these three most effective body parts with the entropy-based DFT gait representation for gait recognition.

We also study to select effective parts adaptively by calculating the weights depends on the variation of gallery gait and probe gait using Zernike and Legendre moments. Experimental results show better performance compared with the others part-based and whole-based approaches.

1.1.2 Gait recognition under walking speed changes

1.1.2.1 Problem definition

Walking speed variation is common for people in daily situations and the most challenging artifacts out of the different cofactors. Person's walking speed variations severely alters the gait pattern, creates large intra-class difference and reduce the recognition rate. The intra-class difference gradually rises by the person's walking speed variation from slower to faster. If the training data set is small, then it fails to model the intra-class variations. Therefore, the performance degraded severely of the gait identification systems. Sample gait images under various walking speeds from the OU-ISIR gait database A [29] and CASIA C [30] are shown in Figure 1.5 and Figure 1.6 respectfully.

Figure 1.5 Sample images of OUISIR treadmill gait database B[5]

[5] Image Source Institute of Scientific and Industrial Research (ISIR), Osaka University (OU) in [29]

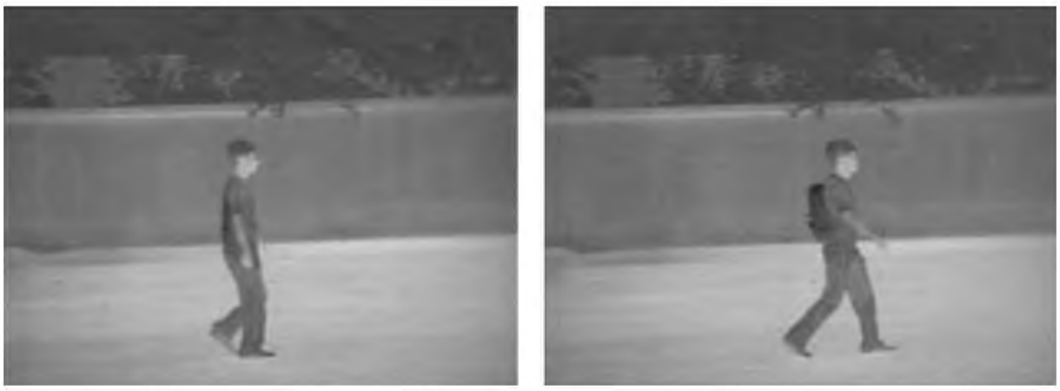

Figure 1.6 Sample images of CASIA-B data set[6]

1.1.2.2 Challenges

Due to increase in walking speed, higher the hands swing, increase the step length and shorten the gait period [31] that changes the shape of the gait. Various studies have shown that walking speed changes can have a very negative impact on recognition rates. For example, Bouchrika and Nixon [32] evaluated the effects walking speed on gait recognition and achieved the rate for both slow and quick walking was 60% and 50% whereas 86% for normal walking leading to the conclusion that dynamic gait features changes with speed. Similarly, Kusakunniran et al. [33] achieved an average rate of 96% for 1 km/h difference and 68% for 4 km/h difference in gallery-probe speed.

1.1.2.3 Motivation and Contribution

In fact, walking speed variation affects some parts of the body (hands, legs, hip, knee and ankle) while some parts (head, neck, torso, hip and thigh) are relatively remain unaffected. Although the dynamic gait features can be significantly affected by the speed changes, the static features can be relatively stable. In this case, the covariate walking speed

[6]Image Source CASIA Gait Database, The Center for Biometrics and Security Research(CBSR) in [30]

has the similar properties with some covariates like clothing and carrying condition, which only affect part of the human silhouette [34]. It indicates the possibility of using certain clothing and carrying condition invariant gait recognition concept to solve the problems caused by different walking speeds.

In this work, we reduce the effect of walking speed changes which affects the dynamic parts of the gait by defining the human gait into six unequal parts and selecting the more effective parts using a lookup table-based technique experimentally. We also study to select effective parts adaptively by calculating the weights depends on the variation of walking speed of gallery gait and probe gait using Zernike and Legendre moments. This method minimizes the intra-class variation by selecting less affected parts and eliminating the more affected body parts dynamically and thus increase the recognition rates considerably.

At the end, we investigate the strength and effectiveness of our proposed part definition and selection approach on OU-ISIR treadmill dataset A [29], OU-ISIR treadmill dataset B [23], CASIA gait database B [24] and CASIA C [30] gait database and compare the results with the existing methods.

1.2 Related Works

A large number of gait recognition techniques have been proposed. Such gait recognition techniques can be divided into two broad categories: model-based approaches [35-48] and model-free (motion-based or appearance-based) approaches [21, 49-61].

1.2.1 Model-based gait recognition

The model-based approaches use a priori knowledge on extracting the physical structure of the human gait by utilizing some static parameters. More specifically, these methods extract the unique gait features such as different body parts shape and motion by fitting the human model to input images. The model-based approaches are still difficult to estimate and their time complexity is high. Although they are known as view and scale invariant. They also require high-quality resolution silhouettes.

These gait features contain kinematics of leg motion by Fourier analysis [44], static shape parameters [36] and gait period with an articulated body model [45], joint angles with an articulated body model [46]. Out of the earliest model-based approaches, Cunado et al. [38] considered legs as an interlinked pendulum. They used phase-weighted Fourier magnitude spectrum for extracting the gait features from the motion of the human leg and then fed the features to K-Nearest Neighbor classifier for the recognition. They then use the Fourier series to extract the gait features from the motion of the human leg and fed them to K-Nearest Neighbor for the classification. Hee et al. [47] constructs a 2D stick model based on human anatomical knowledge [62]. Bobick and Johnson [36] divided and labeled the gait silhouette into three sections (head, pelvis and foot). They calculated the distances among four body part locations (head and foot, head and pelvis, foot and pelvis, left and right foot) to extract static body and stride parameters for gait recognition. Zhang et al. [63] approached a five-link biped locomotion human model to extract trajectory-based kinematic components for clothing invariant recognition. They extracted features from image sequences using the Metropolis–Hasting method. Finally, Hidden Markov Models were trained on the extracted frequency components from these feature trajectories

for classification. Bouchrika and Nixon [37] proposed a model-based method to extract human joints (vertex positions). The motion of the joints was parameterized using elliptic Fourier descriptors. to extract crucial features from human joints. Wang, Tan et al. [64] proposed simple and automatic gait recognition algorithm based on compact statistical shape descriptors of the human body from spatio-temporal motion pattern.

More recently, Ariyanto and Nixon [48] propose a marionette mass-spring model for 3D gait recognition as a more mechanical model. Model-based methods have limited efficiency because of the high computational burden on the basis of complex matching and searching. These methods also often suffer by model fitting errors. In fact, the study [44] reports that high quality gait image sequences are required to achieve a high accuracy.

1.2.2 Model-free gait recognition

The model-free methods typically extract features directly from gait sequences and usually use silhouette to represent gait without any explicit modeling of human body structures. The appearance-based methods usually consider some pre-processing steps such as background modeling, foreground-background subtraction, silhouette alignment and normalization, feature extraction and classification. Motion-based approaches [65, 66] are comparatively insensitive to the quality of gait silhouettes and have the benefit of low computational costs compared to model-based approaches. These types of approaches outperform the model-based methods in general, which is the main reason why the most of the gait recognition approaches adopt the model-free approaches. The model-free approaches can be separated as whole-based and part-based.

1.2.2.1 Whole-based model-free approaches:

Whole-based methods extract features and match the whole human body without any part definition and selection. Tan et al. [54] used six simple projective features to describe human gait and compare eight kinds of frieze features to figure out which projective directions are important for gait recognition. PCA was applied for gait feature dimension reduction and nearest neighbor rule for classification. Abdelkader et al. [67, 68] proposed an eigengait similar way as eigenfaces method using units of self-similarity and applied PCA to reduce the dimensionality of the feature space and k-nearest neighbor rule in the reduced feature space for recognition plots. Cuntoor et al. [69] project the silhouette into a width vector and Liu et al. [70] project it into a frieze pattern, namely, combination of width and height vectors. Considering the periodic property of gait, a discrete Fourier transform (DFT) [71] is computed as pixel-by-pixel amplitude spectra of zero-, one-, and two- times frequency elements. Gait recognition using average silhouette is proposed in [72]. Han et al. [51] proposed the simplest yet the most prevailing baseline algorithm by just averaging the silhouette value pixel-by-pixel over the gait period, known as gait energy image (GEI). As a variant of the GEI, a gait entropy image (GEnI) [73] is computed as pixel-by-pixel entropy of the GEI so as to focus on dynamic regions. A gait flow image (GFI) [74] focuses more directly on the dynamic components, where the optical flow lengths observed on the silhouette contour are averaged over the gait period.

The entropy transformation of gait GEnI from GEI gives more weights in dynamic areas and less in static areas [73]. In GEnI, dynamic areas show more uncertainty and thus more informative than static areas in gait representation. The DFT representation of gait shows better result than GEI for its separated two dynamic higher frequency components

[21]. The one- and two-times frequency elements in the DFT hold only the uncertainty values of the gait. Therefore, the entropy-based transformation of the DFT clearly separates the most uncertainty areas by adding one- and two- times frequency components to the GEI.

1.2.2.2 Part-based model-free approaches

Part-based approaches initially define the body parts manually or experimentally, extract features from the parts and finally select the less affected parts for recognition.

Various studies on human body components [17, 25, 27, 28] suggest that the combination of body parts may increase the recognition accuracy only when it is possible to separate the discriminating and over-fitting parts. The first methods that divide the human body into components for gait identification is described in [17]. They considered each component separately and applied in both person identification and gender classification. Boulgouris et al. [27] proposed a component-based gait recognition that considers the unequal discrimination ability of each part. In [28], seven gait components are defined. The contributions of the components have been studied both individually and in certain combinations for both human gait recognition and gender recognition.

A part-based gait identification method is proposed in [25]. The human body is divided into eight parts based on anatomical statistics. This method can reduce the effect of different clothing combinations by assigning higher weights to the unaffected body parts than the affected areas. Avoiding the least reconstruction error, recently a random subspace method (RSM) is proposed [75]. Although the RSM outperforms other classical methods [51, 72], it does not guarantee the best accuracy for clothing-invariant gait recognition [76].

The method chooses N eigenvectors randomly from all the eigenvectors for creating L random subspaces.

1.2.3 Gait recognition under clothing and carrying conditions

The classification rate for the coat is almost the same as normal clothing but the rate drastically reduced for trench coat [32]. This happens due to nature of the clothing that distract the gait dynamics or occlude the appearance. Matovski et al. [26] claimed that the elapsed time with clothing variation between recording the gallery and the probe affect recognition rate. They collected data in months 9 and 12 where same subjects wearing different types of clothes and performed analysis of different type of clothes over time and over few minutes while keeping all other covariates unchanged. They concluded that the performance could be affected significantly due to clothes change regardless of elapsed time but less significant for similar types of clothes. Guan et al. [75] proposed RSM-based robust clothing-invariant method for gait recognition by combining multiple inductive biases for classification. Hossain et al. [25] proposed a part-based adaptive weight control method for clothing-invariant gait identification. The whole body divided into eight different length parts, including four overlapping parts to overcome the difficulties caused by different types of clothing and dimension-reduced frequency-domain features were used as part-based gait features. They claimed that the larger parts having a higher discrimination capability, whereas the smaller parts are more likely to be unaffected by variations in clothing. The matching weights were determined for all the 8 parts adaptively from the distances between the probe and all the galleries. Islam et al. [77] proposed a random window subspace method (RWSM) for clothing invariant gait recognition by splitting the gait into very small window chunks. The approaches [25, 75, 77] were all

evaluated on large clothing variation OU-ISIR Treadmill database B, which included at most 32 combinations of different types of clothing for 68 subjects with 2746 sequences. The LDA-based method [51] reduces to some extent the effects of intra-class variations, that is, clothing variations, on gait identification. It does not, however, work well when clothing variations exceed individual variations. A convolutional neural networks (CNN) based method is proposed in [78] for clothing invariant gait recognition. They extracted the most discriminative changes of gait features from gait energy image (GEI) as low-level input data and evaluated the performance of their proposed method and achieved better recognition rate compared with other conventional approaches on the challenging clothing invariant dataset OU-ISIR Treadmill B.

1.2.4 Gait recognition under walking speed change

Walking speed changes impacts on accuracy across all modalities of gait recognition. Walking speed variations is the result of a change of applied average energy or strength during walking and alters all the time and spatial based features that makes intra-class difference of human gait. The step length, cadence, double limb stance duration, joint motion and the joint angles at hip, knee and ankle are significantly changed by walking speed [79, 80]. Mason et al. [81] evaluated different ground reaction force (GRF) normalization techniques, including one that linearly stretched the GRF profiles to have the same duration, which is normally correlated with walking speed. Bouchrika et al. [32] evaluated the effects of different covariate conditions in a model-based method and found that the recognition rates drop by 35% for walking speed changes. To reduce the intra-class difference for speed invariant gait recognition, Kusakunniran et al. [82] suggested invariant feature-based methods and speed transformation-based methods.

The first methods minimize intra-class differences by speed invariant features extraction from gait silhouettes. Kusakunniran et al. [33, 82] proposed a potential method Procrustes Shape Analysis (PSA) in handling a large variations of walking speed and cross speed gait recognition. In addition, with [33] Kusakunniran et al. [82] developed Higher-order derivative Shape Configuration (HSC) method to extract features for speed invariant cross speed gait identification. They advanced the HSC framework by using Differential Composition Model (DCM), which adaptively compute and assign weights to different parts of the gait [82]. Compared to Higher-order derivative Shape Configuration, the development of Differential Composition Model reduce the intra-class variation and delivers significant performance on huge speed changes database. Guan et al. proposed an ensemble classifier based on Random Subspace Method (RSM) to deem the unstable dynamic feature caused for speed changes [34]. They claimed that proposed framework is capable to solve the cross-speed gait identification problems in a cross-mode or fixed-mode manner. In this method, they computed eigenvectors and eigenvalues from Gabor-GEI and created random subspaces by removing zero eigenvalue eigenvectors. They randomly selected the eigenvectors, projected and executed the single experiment for ten times, and calculated the mean CCR. However, RSM gained attractive CCR but it does not always assurance the best accuracy because the randomness nature of the system and shows more time complexity [76].

To reduce intra-class difference, the other method is to the transformation of different walking speed data to a general speed before classification. Tsuji et al. [83] proposed a factorization-based speed transformation model to transform dynamic gait features from one speed to another by keeping static features unchanged. The authors claim that the speed

changes are nearly the same effect as camera viewpoint changes, Tsuji et al. utilized the view transformation idea for walking speed changes gait transformation using singular value transformation. The walking speed change mostly affects dynamic body parts like arm swing and stride length, so there are some approaches proposed for cross-speed gait recognition using dynamic part attenuation technique. Tanawongsuwan and Bobick [84] proposed speed normalization procedure, which maps gait features across different speeds and improve the recognition performance. They utilized silhouettes at the single-support phases (mid-stance) as a part of the gait feature, where the limbs are the most closed and are not severely altered as the speed changes. However, the gait recognition performance can drop due to temporary posture changes, silhouette segmentation noise and phase estimation errors that may easily affected the selected particular key-frame at single-support phase of a gait cycle. Recently Chi Xu et al. [85] claimed that existing methods can alleviate the influence of speed on gait recognition task to some extent but most of the methods perform poorly under large speed changes, or suffer from high computational cost, which is an important aspect in real-world applications. They proposed a speed-invariant and stable gait representation called single-support GEI (SSGEI), which realizes a good trade-off between speed invariance and stability by aggregating multiple frames around single-support phases. They performed experiments on two publicly available datasets, the OU-ISIR Treadmill Dataset A and the CASIA Dataset C and showed that their method achieves better accuracies in both identification and verification scenarios with a low computational cost.

1.3 Gait Databases

There are a few databases that were used for experimental evaluation of gait recognition tasks in the past two decades by many researchers. The most of databases were recorded indoors and subjects were different in numbers. In the following section, some standard datasets are described.

1.3.1 NLPR gait database

The Chinese National Laboratory of Pattern Recognition presented three public data-sets namely: CASIA-A [86], CASIA-B [24] and CASIA-C [30].

The CASIA gait database A contains 20 subjects. Each subject has captured 12 video sequences with three viewing angles, namely frontal (90^0), oblique (45^0), and lateral (0^0) views. Each subject walked along a straight-line path from left to right and right to left. In this way, four videos per subject from each viewing angle were recorded. These sequences captured images with 24-bit full color, 352 x 240 pixels of resolution at 25 frames per second.

The CASIA gait database B contains 124 subjects and captured video sequences in different clothing conditions (cl), carrying conditions (bg) and normal walking conditions (nm) from 11 viewing angles. For each subject and each viewing angle ten video sequences were captured including two sequences when wearing a coat, two sequences with carrying a bag and six sequences in normal walking (without wearing coat and carrying bag). Figure 1.2 shows sample images from the CASIA gait database B.

The CASIA gait database C contains 153 subjects (130 males and 25 females) under different weather, speeds and carrying conditions and captured by an infrared (thermal) camera outdoors at night. Ten video sequences were captured for each subject including four sequences for normal walking (fn), two sequences for slow walking (fs), two sequences for fast walking (fq) and two sequences for normal walking with a bag (fnb). The videos were all captured at night by infrared (thermal) cameras.

1.3.2 OU-ISIR gait database

The Institute of Scientific and Industrial Research (ISIR), Osaka University (OU) has OU-ISIR [23] gait database is meant to aid research efforts in the general area of developing, testing and evaluating algorithms for gait-based human identification.

The OU-ISIR has several gait datasets. OU-ISIR treadmill dataset A [23, 29] covers the gait data of 34 subjects from side view. It is captured under nine different speeds with speed variation from 2 km/h to 10 km/h at 1 km/h interval. Two video sequences were recorded for each subject from each speed. Figure 1.7 shows sample size normalized silhouettes from the OU-ISIR gait dataset A. The number of frames recorded for each speed of each sequence is listed in Table 1.1. The OU-ISIR gait database, the treadmill dataset B [23, 29] with large clothing variations. It includes 68 subjects with at most 32 combinations of different types of clothing such as skirt, raincoat, down jacket, long coat, hat, parker, muffler, short pants, casual wears, regular pants, half shirt, full shirt etc. and captured 2746 video sequences. The clothing types are listed in Table 1.2 and the clothing combinations that are used for constructing the dataset is in Table 1.3. Figure 1.8 shows the sample images of clothing combinations.

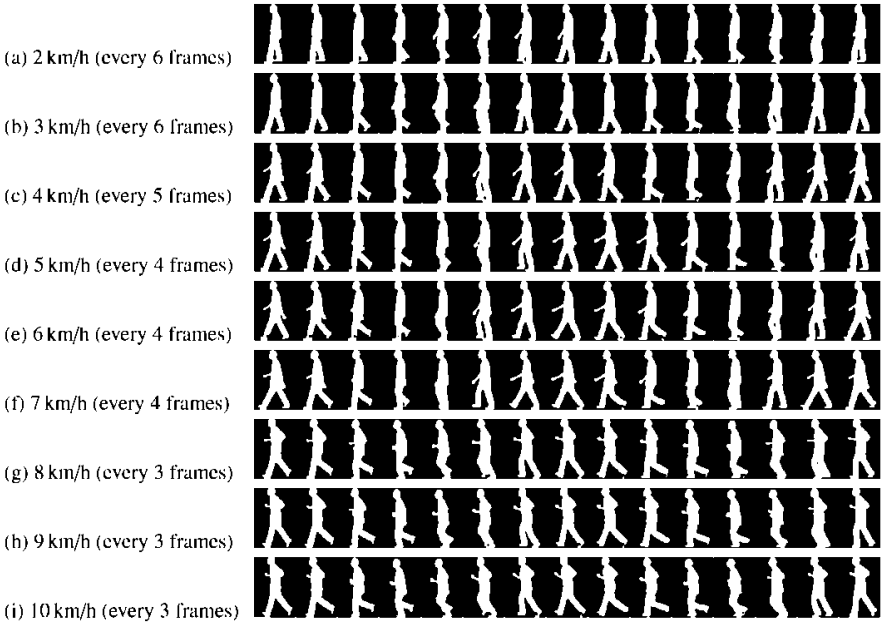

Figure 1.7 Sample size normalized silhouettes from the OU-ISIR gait dataset A [29]

Table 1.1 Number of frames recorded for each speed of each sequence [29].

Speed (km/h)	2	3	4	5	6	7	8	9	10
No. of frames	420	360	360	420	360	240	240	240	300

Table 1.2 Types of clothing used in dataset B [25] (abbreviation: name).

RP: Regular Pants	HS: Half Shirt	CW: Casual Wear
BP: Baggy Pants	FS: Full Shirt	RC: Rain Coat
SP: Short Pants	LC: Long Coat	Ht: Hat
Sk: Skirt	Pk: Parker	Cs: Casquette Cap
CP: Casual Pants	DJ: Down Jacket	Mf: Muffler

Table 1.3 Different clothing combinations [25].

#	S_1	S_2	S_3	#	S_1	S_2	S_3	#	S_1	S_2	#	S_1	S_2
2	RP	HS	-	7	RP	LC	Ht	L	BP	Pk	V	Sk	DJ
3	RP	HS	Ht	8	RP	LC	Cs	M	BP	DJ	D	CP	HS
4	RP	HS	Cs	C	RP	DJ	Mf	N	SP	HS	F	CP	FS
9	RP	FS	-	A	RP	Pk	-	Z	SP	FS	E	CP	LC
X	RP	FS	Ht	B	RP	DJ	-	P	SP	Pk	G	CP	Pk
Y	RP	FS	Cs	I	BP	HS	-	S	Sk	HS	H	CP	DJ
5	RP	LC	-	K	BP	FS	-	T	Sk	FS	O	CP	CW
6	RP	LC	Mf	J	BP	LC	-	U	Sk	Pk	R	RC	RC

The OU-ISIR gait database, the treadmill dataset D is composed of gait silhouette sequences of 185 subjects from side view with various gait fluctuations among gait cycle. The OU-ISIR Gait Large Population Dataset covers gait data of 4007 subjects. It is captured under four different viewing angles.

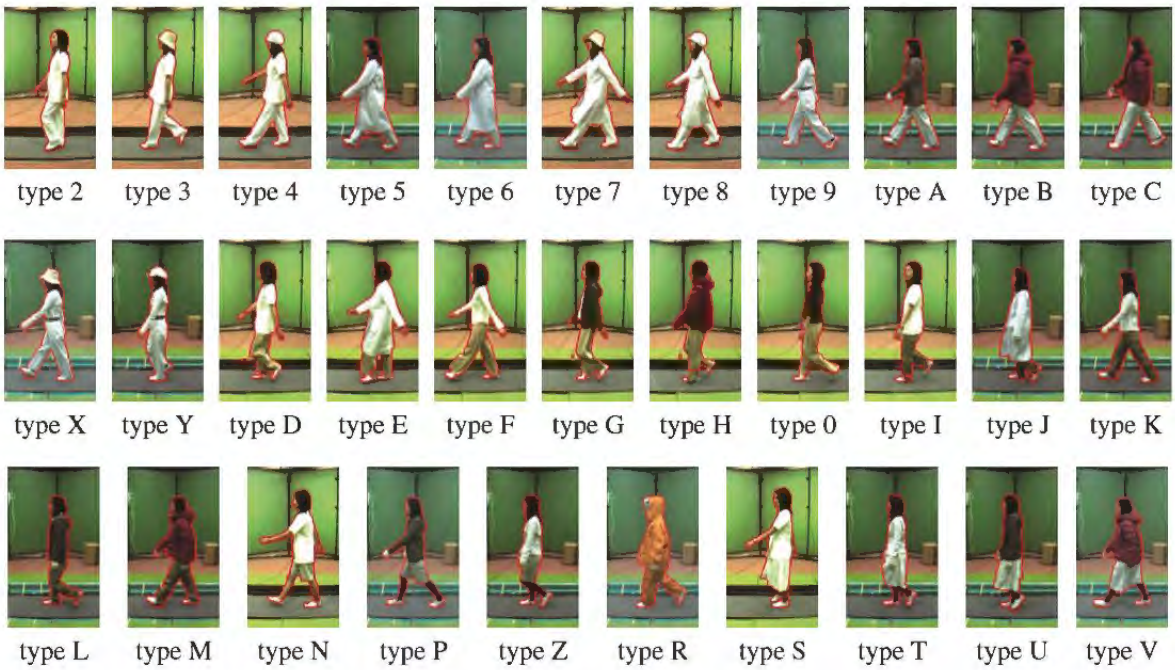

Figure 1.8 Sample clothing combinations [25].

1.3.3 The CMU Mobo gait database

The CMU Mobo gait database [87] contains 25 subjects from 2 different walking speeds, namely slow walking (3.3 km/h) and fast walking (4.5 km/h). The videos were captured in an indoor scenario. Each subject was recorded under four walking conditions, slow walking, fast walking, slow walking at a certain slope, and slow walking when holding a ball.

1.3.4 USF database

The USF [88] is a large gait dataset that covers the data of 122 subjects. The gait sequences are filmed outdoors under several walking variations: two viewpoints, surface, shoes, carrying condition, and time.

1.3.5 Southampton database

The Southampton [89] has two gait datasets. The Soton Small dataset covers the data of 12 subjects, captured inside track, with a chroma-key green screen backdrop, under several walking variations, which are: footwear, clothes and carrying bags, and different speeds. The Soton Large database covers the data of 115 subjects, captured outdoors on an inside track and on a treadmill under six different views.

1.3.6 Other gait databases

There are other gait datasets including the HID-UMD gait databases [90] and the MIT Artificial Intelligence Lab data set (MIT AI) [91]. Details of the existing datasets are given in Table 1.4.

Table 1.4 The existing different gait datasets.

Dataset	Number of Subjects	Number of Sequences	Environment	Year	Walking Variations
CASIA A [86]	20	240	Outdoor	2001	3 viewing angle
CASIA B [24]	124	13640	Indoor	2005	Clothing, carrying and viewing conditions
CASIA C [30]	153	1530	Outdoor, thermal camera (at night)	2005	Speed, carrying condition
OU-ISIR A [29]	34	612	Indoor (Treadmill)	2010	9 walking speeds conditions
OU-ISIR B [23]	68	2746	Indoor (Treadmill)	2010	clothing condition
OU-ISIR D	185		Indoor (Treadmill)	2010	gait fluctuations
OU-ISIR Gait Large Population Dataset	4007		Indoor		Different age ranges, 4 viewing angles
USF [88]	122	1870	Outdoor	2001	view, surface shoe, carrying, time conditions
CMU [87]	25	600	Indoor	2001	view, walking speed, carrying, surface
Soton Small [89]	12		Indoor		Carrying condition, clothing, footwear (shoe), viewing angles
Soton Large [89]	115	2128	Indoor (Treadmill and track), outdoor		6 different viewing angles
HID-UMD 1 [90]	25	100	Outdoor		4 viewing angles
HID-UMD 2 [90]	55	220	Outdoor		2 viewing angles
MIT AI 24 194 Indoor [91]	24	194			View, time conditions

1.4 Thesis Outline

The rest of the dissertation is organized as follows.

CHAPTER 2 explains preprocessing, different gait representation technique and background knowledge that is used in different proposed methods.

CHAPTER 3 presents the experimental setup to define the body parts of whole gait considering clothing condition. The selection procedure of most effective body parts by rejecting most affected parts is established here.

CHAPTER 4 introduces a novel gait feature representation technique Entropy-based DFT (EnDFT). EnDFT highlights the dynamic areas of gaits and this is useful for clothing and carrying conditions to enhance the recognition performance.

In CHAPTER 5, The parts definition and look-up table-based parts selection procedure for speed changes is presented. The benefits of look-up table for parts selection are to select different body parts with speed changes of a probe.

CHAPTER 6 describes a common frame work for clothing and carrying conditions and speed changes. For selecting body parts adaptively, Legendre moments and Zernike moments is introduced to calculate the weight of each part and used that weight as threshold. If the weight of certain part of a probe is greater than the threshold we discard that part otherwise accept for recognition.

CHAPTER 7 presents the summery of this thesis and express some ideas and extensions of current works.

CHAPTER 2. OVERVIEW OF PREPROCESSING, GAIT CYCLE ESTIMATION, GAIT REPRESENTATION TECHNIQUES AND FUNDAMENTAL KNOWLEDGE

This thesis proposes several techniques to address the issues of various walking conditions focusing on most challenging clothing and carrying changes and speed variations. Thus, many techniques are adopted and adapted accordingly in the proposed methods. This chapter explains and discusses about different existing and proposed gait representation and background knowledge of these techniques.

We used the OU-ISIR Gait Database- Treadmill Dataset A, OU-ISIR Gait Database- Treadmill Dataset B, CASIA-B and CASIA-C dataset. We have conducted several different experiments on these datasets using our proposed model-free methods.

2.1 Preprocessing

To represent the gait features, most of the model-free gait recognition approaches use silhouettes. Silhouettes are extracted from each frame of a sequence by background subtraction-based graph-cut segmentation [92]. Mathematical morphological operations are used on extracted silhouettes to reduce minor segmentation errors and noise elimination. Now, background-subtracted silhouette is registered to obtain the spatio-temporal gait silhouette volume (GSV) [71]. Then, the silhouettes are scaled and normalized into a fixed size of 128 × 88 pixels. Size normalized gait silhouettes are shown in Figure 2.1 as an example.

The initial step for matching measure is gait period detection. In our study, the similar method normalized autocorrelation (NAC) as that one in [71] is applied to determine gait periods of size-normalized silhouettes for the temporal axis on each gait sequence.

Figure 2.1 Size normalized gait silhouettes [23]

We calculate the normalized autocorrelation (NAC) of a GSV for the temporal axis as:

$$C(N) = \frac{\sum_{x,y} \sum_{n=0}^{T(N)} g_{x,y,n}\, g_{x,y,n+N}}{\sqrt{\sum_{x,y} \sum_{n=0}^{T(N)} g_{x,y,n}^2} \sqrt{\sum_{x,y} \sum_{n=0}^{T(N)} g_{x,y,n+N}^2}} \tag{2.1}$$

$$T(N) = N_{total} - N - 1 \tag{2.2}$$

$$N_{gait} = \arg \quad max_{N \in [N_{min}, N_{max}]}\, C(N) \tag{2.3}$$

where *C(N)* is the NAC for an N-frame shift, *g(x,y,n)* is the silhouette value at position *(x,y)* in the n_{th} frame, and N_{total} is the total number of frames in the GSV.

2.2 Human Gait Representation Technique

Several gait representations have been proposed that use the whole number of silhouettes in one gait period instead of matching sequences on a frame by frame basis.

2.2.1 Gait Energy Image (GEI)

The spatio-temporal average silhouette over a complete gait cycle is called GEI [64]. Examples of GEI's are shown in Figure 2.2 from three dataset. Most of the appearance-based approaches [51, 72, 75, 89, 93] used GEI as input gait features. GEI represents both the static (head and body) and dynamic areas (swings of legs and arms) of the gait.

Given the pre-processed binary gait silhouette images $B(x, y, n)$ at time n in a sequence, the GEI is defined as:

$$GEI(x, y) = \frac{1}{N} \sum_{n=1}^{N} B(x, y, n), \tag{2.4}$$

where N is the total number of frames in a gait cycle, n is the frame number and x and y values in the 2D image coordinates.

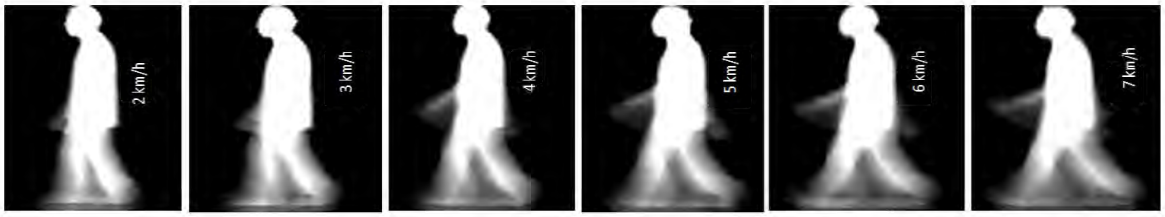

(a)

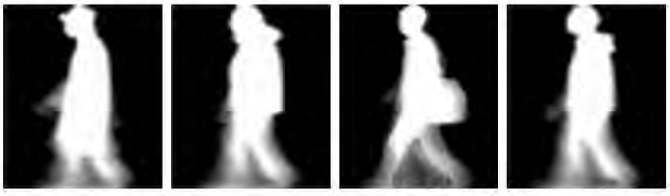

(b)

Figure 2.2 Examples of Gait Energy Images of (a) walking speed changes and (b) clothing and carrying conditions.

2.2.2 Gait Entropy Image (GEnI)

In mathematics, entropy is used to measure the uncertainty of problems. While in information science, entropy is the average uncertainty of information source. In other word, entropy is a measure of irregularity of states such as imbalance, uncertainty like as dynamic areas of human gait. If *k* symbols are generated from the source, then the average self- information obtained from *k* output is:

$$-k\sum_{j=1}^{J} P(a_j)\log P(a_j) \tag{2.5}$$

where a_j are symbols and $P(a_j)$ are source symbols probability. The average information per source output i.e. entropy is:

$$H(Z) = -\sum_{j=1}^{J} P(a_j)\log P(a_j) \tag{2.6}$$

As $H(Z)$ increase means more information is associated with the source and if the source symbols are equally probable then the entropy will be the maximum. The intensity value of the binary silhouettes for a fixed pixel location as a discrete random variable, the entropy of this variable over each gait period can be computed as:

$$H(x,y) = -\sum_{j=0}^{1} P_j(x,y)\log_2 P_j(x,y) \tag{2.7}$$

GEnI [21, 73] is extracted by computing entropy directly from GEI using Equation (2.7), where $P_1(x, y)$ represent the value from GEI and $P_0(x, y) = 1 - P_1(x, y)$, as are shown in Figure 2.3. The GEnI contains dynamic body areas (e.g., leg, arms) which undergo consistent relative motion during a gait cycle will lead to high gait entropy value, whereas those areas that remain static (e.g., torso) would give rise to low values.

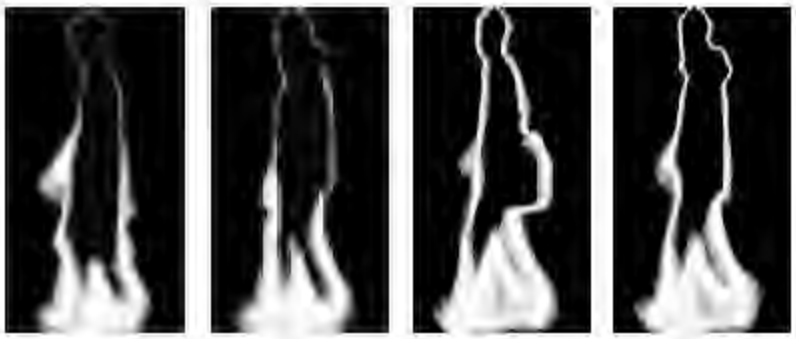

Figure 2.3 Examples of Gait Entropy Images of different clothing and carrying conditions.

2.2.3 Discrete Fourier Transform Image (DFT)

Another popular gait representation technique is the frequency domain gait features. The amplitude spectra of the GSV are calculated by DFT analysis based on the gait period [21, 71] are shown in Figure 2.4. A DFT $G(x, y, k)$ and amplitude $A(x, y, k)$ for the temporal axis are calculated as;

$$G(x, y, k) = \sum_{n=0}^{N-1} B(x, y, n) e^{-j\omega_0 kn} \tag{2.8}$$

$$A(x, y, k) = \frac{1}{N}|G(x, y, k)| \tag{2.9}$$

where N is the number of frames in a gait cycle, ω_0 is a base angular frequency for a gait cycle and k is the frequency component. Usually, only 0-2 time's frequencies are considered. Higher frequency elements are removed as noise. Therefore, DFT consists of three components where the first component is equivalent to GEI, middle component represents the asymmetry of the left and right motion and the last component represents the symmetry thereof.

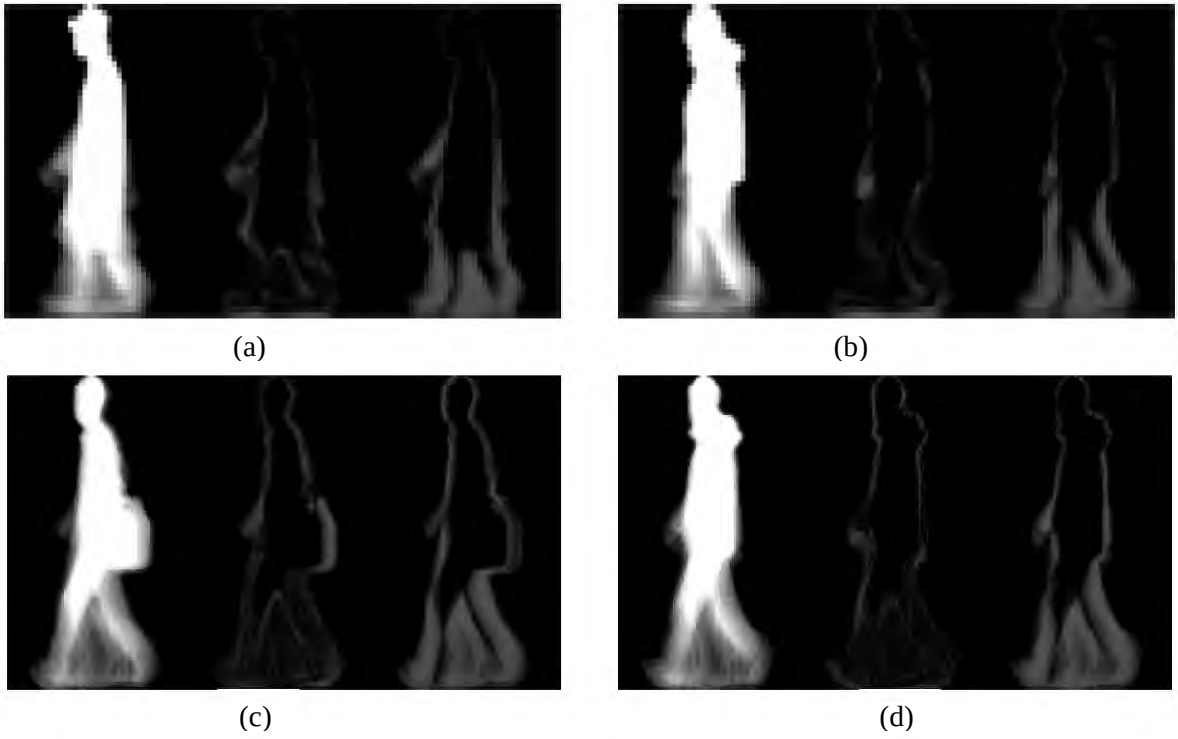

Figure 2.4 Examples of Discrete Fourier Transform images (a-d) of different clothing and carrying conditions where each of with 0, 1 and 2-times frequency components.

2.2.4 DFT Entropy Image (EnDFT)

Both GEI and DFT include static (e.g. torso) and dynamic (e.g. leg, arms) components together. However, it was reported in [73] that they are vulnerable in the presence of significance change in appearance due to different covariate condition. GEnI usually outperforms GEI, but it produces similar result to the DFT because the last two components of DFT represent the most dynamic nature of the gait.

We propose frequency domain-based entropy gait features EnDFT in [21]. The intensity value of the proposed EnDFT is computed using Equation (2.7) from the DFT. Where $P_1(x, y)$ is the intensity value of DFT and $P_0(x, y) = 1 - P_1(x, y)$.

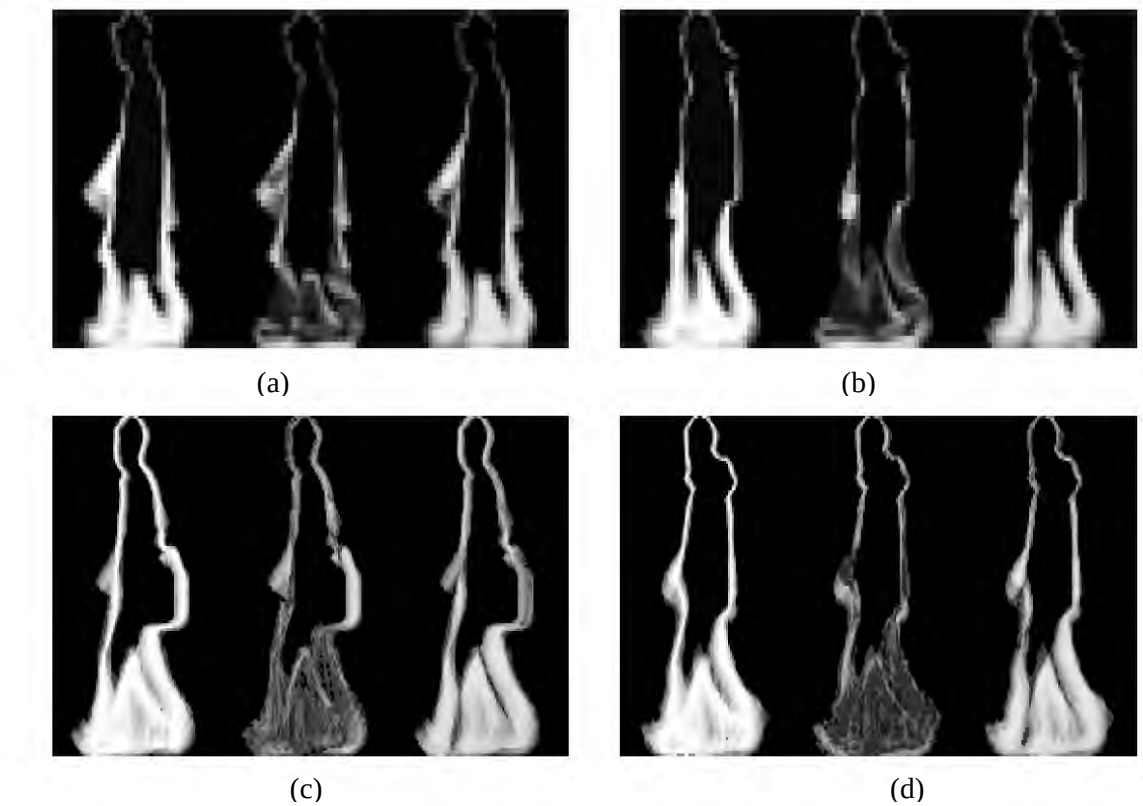

Figure 2.5 Examples of Entropy-based Discrete Fourier Transform (EnDFT) images (a-d) of different clothing and carrying conditions each of with 0, 1 and 2-times frequency components.

The main difference between GEnI and EnDFT gait feature is that GEnI is calculated from GEI whereas EnDFT is derived from DFT representation.

The DFT representation of gait shows better result than GEI for its separated two dynamic higher frequency components. The one- and two-times frequency elements in the DFT hold only the uncertainty values of the gait. Therefore, the entropy-based transformation of the DFT clearly separates the most uncertainty areas by adding first- and second-times components of the DFT to the GEI. It is visible from Figure 2.5 that proposed EnDFT gives more weights into dynamic areas and less near to zero into static areas by using all three components of the DFT. It is simple to generate EnDFT directly from DFT features just computing the entropy.

2.3 Subspace Analysis

Principal Component Analysis (PCA) and Linear Discriminant Analysis (LDA) are extensively used and well-known subspace learning methods. Direct template matching for recognition or identification is sensitive to small silhouette distortions and noise [51, 94]. This is due to the dimensionality of the gait feature space is high even after feature selection. To overcome this issue, PCA and LDA can be used to project the original gait features to a subspace of lower dimensionality for achieving better lower dimensional data representation and important optimal discriminant information simultaneously [95]. Their fundamental concepts are briefly explained as below.

2.3.1 Principal Component Analysis

Suppose we have *N* number of *M*-dimensional gallery gait image template $\{x_1, \ldots, x_n, \ldots, x_N\}$ belonging to *C* different classes (subjects), where each template is a column vector obtained by concatenating the rows of the corresponding gait image. Let $D_{i,j}$ indicate the *j*th distance signal in class *i*, each distance signal contain *M* normalized pixel points (dimensionality), the sample number of distance signal in class *i* is N_i, then the total training sample number is, $N = N_1 + N_2 + \ldots + N_c$.

The training set is

$$D = \lfloor D_{11}, D_{12}, \ldots, d_{1n}, d_{21}, \ldots, d_{CN} \rfloor, D \in R^{M \times N} \tag{2.10}$$

The mean value m_D and covariance matrix $\sum$ are

$$m_D = \frac{1}{N} \sum_{i=1}^{C} \sum_{j=1}^{N} D_{i,j} \tag{2.11}$$

$$\Sigma = \frac{1}{N-1} \sum_{i=1}^{C} \sum_{j=1}^{N} (D_{ij} - m_D)\,(D_{ij} - m_D)^T \tag{2.12}$$

where $\sum$ is real symmetric matrix and $\sum \in R^{M \times N}$.

According to singular value decomposition (SVD) theory, the nonzero eigenvalue of *M* are $\lambda_1, \lambda_2, \ldots, \lambda_M$ and its corresponding eigenvector are $e_1, e_2, \ldots, e_M$. The former eigenvectors with relatively large eigenvalue have relatively large change in training mode. And higher order eigenvector is to indicate relatively little change. Considering with storage and

effectiveness of calculation, set a threshold value T_s on accumulated variance curve to remove relatively small eigenvalue and corresponding eigenvector. If we select *K (K<M)* biggest eigenvalues and their eigenvector, the eigen mapping matrix E_{PCA} can be formed as:

$$E_{PCA} = [e_1, e_2, \dots, e_K] \tag{2.13}$$

By projecting each distance signal D_{ij} into *K*-dimensional eigenspace, we get R_{ij} as:

$$R_{ij} = E_{PCA}^T D_{ij} = [e_1, e_2, \dots, e_K]^T D_{ij} \tag{2.14}$$

2.3.2 Linear Discriminant Analysis

LDA is a feature extraction method in which the optimal projection directions are obtained by seeking the extreme of Fisher criterion function. It is expected that the projected samples can be achieved the largest between-class scatter and the smallest within-class scatter. After projecting *D* by PCA we get, $R = \lfloor R_{11}, R_{12}, \dots, R_{1N}, R_{21}, \dots, R_{CN} \rfloor, R \epsilon R^{K \times N}$ and its dimension is reduced from *M* to *K*.

Between-class scatter matrix S_b of samples and within-class scatter matrix S_w of samples are defined as follows:

$$S_b = \frac{1}{N} \sum_{i=1}^{C} \sum_{j=1}^{N} N_i (R_{i,j} - m_i) \, (R_{i,j} - m_i)^T \tag{2.15}$$

$$S_w = \frac{1}{N}\sum_{i=1}^{C}\sum_{j=1}^{N}(m_i - m)\,(m_i - m)^T \tag{2.16}$$

where m_i is the mean of samples *i*th class and *m* is mean of all class.

Then compute $S_w^{-1}S_b$to get the matrix for singular value decomposition (SVD) and can obtain *P (P<K)* nonzero eigenvalue $\lambda_1, \lambda_2, \ldots, \lambda_P$ and their corresponding eigenvector $e_1, e_2, \ldots, e_P$. The relatively large eigenvalue and their eigenvector have relatively higher separability, and higher order eigenvector has comparatively lower separability. By selecting first *t* largest eigenvalues, where $t \leq C\text{-}1$ and with their eigenvector to construct eigen mapping matrix W_{LDA}, which is:

$$W_{LDA} = \left[e_{1,}e_2, \ldots, e_t\right] \tag{2.17}$$

By projecting each sample $R_{i,j}$ to t-dimensional eigenspace as:

$$P_{i,j} = W_{LDA}^T \,.\, R_{i,j} = [e_{1,}e_2, \ldots, e_t]^T \,.\, R_{i,j} \tag{2.18}$$

Put $R_{ij} = E_{PCA}^T D_{ij}$ into Equation (2.18) and gets:

$$P_{i,j} = W_{LDA}^T \,.\, E_{PCA}^T D_{ij} \tag{2.19}$$

where, $P_{i,j}$ is a point in the *t*-dimensional eigenvector and each gait sequence appears as a way in eigenspace. It is apparent that PCA enormously reduces the dimensionality of sample and optimal class separation after LDA training.

2.4 Orthogonal Moments Computation

The mathematical concept of moments has been used in different fields ranging from physics and statistics to image processing and pattern recognition for many years. Moments has been used to extract a set of proper numerical attributes of features from the objects for classification in the design of an imagery pattern recognition system. In this research, Legendre moments and Zernike moments have been used for effective human body part selection for clothing and walking speed invariant gait recognition.

2.4.1 Legendre Moments

Legendre moments, were first introduced by Teague [96]. Legendre moments are orthogonal moments and were used in several pattern recognition applications [97]. The Legendre moments used Legendre polynomials as its basis set [98]. The two-dimensional Legendre moments of order *(p + q)*, with an image intensity function *f(x, y)*, are defined on the square [-1, 1] × [-1, 1] as:

$$L_{pq} = \lambda_{pq} \iint_{-1}^{1} P_p(x) P_q(y)\, f(x,y) dx dy \tag{2.20}$$

where $\lambda_{pq} = \frac{(2p+1)(2q+1)}{4}$, *p, q = 0, 1, 2, ..., ∞,* and $P_p(x)$ is the p_{th} order Legendre polynomial defined by:

$$P_p(x) = \sum_{k=0}^{p} \alpha_{pk} x^k = \frac{1}{2^p p!} \frac{d^p}{dx^p} (x^2 - 1)^p \tag{2.21}$$

or,

$$P_p(x) = \sum_{k=0}^{p} \left\{ \frac{(-1)^{\frac{p-k}{2}} x^k (p+k)!}{2^p k! \left(\frac{p-k}{2}\right)! \left(\frac{p+k}{2}\right)!} \right\}, \qquad p-k = even \tag{2.22}$$

The Legendre polynomials have the generating function:

$$\frac{1}{\sqrt{1-2rx+r^2}} = \sum_{p=0}^{\infty} r^p P_p(x)\,, \;\; r \prec 1 \tag{2.23}$$

By dividing the two parts of the generating function in Equation (2.23), the recurrent formula of the Legendre polynomials can be acquired straightforwardly:

$$\frac{d}{dr}\left(\frac{1}{\sqrt{1-2rx+r^2}}\right) = \frac{d}{dr}\left(\sum_{p=0}^{\infty} r^p P_p(x)\right)$$

$$\Leftrightarrow \;\; \frac{1}{\sqrt{1-2rx+r^2}} \times \frac{x-r}{1-2r+r^2} = \sum_{p=0}^{\infty} p r^{p-1} P_p(x)$$

Then we have:

$$(x-r)\sum_{p=0}^{\infty} r^p P_p(x) = (1-2rx+r^2)\sum_{p=0}^{\infty} p r^{p-1} P_p(x)$$

And, the recurrent formula of Legendre polynomials is:

$$\begin{cases} P_{p+1}(x) = \dfrac{2p+1}{p+1} x P_p(x) - \dfrac{p}{p+1} P_{p-1}(x) \\ P_1(x) = x, \;\; P_0(x) = 1 \end{cases} \tag{2.24}$$

The Legendre polynomials are a complete orthogonal basis set on the interval [-1, 1]:

$$\int_{-1}^{1} P_p(x)P_q(x)dx = \frac{2}{2p+1}\delta_{pq} \tag{2.25}$$

where,

$$\delta_{pq} = \begin{cases} 1 & if\ p = q \\ 0 & if\ p \neq q \end{cases}$$

is the Kronecker symbol.

The orthogonal property of Legendre polynomials implies no redundancy or overlapping of information between the moments with different orders. This property enables the contribution of each moment to be unique and independent from the information in an image [96].

To compute Legendre moments from a digital image, the integrals in Equation (2.20) are replaced by summations and the coordinates of the image must be normalized into [-1, 1]. Therefore, the numerical approximate form of Legendre moments, for a discrete image of $M \times N$ pixels with image intensity function $f(x, y)$, is [99]:

$$L_{pq} = \lambda_{pq} \sum_{i=0}^{M-1} \sum_{j=0}^{N-1} P_p(x_i)P_q(y_j)\, f(x_i, y_j) \tag{2.26}$$

where $\lambda_{pq} = \frac{(2p+1)(2q+1)}{M \times N}$, x_i and y_j denote the normalized pixel coordinates in the range of [-1, 1], which is given by:

$$x_i = \frac{2i-(M-1)}{M-1}, \qquad y_j = \frac{2i-(N-1)}{N-1} \tag{2.27}$$

The formula defined in Equation (2.20) is obtained by replacing the integrals in Equation (2.26) by summations and by normalizing the pixel coordinates of the image into the range of [-1, 1] using Equation (2.27).

Function LegendrePolinomials (x,p)
px=0;
for k=0 to p
if mod (p-k,2)=0
$c = \frac{(-1)^{\frac{p-k}{2}} x^k (p+k)!}{2^p k! \left(\frac{p-k}{2}\right)! \left(\frac{p+k}{2}\right)!}$;
px=px+c;
end if
end for
return px;

Function LegendreMoments (p,q)
L=0;
for i=0 to (M-1)
for j=0 to (N-1)
$x_i = \frac{2i-(M-1)}{M-1}$; $y_j = \frac{2j-(N-1)}{N-1}$;
px = LegendrePolinomials (x_i, p);
py = LegendrePolinomials (y_i, q);

*L = L + f(x_i, y_j) * px * py;*

end for

end for

return $\frac{L(2p+1)(2q+1)}{M \times N}$;

Figure 2.6 Pseudo code for Legendre Moments Computation [98].

Figure 2.6 shows the pseudo code for computing Legendre moments of order (p + q) by equation defined in Equation (2.26) and by using direct method for calculating Legendre polynomials [98]. In this work the recurrent formula is used for calculating Legendre polynomials in order to increase computation speed.

2.4.2 Zernike Moments

Teague [96] introduced the rotationally invariant Zernike moment, which employs the complex Zernike polynomials as the moment basis set. Zernike moments show the properties with no overlapping or redundancy of information between the moments of an image [100]. Zernike moments have been utilized as features set in many researches for that properties [101]. The three steps to compute the Zernike moments of an image are computation of (i) radial polynomials, (ii) Zernike polynomials, and at last (iii) Zernike moments by projecting the image onto the Zernike polynomials [98].

The first step to obtain Zernike moments from an image is the computation of radial polynomials. The real-valued radial polynomial is defined as:

$$R_{p,q}(r) = \sum_{s=0}^{(p-|q|/2} \frac{(-1)^s (p-s)!\, r^{p-2s}}{s!\left(\frac{p+|q|}{2}-s\right)!\,\left(\frac{p-|q|}{2}-s\right)!} \tag{2.28}$$

where $R_{p,q}(r) = R_{p,-q}(r)$ and p, q is order and repetition respectively. The order is non-negative integer and repetition is integer satisfying p - $|q|$ = *even* and $|q| \leq p$. The radial polynomials satisfy the orthogonal properties for the same repetition q.

$$\int_0^{2\pi}\int_0^1 R_{p,q}(r,\theta)R_{p',q}(r,\theta)\, r\, drd\theta = \frac{\delta_{pp'}}{2(p+1)} \tag{2.29}$$

The next step is to compute complex-valued 2-D Zernike polynomials within a unit circle using radial polynomial as:

$$V_{pq}(x,y) = V_{pq}(r\, sin\theta, r\, cos\theta) = R_{p,q}(r)e^{jq\theta} \tag{2.30}$$

where $j = \sqrt{-1}, |r| \leq 1$ is the length of complex-valued functions orthogonal on the unit circle $x^2 + y^2 \leq 1$.

$$\iint_{x^2+y^2\leq 1} [V_{nm}(x,y)]^*\ V_{pq}(x,y)dxdy = \frac{\pi\delta_{mp}\delta_{nq}}{m+1} \tag{2.31}$$

or, in polar coordinates:

$$\int_0^{2\pi}\int_0^1 [v_{nm}(r,\theta)]^*\, V_{pq}(r,\theta) r\, drd\theta = \frac{\pi\delta_{mp}\delta_{nq}}{m+1} \tag{2.32}$$

where the asterisk (*) denotes the complex conjugate. The last step is to compute complex Zernike moments of order p with repetition q for an image function $f(x; y)$ as:

$$Z_{pq} = \frac{p+1}{\pi} \iint_{x^2+y^2\leq 1} [V_{pq}(x,y)]^*\, f(x,y)\, dxdy \tag{2.33}$$

or, in polar coordinates:

$$Z_{pq} = \frac{p+1}{\pi} \int_0^{2\pi} \int_0^1 [V_{pq}(r,\theta)]^* \, f(r,\theta) r \, dr d\theta \tag{2.34}$$

To compute Zernike moments from a digital image, the integrals in Equation (2.33) and in Equation (2.34) are replaced by summations in addition to the coordinates of the image which must be normalized into [0, 1] by a mapping transform. The discrete form of the Zernike moments on an image of size $M \times N$ is expressed as:

$$Z_{pq} = \frac{p+1}{\lambda} \sum_{x=0}^{M-1} \sum_{y=0}^{N-1} [V_{pq}(x,y)]^* \, f(x,y) = \frac{p+1}{\lambda} \sum_{x=0}^{M-1} \sum_{y=0}^{N-1} R_{pq}(r_{xy}) \, e^{-jq\theta_{xy}} \, f(x,y) \tag{2.35}$$

where $0 \leq r_{xy} \leq 1$ and λ is a normalization factor. In the discrete implementation of Zernike moments, the normalization factor λ must be the number of pixels located in the unit circle by the mapping transformation and corresponds to the area of a unit circle π in the continuous domain. The transformed θ_{xy} phase and the distance r_{xy} at the pixel of coordinates (x, y) are given by:

$$\theta_{xy} = \tan^{-1}\left(\frac{(2y-(N-1))/(N-1)}{(2x-(M-1))/(M-1)}\right) \tag{2.36}$$

$$r_{xy} = \sqrt{\left(\frac{2x-(M-1)}{M-1}\right)^2 + \left(\frac{2y-(N-1)}{N-1}\right)^2} \tag{2.37}$$

Most of the computation time of Zernike moments is because of computation of radial polynomials. Therefore, researchers have proposed faster methods that reduce the

factorial terms by utilizing the recurrence relations on the radial polynomials. Prata et al. [94] proposed a recurrence relation that uses radial polynomials of lower order than p as follows:

$$R_{pq}(r) = \frac{2rp}{p+q} R_{(p-1)(q-1)}(r) - \frac{p-q}{p+q} R_{(p-2)q}(r) \tag{2.38}$$

Function RadialPolinomial (r,p,q)
radial=0;
for s=0 to (p-q)/2
$c = \frac{(-1)^s (p-s)!}{s!\left(\frac{p+|q|}{2}-s\right)!\left(\frac{p-|q|}{-2}-s\right)!}$;
radial=radial + c * r^{p-2s};
end for
return radial;

Function ZernikeMoments (p,q)
Zr=0; Zi=0;
for x=0 to (M-1)
for y=0 to (N-1)

$r = \sqrt{\left(\frac{2x-(M-1)}{M-1}\right)^2 + \left(\frac{2y-(N-1)}{N-1}\right)^2}$;

$\theta = \tan^{-1}\left(\frac{(2y-(N-1))/(N-1)}{(2x-(M-1))/(M-1)}\right)$;
if r ≤ 1
radial = RadialPolinomial (r, p, q);
$Zr = Zr + f(x,y) * radial * \cos(q * \theta)$;
$Zi = Zi + f(x,y) * radial * \sin(q * \theta)$;
count=count + 1;
end if

end for

end for

return $\frac{(p+1)(Zr+i*Zi)}{count}$;

Figure 2.7 Pseudo code for Zernike Moments Computation [98].

It is quite evident from the precedent equation that we can't compute all cases of p and q while computing the radial polynomials. It is not possible to use Prata's equation in cases where $q = 0$ and $p = q$. Those cases can be obtained by other methods. The direct method can be used in cases where $q = 0$, whereas the equation $R_{pp}(r) = r^p$ is used for $p = q$. The usage of direct method to compute radial polynomials in the case of $q = 0$ will considerably increase the computation time, especially when p is large. Figure 2.7 shows the pseudo code for computing Zernike moments of order p and repetition q by equations defined in Equation (2.28), (2.36) and (2.37) by using direct method for calculating Zernike radial polynomial [98].

2.5 Matching Measure

At first calculate the Euclidean distances between feature vectors for each gallery and probe for the subsequences with N_{gait} frames. There are different methods for matching measure. One of the first methods is the mean value of the minimum distances of the subsequences. The other second method is the median value of the minimum. Next is the minimum value of the minimum. In our case, we use the second method as it can overcome some effect of outlier.

Let $\{x_j^p\}$(j=1 to N_{gait}) and $\{x_k^g\}$(j=1 to N_{gait}) be the subsequences for the probe $\boldsymbol{x^p}$ and gallery $\boldsymbol{x^g}$ respectively. The Euclidean distance between probe and gallery is $d^{subs}(x^p, x^g)$ is the matching measure for the subsequences.

The median value of the minimum distances of the combinations of subsequences of each probe and gallery is defined as:

$$d^{Med}(x^p, x^g) = Median_j[\min_k\{d^{subs}(x_j^p, x_k^g)\}] \quad (2.39)$$

2.6 Conclusion

In this chapter explains overview of preprocessing, gait period estimation and different gait representation techniques and background knowledge that is used in different proposed methods in the following chapters of thesis. Out of the different gait representations, we proposed the EnDFT to highlight the dynamic areas of gait and useful for improving performance with clothing and carrying conditions. It is also explained principal component analysis and linear discriminant analysis for gait dimensionality reduction. Legendre moments and Zernike moments are used for effective parts selection adaptively for different covariate conditions. Matching measure is used for all experiments with k-nearest neighbors (k-NN) based classifier.

CHAPTER 3. PART DEFINITION AND EFFECTIVE PART SELECTION FOR PART-BASED GAIT IDENTIFICATION

3.1 Introduction

Gait identification is more difficult due to various covariate conditions such as clothing (changes different body parts on different cloth combination), carrying object (hand bag, backpack, briefcase, etc.), walking speed, viewing angle and different shoe-wearing [25, 65]. The study [102] showed that the results of statistical analysis and/or recognition rate are not significantly changed if a subset of the feature is used. So, the remaining features are redundant. They found that the upper body part contains the most important information for recognition. In another analysis, they suggested the lower body part (lower 30%) is significant for recognition. Generally different cofactors can affect different body parts and make further difficulties for gait identification. To overcome these difficulties, different part-based approaches have been proposed [25, 28, 62, 103]. However, there is no systematic study for dividing the body into different parts. Most of the techniques involved body parts based on anatomical knowledge some divided in some equal parts.

The main contribution of the proposed system is to define the parts of human gait automatically from a training data set depending the effectiveness of the covariate condition. The next step to select the most effective parts and discard the redundant part to overcome the difficulties arises in various cofactor conditions specifically for clothing and carrying conditions. The experimental result shows better performance for gait

identification. For dividing the body horizontally into different parts, we study the contribution of small segment of gait in terms of identification rate in training dataset. The smallest segment in this case is a row as a pixel has no effect for horizontal part selection.

3.2 Pre-processing and Feature Representation

The pre-processing including gait period estimation for the standard gait recognition is explained in Preprocessing section 2.1. The details of different gait feature representation techniques GEI, GEnI, DFT and EnDFT, and example images are presented in section 2.2.

3.3 Matching Measure

At first calculate the Euclidean distances between feature vectors for each gallery and probe for the subsequences with N_{gait} frames. There are different methods for matching measure. One of the first methods is the mean value of the minimum distances of the subsequences. The other second method is the median value of the minimum. Next is the minimum value of the minimum. In our case, we use the second method as it can overcome some effect of outlier.

Let $\{x_j^p\}$(j=1 *to* N_{gait}) and $\{x_k^g\}$(j=1 *to* N_{gait}) be the subsequences for the probe $\boldsymbol{x^p}$ and gallery $\boldsymbol{x^g}$ respectively. The Euclidean distance between probe and gallery is $d^{subs}(x^p, x^g)$ is the matching measure for the subsequences.

The median value of the minimum distances of the combinations of subsequences of each probe and gallery is defined as:

$$d^{Med}(x^p, x^g) = Median_j[\min_k\{d^{subs}(x_j^p, x_k^g)\}] \quad (3.1)$$

3.4 Human Gait Part Definition

The whole human body is divided into very small segments each of which is considered as a single row for part definition. We start from the bottom single row and measure rank - 1 recognition rate. Then each immediate upper single row is merged to form sub-segments and calculated the recognition rate in each step until the top row is reached. The training subset of the OU-ISIR Gait Database, the Treadmill Dataset B is divided into gallery and probe subset for finding the recognition rate. Gallery subset contains only the standard clothing type and probe subset consists with other clothing types. The effect of cumulative row-wise recognition rate is shown in **Algorithm 1**.

It is clear from the **Algorithm 1** that each row has either positive or negative effect in total recognition accuracy. From this observation, we can define the body parts based on the positive or negative contributions of the consecutive rows.

First local minima and maxima are explored from the row-wise recognition rate. The local minima correspond to the less effective and maxima corresponds more effective areas of the human body. The body areas containing local maxima contributed the most in gait recognition while the body areas consisting of local minima have less contribution. Therefore, human body can be divided into parts with some consecutive rows containing local minima and maxima. In one way, the local minimum and maximum bound the area of a part. The part consists of consecutive rows with either positive or negative contributions for row-wise recognition. In this case, the body parts can be mixed up with

static and dynamic area of the body that reduce the recognition accuracy. Another alternative is that the area of a part is bounded by the median between the maximum. The part may consist of consecutive rows with positive or negative contributions for row-wise recognition. The body parts correspond to the static and dynamic area without combining them together. The median balances the distribution between minimum and maximum that can reduce the outlier effect for a part. We follow the later technique here.

We start the curve from top row (maximum here) until a local minimum is found. After getting one local minimum, we find out median between maximum and minimum and divide the body here. We then search for another local maximum and calculate the median of the first minimum and second maximum and divide the body. Similarly, we search for every pair of adjacent local maximum and minimum, and divides the body at their median. We repeat this process until reaching to the bottom row. If the last minimum is the bottom, there is no division of the body. Following the procedure, human body is divided into five parts as shown in **Algorithm 1**.

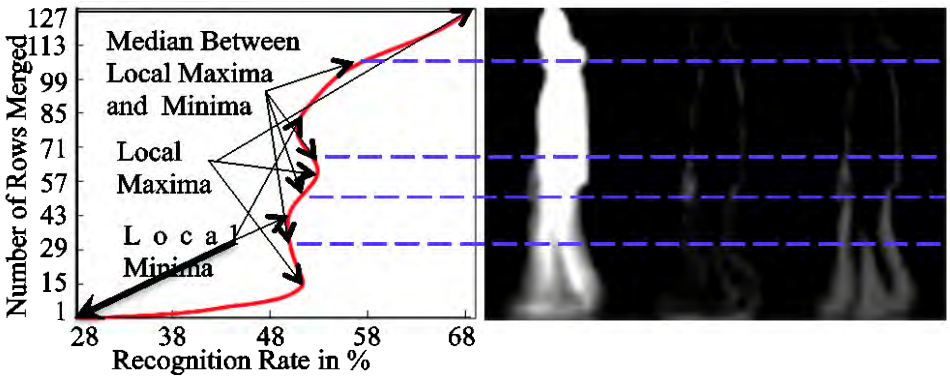

Figure 3.1 Recognition rate for each row merged form bottom to top.

The implementation algorithm is given in **Algorithm 1**.

Let $f(x)$ be the function representing the recognition rate in percentages. It can be defined as

$f(x) = f(P_k) =$ % of recognition rate

where P_k be sub-segments and k = 1, 2, 3, …, n.

The local maximum points of the function $f(x)$ can be written as:

$$\eta_{l\,max} = \begin{Bmatrix} \frac{\partial f(R)}{\partial R} = 0 \; and \; \frac{\partial^2 f(R)}{\partial R^2} < 0 \\ 0 \; otherwise \; (saddle \; points) \end{Bmatrix} \tag{3.2}$$

Similarly, the local minimum points of the function $f(R)$ can be written as:

$$\eta_{l\,max} = \begin{Bmatrix} \frac{\partial f(R)}{\partial R} = 0 \; and \; \frac{\partial^2 f(R)}{\partial R^2} > 0 \\ 0 \; otherwise \; (saddle \; points) \end{Bmatrix} \tag{3.3}$$

Algorithm 1

Algorithm INDEX-OF-MEDIAN takes a series F as input. It maintains three arrays LX[], LN[], and M[] to store indices of local maxima, local minima and median found in the series F and return M.

INDEX-OF-MEDIAN(F)

1. m=1 and n=1
2. For x=1 to length(F)
3. $F'(x) = F(x) - F(x-1)$
4. $F''(x) = F'(x) - F'(x-1)$
5. If $F'(x) = 0 \; and \; F''(x) < 0$
6. then LX[m]=x and m++
7. Else If $F'(x) = 0 \; and \; F''(x) > 0$
8. then LN[n]=x and n++
9. Else
10. It is a saddle point
11. End of for loop
12. M[1]=LN[1]
13. For j=2 to length(LX)
14. $\mathrm{M}[j] = \mathrm{MEDIAN}(F(\mathrm{LX}[j-1]) + F(LN[j]))$
15. End of for loop
16. Return M

3.4.1 Effective Part Selection

The body parts that include local minimum show negative effect in overall recognition rate and the parts that include local maximum have very good positive effect in overall recognition rate (the validity of effective parts selection is presented in section

4.5.2). Therefore, the parts that include local maximum are selected as effective parts and the parts that include local minimum are discarded as redundant parts empirically. Figure 3.2 shows the three effective parts (EP i) {i = 1, 2, 3} and two less effective body parts (LEPj) {j = 1, 2}.

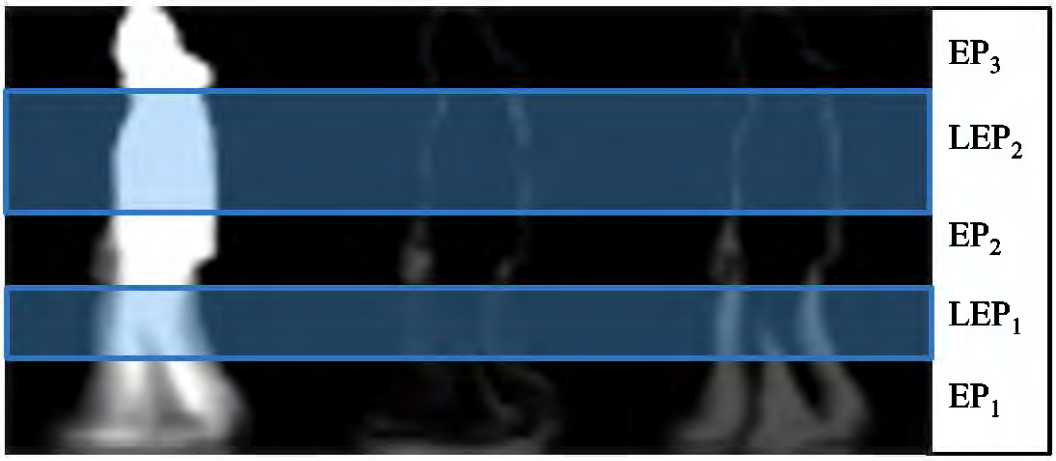

Figure 3.2 Selected Effective and Redundant (blue shaded) Parts.

3.5 Experiment

We use clothing invariant dataset to show the performance of the proposed effective part-based method although the system can be used in any kind variation like backpacks, shows etc.

3.5.1 Datasets

For effective part selection, we use OU-ISIR Gait Dataset B [23]. We used a training dataset containing 446 sequences of 20 subjects (10 males and 10 females) from the gait dataset. The sequences consist of different clothing types ranging from 15 to 28 for each subject.

For testing, we used a gallery set from the dataset consisting of the standard clothes sequences of 48 subjects, excluding the 20 training subjects. The probe set included 856 sequences for these 48 subjects with other clothes types, excluding the standard clothes.

3.5.2 Result Analysis

We compare the proposed method with whole-based i.e. effective-parts with redundant parts, eight part-based method without weight control and component-based method. The result shows Figure 3.3 as CMC curve. The effective parts-based method outperforms the other methods with reduced features.

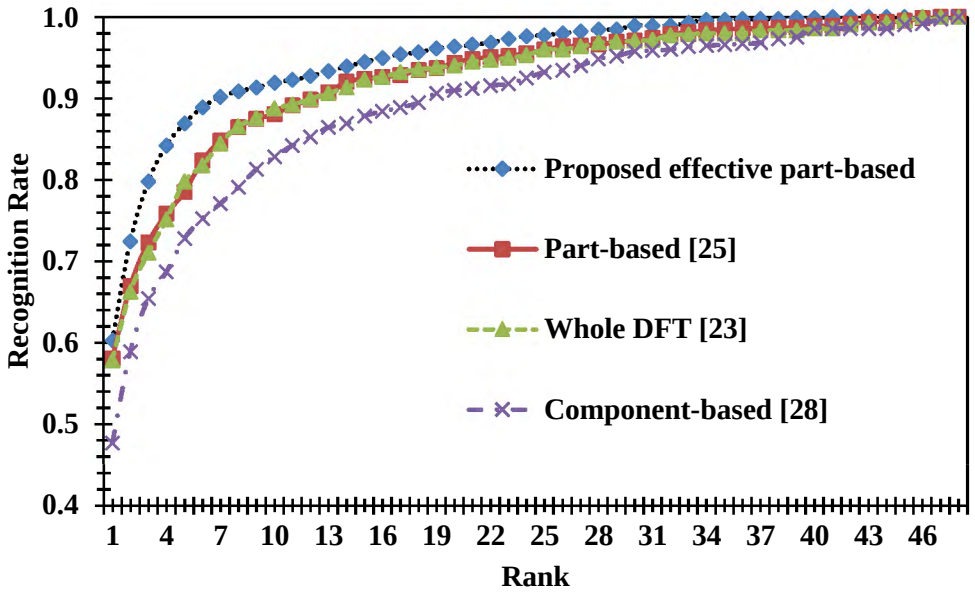

Figure 3.3 Cumulative Matching Curve (CMC) for proposed method.

3.6 Conclusion

We study the contributions of very small segment in term recognition rate for dividing the body into different parts. Based on local maxima and minima human body is

divided into five unequal parts. Then depending on the positive or negative effect three parts are selected as effective parts and other two parts discarded as redundant for gait recognition. Experimental result shows promising performance in comparison with other part-based methods.

CHAPTER 4. EFFECTIVE PART-BASED GAIT IDENTIFICATION USING FREQUENCY-DOMAIN GAIT ENTROPY FEATURES

4.1 Introduction

The aim of this study is to develop robust gait recognition technique which can accept huge clothing and carrying changes. Gait identification task becomes more difficult due to the change of appearance by different cofactors (e.g., shoe, surface, carrying, view, and clothing). The cofactors may affect some parts of gait while other parts remain unchanged and can be used for recognition. From our point of view, there are two important ways to improve the recognition accuracy in case of different cofactors like clothing, carrying objects, etc. are as following:

1. For selecting the appropriate parts, more affected and less affected body parts should be considered.
2. Gait features should be represented with the most discriminating information.

From these observations, we propose a robust technique to define which parts are more effective or less affected by cofactors and which parts are less effective or mostly affected by cofactors like clothing, carrying objects etc. To find out the effective body parts, the whole body is divided into small segments where each segment is a single row [104]. Based on positive and negative effect of each segment, three most effective parts and two less effective parts are defined. Usually, the dynamic areas (e.g., legs, arms swing)

are comparatively less affected than static areas (e.g., torso) by different cofactors in appearance-based gait representation. To give more emphasis on dynamic areas and less on static areas, we also propose the DFT based frequency-domain gait entropy termed as EnDFT representation which is computed from frequency domain gait representation.

We use the three most effective body parts with the entropy-based gait representation for gait recognition and totally discard the two less effective parts. Experiments are conducted on two comprehensive benchmarking databases: The OU-ISIR Gait Database, the Treadmill dataset B [23] with clothing variations and CASIA Gait Database, Dataset B [24] with clothing and carrying conditions. Experimental results show better performance compared with the others part-based and whole-based approaches.

4.2 Pre-processing and Feature Representation

The pre-processing including gait period estimation for the standard gait recognition is explained in section 2.1. The different gait feature representation techniques GEI, GEnI, DFT and EnDFT and example images are presented in section 2.2.

4.3 Part Definition and Effective Part Selection

Based on the recognition accuracy of each row of DFT gait features, Rokanujjaman et al. [104] defined three effective parts and two less effective parts and preliminary results are reported. For part definition and selection, the training subset of the OU-ISIR gait database, Treadmill dataset B [23] is used. The effectiveness of the proposed method was shown using the same database. The whole procedure of part definition and effective part selection is discussed in section 3.4.

4.4 Effective Part-based Features Extraction and Classification

From the five parts of the human body when two parts are discarded dimension of the data is automatically reduced. Principal component analysis (PCA) is applied to each effective part for further reduction of the dimension. The dimension reduced features are used for gait identification.

4.4.1 Effective part-based dimension reduced gait features

The dimension of the represented gait features is usually higher than training data. The statistical dimension reduced approach such as PCA, linear discriminant analysis (LDA) [105] only preserves the features, which contribute the most.

The part selection method (discussed in section 3.4) defined two less effective body parts. These parts may change frequently due to different cofactors, in particular, some challenging cofactors such as clothing variations and carrying objects. Discarding these two less effective body parts, it is possible to reduce the dimension of the gait features as well as increase the recognition performance. The system can reduce 47 % dimension by discarding the two less effective body parts as redundant. Therefore, it can be a considerable technique for representing the gait features in lower dimensional space.

Each of these three effective parts is trained individually in the PCA and LDA subspace using the proposed EnDFT features to further reduction of the dimension. The dimension-reduced gait features are used for part-based gait identification.

4.4.2 Effective part-based classification

Let a probe sequence P with m subsequences Pr $\{r = 1, .., m\}$ and a gallery sequence G with n subsequences G_s $\{s = 1, ..., n\}$. The matching measure for the subsequences is simply chosen as the Euclidean distance between P_r and G_s (let $d^{sub}(P_r, G_s)$). First, we compute the minimum distances for each of the probe subsequence P_r to a gallery sequence G is defined with i^{th} body part as:

$$d_i^{sub}(P_r, G) = \min_s \left[d_i^{sub}(P_r, G_s \right] \tag{4.1}$$

Then, we compute the median of the minimum distances for each of the probe subsequence P_r as the distance between a probe P and a gallery G sequence is defined as:

$$D_i(P, G) = \operatorname{median}_r \left[d_i^{sub}(P_r, G) \right] \tag{4.2}$$

4.5 Experimental Result and Discussion

This section shows experimental results using different datasets. The experimental results show the effectiveness of the effective and less effective body parts for human gait recognition using proposed EnDFT features.

4.5.1 Datasets

We have used two benchmarking gait datasets: the OU-ISIR Gait Database, the treadmill dataset B [23] and CASIA Gait Database, dataset B [24] to evaluate the performance of the proposed approach against the clothing and carrying object cofactors.

4.5.1.1 The OU-ISIR Gait Database, the Treadmill Dataset B

This dataset was chosen due to its largest clothing variations. Considering one of the most challenging cofactors: clothing, recent work [23] created the OU-ISIR Gait Database, the Treadmill Dataset B with large clothing variations. It includes 68 subjects with at most 32 combinations of different types of clothing such as skirt, raincoat, down jacket, long coat, hat, parker, muffler, short pants, casual wears, regular pants, half shirt, full shirt etc. The whole dataset is divided into three subsets: training set, gallery set and probe set. In training set there are 446 sequences of 20 subjects (10 males and 10 females) with the range of 15 to 28 different combinations of clothing. The testing set (gallery and probe sets) consists of other sequences of the rest 48 subjects excluding the 20 training subjects. Gallery set containing only standard clothing type, i.e., regular pant and full shirt of 48 subjects. Probe set containing 856 sequences of these 48 subjects considering all types of different clothing combinations excluding the standard one type.

4.5.1.2 CASIA Gait Database, Dataset B

This dataset was chosen due to its subject diversity with multiple sequences with clothing and carrying object cofactors. More specifically, this dataset comprises three cofactors normal walking sequences, carrying objects (i.e., carrying a bag) and only one clothing type (i.e., wear a bulky coat). There are total 124 subjects and each subject contain 10 walking sequences. Based on the three cofactors the whole dataset is divided into three subsets. CASIASetA consists of six normal walking sequences where the subject does not carry a bag or wear a bulky coat. CASIASetB consists of two carrying-bag sequences and set CASIASetC consists of two wearing-coat sequences. The gallery set is constructed by

taking the first four sequences of each subject in CASIASetA (CASIASetA1). The probe set is the rest two sequences in CASIASetA (CASIASetA2), two sequences in CASIASetB and two sequences in CASIASetC. The gallery set is used as training set for CASIA Gait Database, Dataset B.

Although we notice that the USF HumanID Gait Challenge Dataset [88] is also one of well-known benchmarking gait databases, we did not include it in our experiments due to smaller clothing variations than those with the OU-ISIR Gait Database, the Treadmill Dataset B [23], and the smaller number of sequences per subject per cofactor than that of CASIA Gait Database, Dataset B [24].

4.5.2 Experimental validation of three effective parts

The human body is divided into five parts: three effective parts *(EP i)* $\{i = 1, 2, 3\}$ and two less effective parts *(LEPj)* $\{j = 1, 2\}$. Figure 4.1 shows the recognition rate for each individual part separately. The consecutive merging or discarding effect of the effective and less effective parts is shown in Figure 4.2.

It is observed from Figure 4.2 that when each of the three effective parts are combined then the recognition rate is increased dramatically and when each of the two less effective parts are combined with the other effective parts cumulatively then the recognition rate are decreased. Although the recognition rates of some effective parts are lower than the less effective parts, the combined performance of effective part is better. The reason is that the less effective parts recognize the similar subjects where the effective parts can recognize different individual with cofactors.

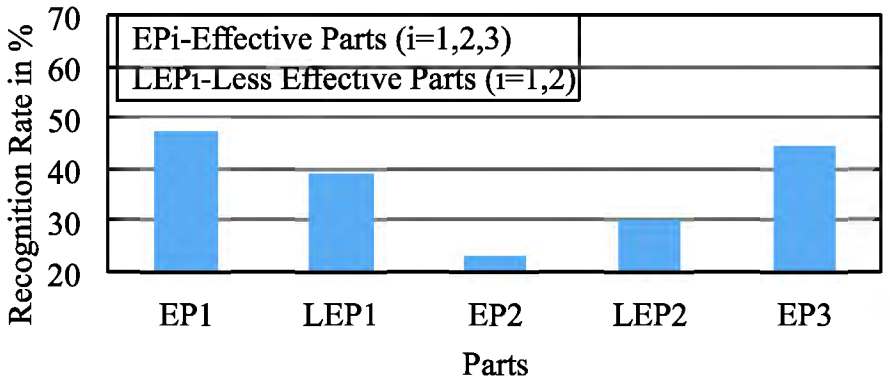

Figure 4.1 Part-wise recognition rate.

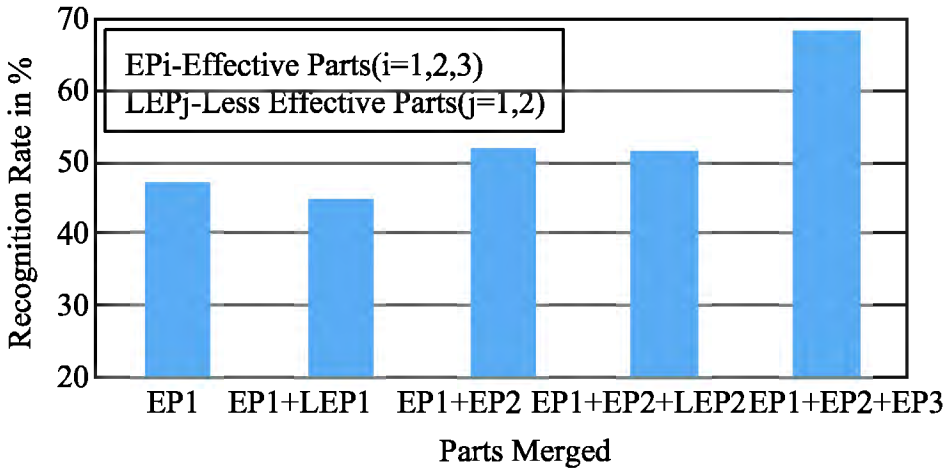

Figure 4.2 Combining effect of the effective and less effective parts in overall recognition.

4.5.3 Effective parts on different gait representations

To show the further effectiveness of the proposed parts definition, we perform experiment for different gait representation techniques separately on both the OU-ISIR Gait Database, the Treadmill Dataset B and CASIA Gait Database, Dataset B. The Cumulative Matching Curve (CMC) of Figure 4.3 shows the comparison of the whole-based and the effective part-based recognition rate for different gait representation

techniques using the OU-ISIR Gait Database, the Treadmill Dataset B. On the other hand, Figure 4.4 shows the CMC curves comparing the whole-based and the effective part-based recognition rate for different gait representation techniques using CASIA Gait Database, Dataset B. Table I shows the rank - 1 recognition rate for the whole-based and the effective part-based methods using all representations. It also shows the reported result of the popular methods [24, 51, 65] using the CASIA Gait Database, Dataset B.

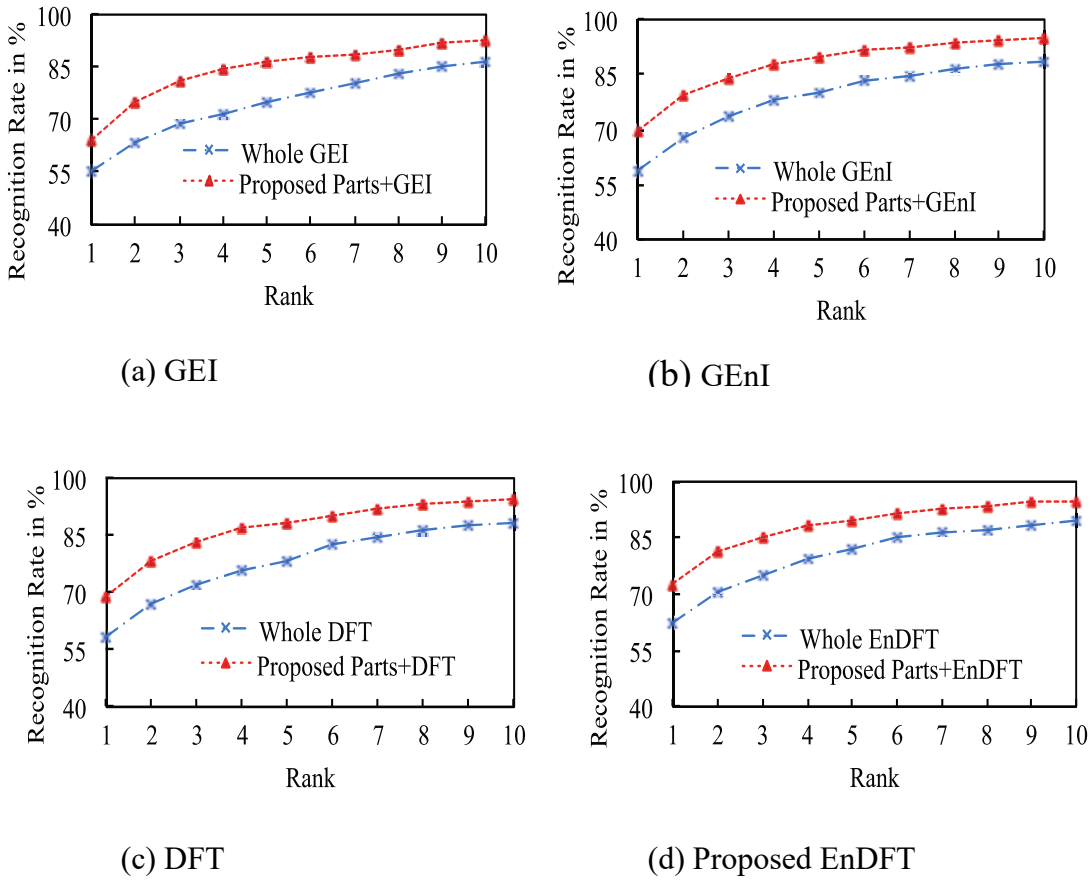

Figure 4.3 Comparison of the proposed effective part-based with whole-based methods using different gait representations (i.e., GEI, DFT, GEnI and proposed EnDFT) in the OU-ISIR Gait Database, the Treadmill Dataset B.

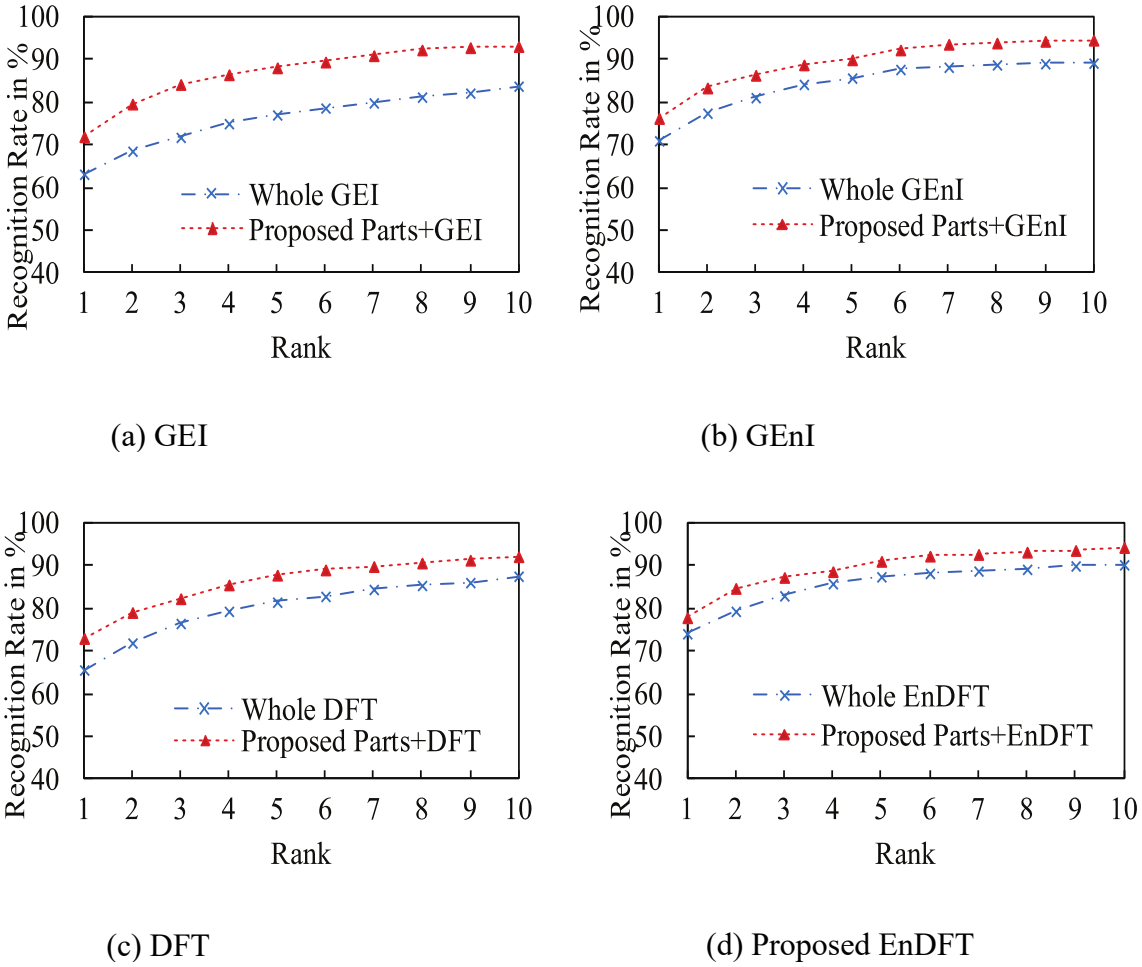

Figure 4.4 Comparison of proposed effective part-based with whole based methods using the different gait representations (i.e., GEI, DFT, GEnI and Proposed EnDFT) in CASIA Gait Database, Dataset B.

It is obvious that the proposed effective part-based method produces always better results than other whole-based methods in all of the reported gait representation techniques for the OU-ISIR Gait Database, the Treadmill Dataset B and the whole CASIA Gait Database, Dataset B datasets except for the subset of CASIA dataset CASIASet2 (Table 4.1).

Table 4.1 Comparison of proposed effective part-based with whole based methods using different gait representation.

Methods / Datasets	OU-ISIR	CASIA Set A2	CASIA Set B	CASIA Set C
Yu et al. [24] (%)	--	97.60	52.00	32.70
Han et al. [51] (%)	--	99.40	60.20	30.00
Bashir et al. [65] (%)	--	100.00	78.30	44.40
Whole GEI (%)	55.25	99.04	60.08	30.24
Whole DFT (%)	58.06	99.04	64.92	32.66
Whole GEnI (%)	58.87	98.56	80.64	33.47
Whole proposed EnDFT (%)	62.15	98.56	83.87	39.51
Proposed Parts+GEI (%)	64.01	98.56	75.00	41.93
Proposed Parts+DFT (%)	68.49	96.65	79.03	42.74
Proposed Parts+GEnI (%)	69.62	97.61	83.46	47.17
Proposed Parts+Proposed EnDFT (%)	72.90	97.61	83.87	51.61

4.5.4 Effect of frequency domain gait entropy features

The proposed frequency domain gait entropy features (EnDFT) are compared with three others gait representations GEI, DFT, and GEnI in both the OU-ISIR Gait Database, the Treadmill Dataset B and CASIA Gait Database, Dataset B (CASIASetA2, CASIASetB, CASIASetC) datasets (Figure 4.5). The EnDFT gait features show much better

performance in all datasets except CASIAsetA2. The EnDFT highlights the most discriminative dynamic areas while minimizing the effect of the static areas. It was also reported in [73] that static areas can be over-fitted when the appearance is significantly changed by clothing and carrying cofactors.

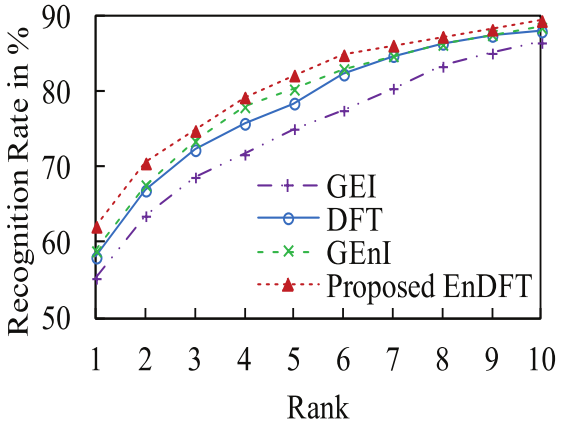

(a) Whole-based methods on the OU-ISIR Gait Database, the Treadmill Dataset B

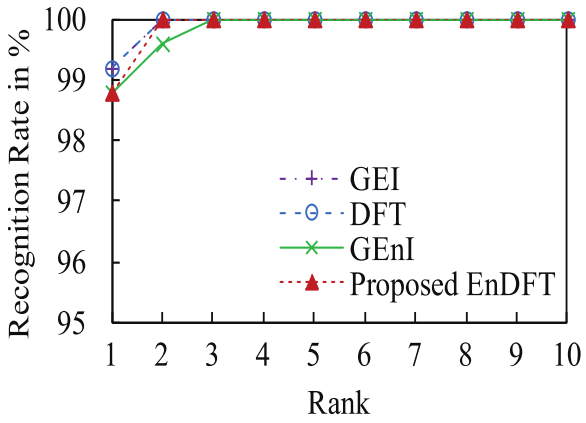

(b) Whole-based methods on CASIASetA2

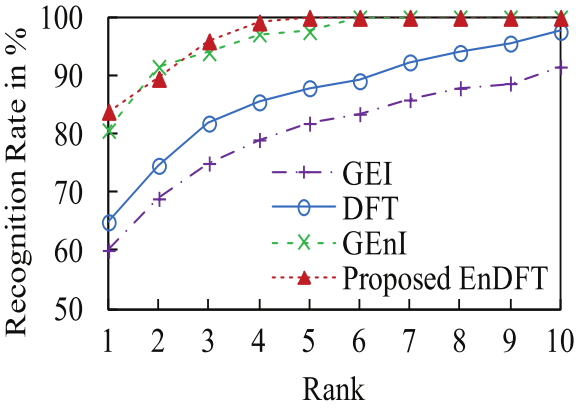

(c) Whole-based methods on CASIASetB

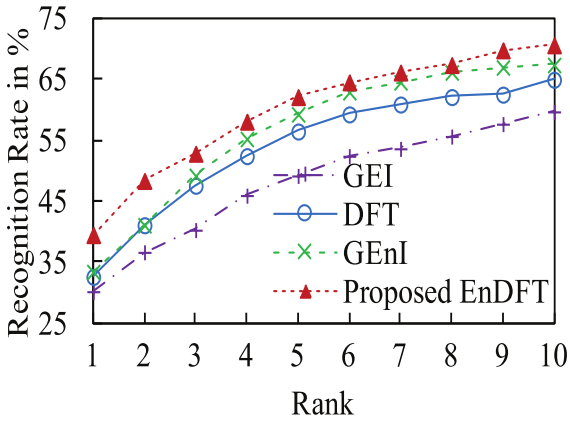

(d) Whole-based methods on CASIASetC

Figure 4.5 Whole-based methods comparison using proposed EnDFT representation with other existing representations (GEI, GEnI and DFT) in both datasets (the OU-ISIR Gait Database, the Treadmill Dataset B and CASIA Gait Database, Dataset B).

4.5.5 Effective parts with EnDFT feature on clothing complexity

To find out the complexity of individual clothing of the OU-ISIR Gait Database, the Treadmill Dataset B, the training set is divided into two subsets: gallery with standard clothing and probe contains the rest clothing types. We compute the recognition rate for all clothing types and arrange them in descending order as shown in Figure 4.6. Figure 4.7 shows the sample images according the sorted clothing types with gallery.

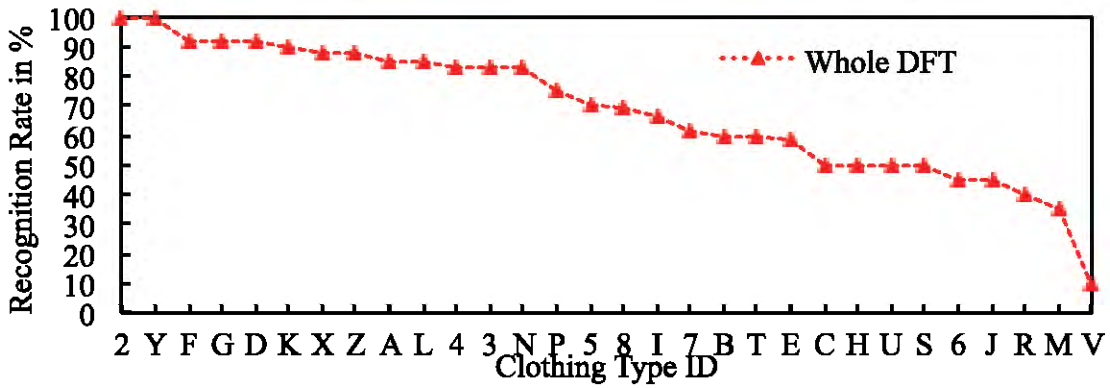

Figure 4.6 Sorted clothing types according to recognition rate.

Clothing types that are similar with gallery gives better recognition rate. On the other hand, recognition rate decreases for dissimilar clothing types. It is observed in Figure 4.6 and Figure 4.7, that the recognition rate decreases with increasing the clothing complexity. For analyzing the clothing complexity and the effect of the proposed system, we make three groups of all the clothing types using k-means clustering techniques. The training probe subset is used here. Table 4.2 shows the three clusters with clothing Ids and cluster 1 to cluster 3 are arranged from simple to complex clothing types. To evaluate the performance, we compare the proposed system with the system using whole DFT and EnDFT features for the test dataset. Figure 4.8 shows the comparison results.

Table 4.2 Clothing clusters.

Cluster ID	Clothing IDs	Percentages of clothing types
Cluster 1	Y,X,Z	10.00 %
Cluster 2	2,F,G,D,K,A,L,4,3,N,P, 5,8,I,7,T,E,U,S,6,J,R	73.33 %
Cluster 3	H,B,M,C,V	16.67 %

For relatively simple clothing types, whole-based methods are slightly better for recognition than the proposed method. However, for complex clothing types in cluster 2 and cluster 3, the performance of the proposed method is much better than whole-based methods. It is noticeable that cluster 1 contains only 10 % of the clothing types and the performance of the proposed part-based EnDFT method is increasing with the increases of clothing complexity. Thus, it is validated that the proposed features can represent the gait with the most discrimination capability and the effective parts selection enhance the recognition rate with reduced data. It is also supported by the result shown in Table 4.1 that the proposed system outperforms in clothing and carrying conditions for CASIA Gait Database, Dataset B [24].

4.5.6 Comparisons with other methods

The performance of the proposed effective parts with EnDFT features based method is compared with four widely used whole-based methods [51, 71, 72, 73] and one part-based methods [25]. The whole-based methods [72] used GEI and [71] used frequency domain FFT gait features that are dimension reduced by the PCA.

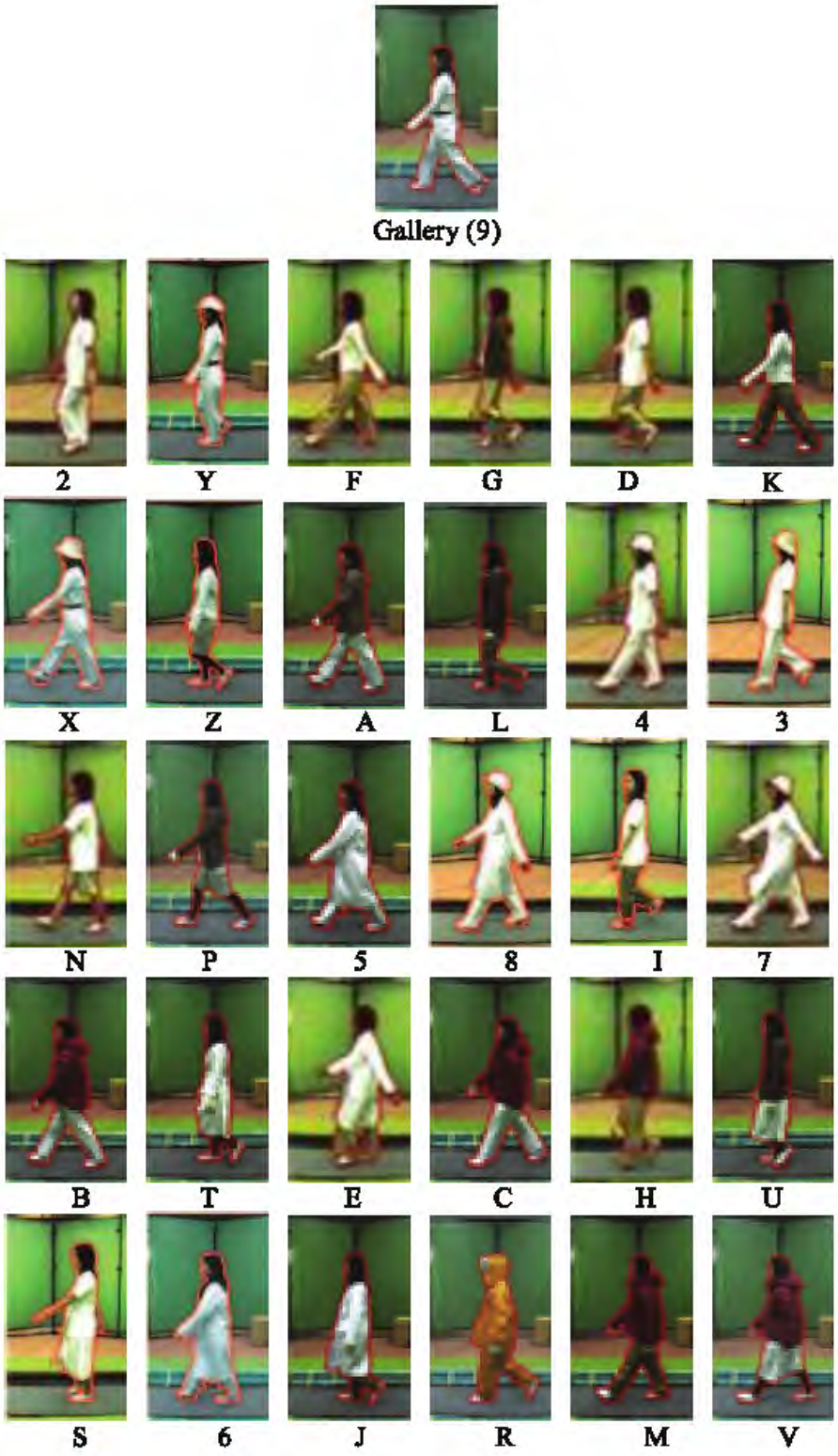

Figure 4.7 Sample clothing images [25] of the OU-ISIR Gait Database, the Treadmill Dataset B according to sorted ID and clothing complexity.

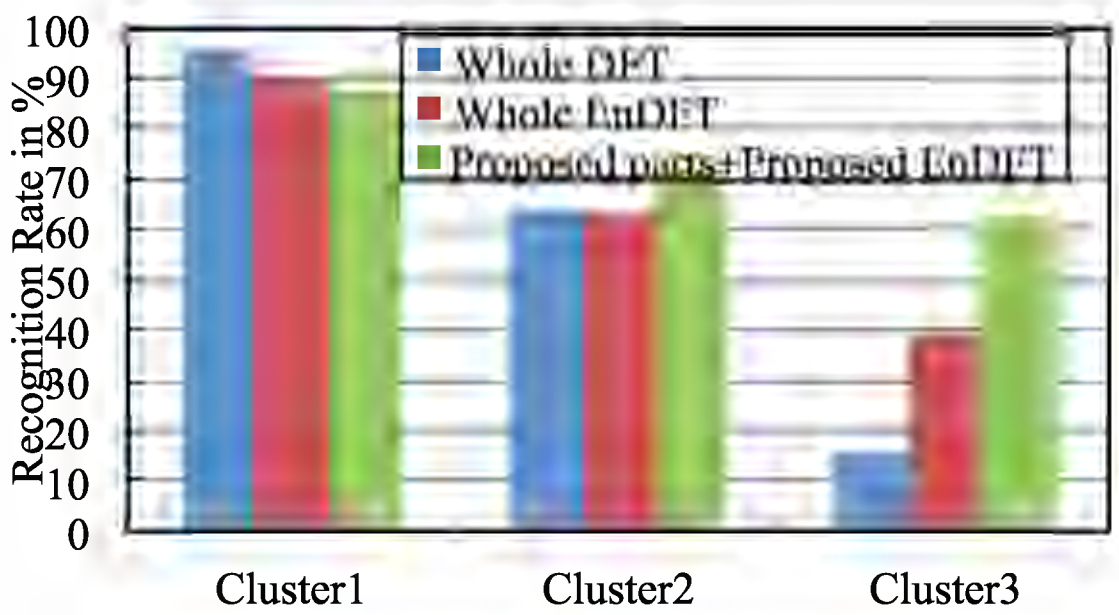

Figure 4.8 Comparison of cluster-wise recognition rate.

The LDA based methods [51] and [73] used GEI and GEnI gait features respectively. In the LDA based methods, we have used the training set for both datasets in the training stage where first the dimensions are reduced by PCA, and then LDA is applied. The part-based method [25] defined eight parts: four consecutive parts and four overlapping parts based on anatomical statistics on DFT gait features. The performance is evaluated using these eight parts without adaptive weighting.

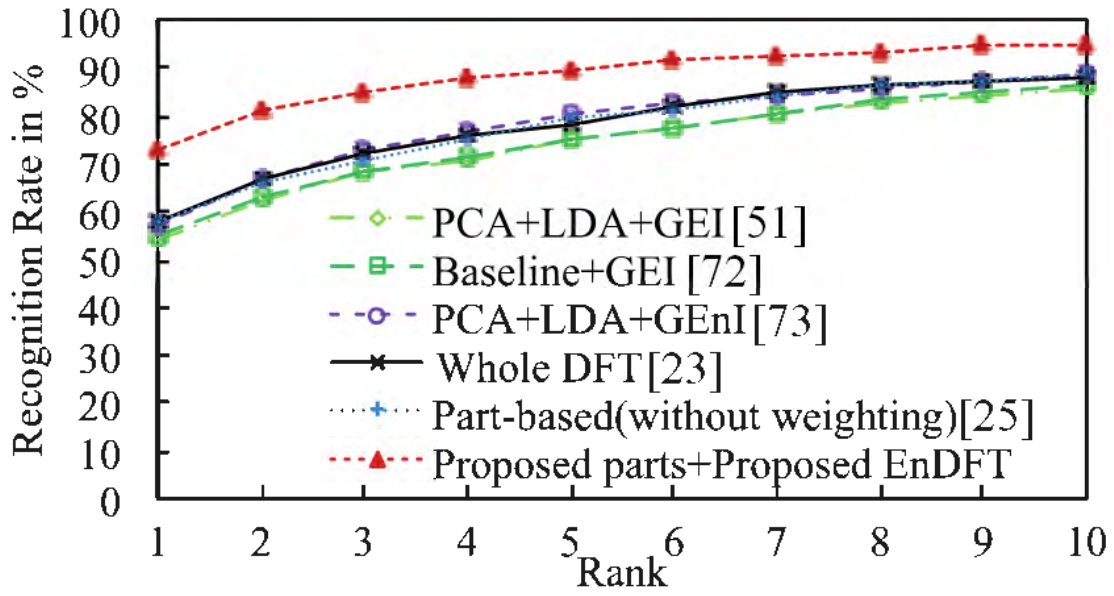

Figure 4.9 Comparison with other methods on the OU-ISIR Gait Database, the Treadmill Dataset B.

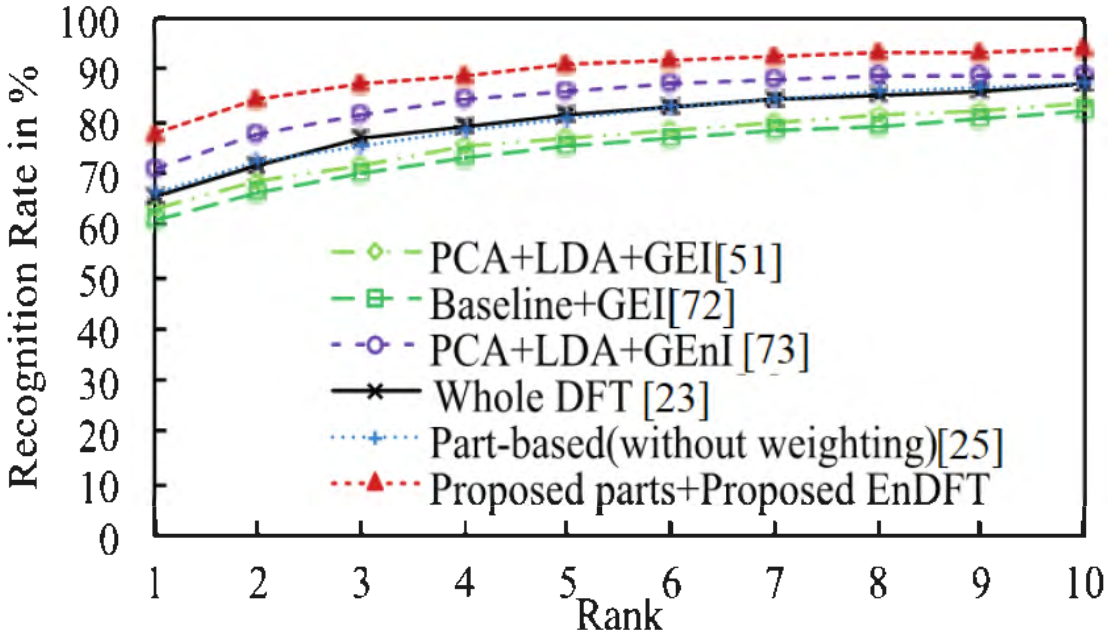

Figure 4.10 Comparison with other method on CASIA Gait Database, Dataset B.

4.5.7 Discussion

The main contribution is to define the effective body parts definition with proposed frequency domain-based entropy gait features (EnDFT). The comparison results are shown in Figure 4.3 to Figure 4.5.

The proposed method is always showing better performance for both the OUISIR Gait Database, the Treadmill Dataset B and CASIA Gait Database, Dataset B datasets. The experimental results are summarized in Table 4.1. The results clearly show that the proposed EnDFT based gait features produced better performance in comparison with others reported representation techniques. The proposed effective parts definition show much better result than whole-based representation on all of the gait representation techniques especially for the new proposed gait representation techniques (EnDFT).

The proposed effective parts definition is very much effective in the presence of significant change of appearance due to challenging clothing cofactors on the both datasets. One interesting observation is that discarding the two less effective body parts i.e., using the three effective body parts with the EnDFT gait features is still give the same result as for the whole based representation in presence of carrying-bag conditions for CASIASetB dataset. Another observation is that in case of the OU-ISIR Gait Database, the Treadmill Dataset B (Figure 4.8) and CASIASetA2 dataset (Table 4.1) where normal clothing are used the whole based representation gives slightly better result than effective part-based method although the result is comparable. However, in real application, we cannot always expect uniform normal clothing. The performance of the proposed part-based EnDFT method increases with the increases of the clothing complexity (Figure 4.8).

4.6 Conclusion

We propose the effective part-based gait identification using frequency domain-based gait entropy features (EnDFT). To find out the effective body parts, we have proposed a more robust technique by dividing the whole body into small segments where each segment is a single row in this paper. Based on positive and negative effect of each segment, three effective parts and two less effective parts are defined. We have also investigated different gait representation techniques and the proposed a new frequency domain-based gait entropy features EnDFT. The proposed method outperforms other classical gait recognition algorithms and representation techniques in both the OU-ISIR Gait Database, the Treadmill Dataset B and CASIA Gait Database, Dataset B datasets.

Since our part definition and effective part selection method is applicable to any types of the gait features which are represented as a set of point statistics (e.g., gait flow image [74], chrono-gait image [56], Masked-GEI [65]) without any changes.

CHAPTER 5. PART-BASED SPEED INVARIANT HUMAN GAIT IDENTIFICATION

5.1 Introduction

This chapter proposes a novel method that can reduce the intra-class difference that creates by walking speed changes. Gait is an effective behavioral biometric signature to recognize a person at a remote with low quality image sequence of non-cooperative person by inspecting their walking pattern. Among many cofactors, person's walking speed variations due to different situation is one of the challenging artifacts that alters the gait pattern and reduce the recognition rate. The intra-class difference gradually rises by the person's walking speed variation from slower to faster. If the training data set is small, then it fails to model the intra-class variations. Therefore, the performance degraded severely of the gait identification systems. The situation when some portion of human body affects due to speed changes, it is possible to recognize the person by considering the less affected body parts by neglecting parts that are more affected.

Our objective is to design a robust model free approach for the gait recognition problem where the gait contaminated with cofactor of large walking speed changes. In this work, we reduce the effect of walking speed changes which affects the dynamic parts of gait by defining the gaits into six unequal parts and selecting the more effective parts using a lookup table dynamically. We minimize the intra-class variation by eliminating the more affected body parts depending the speed differences of gallery-probe pair, and thus increase the recognition rates.

Experiments on largest walking speed variation OU-ISIR Treadmill Database A [29] and CASIA database C [30] is used to show the robustness, efficiency and performance of the proposed method. Our experimental results have also indicated that the proposed lookup table based effective part selection method outperforms the state-of-the-arts for cross speed gait recognition.

5.2 Gait speed estimation and representation

The publicly available popular large speed changes OU-ISIR dataset A [29] is frame size of 640 × 480 pixels and captured at 60 frames/second and the CASIA dataset C at 25 frames/second of 240 × 320 pixels. Most of the literature of appearance-based approaches use silhouettes to represent the gait features. The first step is to extract human silhouettes by subtracting of earlier modelled background from the video frames. Each silhouette size is normalized into fixed size 128 × 88 pixels and registered based on the extracted regions height, and centre to find gait silhouette volume (GSV) [63]. We detect gait period N_{gait} by maximizing the autocorrelation from the size normalized and registered silhouettes as describe in section 2.1. Gait Energy Image (GEI) feature is used for walking speed estimation, part definition and selection because both the non-stationary parts (i.e. hands and legs) and stationary parts (head and torso) of the gait are clear in these features.

5.2.1 Gait Representation

The detail of Gait Energy Image (GEI) and Discrete Fourier Transform (DFT) gait representation is discussed in section 2.2.1. The images of these representation with different walking speed from the two datasets are shown in Figure 5.1.

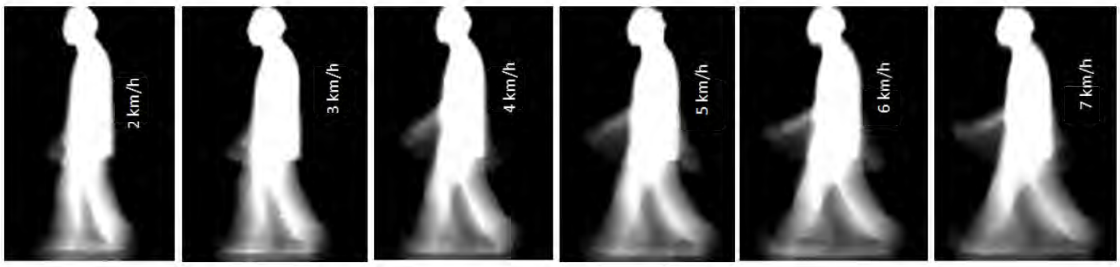

(a)

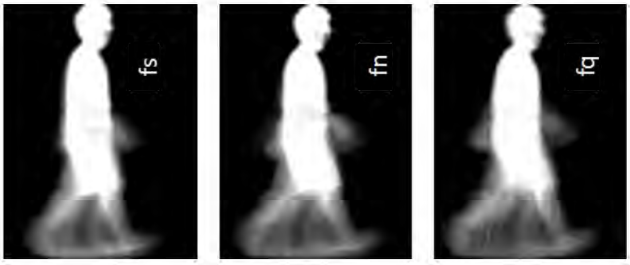

(b)

Figure 5.1 GEI representation of different speeds (a) OU-ISIR database A and (b) CASIA database C.

5.2.2 Walking Speed Estimation

Walking speed estimation of unknown gaits are done by using classifier from the training set that contains the different known walking speed of gaits. The unit of walking speed is km/h. The total number of silhouettes in a single gait period may vary with speed changes. The average number of silhouettes per gait period and elapsed time is estimated from the training set of different speeds is represented in Table 5.1. The Table 5.1 clearly shows that the total number of silhouettes increases with speed changes from faster to slower. The CASIA dataset C has recorded at 25 f/s and treadmill dataset OU-ISIR set A at 60 f/s. The elapsed time for a gait period is calculated as [82] by utilizing earlier known and estimated information of the datasets as:

$$\text{Time} = \frac{\text{N}_{\text{frame}}/\text{gait period}}{\text{frame rate}} \text{ in second} \tag{5.1}$$

The CASIA does not mention any absolute walking speed for their dataset. It contains three dissimilar walking speed as fq for quick, fn for normal and fs for slow. By using the elapsed time of a gait period and compare with the information estimated for OU-ISIR dataset, we could find the approximated walking speed of fs, fn and fq are 4 km/h, 5 km/h and 7 km/h respectively.

Table 5.1 Estimation of number of frames and elapsed time of a gait period of different speeds.

OU-ISIR Gait Dtatbase A			**CASIA Gait Database C**		
Speed (km/h)	**N_{frame}/gait period**	**Time (second)**	**Speed**	**N_{frame}/gait period**	**Time (second)**
2	88	1.47	fs	29	1.16
3	75	1.25	fn	26	1.04
4	69	1.15	fq	23	0.90
5	63	1.05			
6	59	0.98			
7	55	0.92			

5.3 Classification

The gallery set has *c* subjects or classes and has N_{gait} sub-sequences of each gait sequence. For matching criterion, the Euclidean distance is used. It is assumed that x_k^g with k=1 to N_{gait} and x_j^p with j=1 to N_{gait} are the sub-sequences for the gallery $\boldsymbol{x^g}$ and the probe $\boldsymbol{x^p}$ gait sequences. The Euclidean distances $d^{subs}(x^p, x^g)$ are computed among probe and gallery for N_{gait} sub-sequences as follows:

$$d^{subs}(x^p, x^g) = \left\| x_j^p - x_k^g \right\| \tag{5.2}$$

As [13], the median value of the minimum distances of the combinations of sub-sequences of each probe and gallery is defined as:

$$d^{median}(x^p, x^g) = median_j[\min_k\{d^{subs}(x^p, x^g)\}] \tag{5.3}$$

Then we select the minimum distance for a probe to all *c* subjects of the gallery as follows:

$$D^{min} = min_{g=1}^{c} d^{median}(x^p, x^g) \tag{5.4}$$

5.4 Human body Parts Division and Selection

To reduce intra-class difference and determine the discriminate feature for improving the recognition performance we will divide the human body parts [93]. Experimentally dividing the human body row wise into several sections, we measure the impact of minor section here a single row as recognition rate of the training set. The training set of OU-ISIR database A [29] is utilized for human body division horizontally and selection the more effective parts.

5.4.1 Parts Division

Stepwise recognition rate is measured from the top row of GEI, combine immediate next lower single row in each step, and continue the procedure until reach the bottom row. The recognition rate in percentage for each step beside the GEI is shown in Figure 5.2. From this Figure, some steps the recognition rate increases (positive contribution) and

some steps the rate decreases (negative contribution). Considering the states of contributions, we can divide the human gait in to some unequal parts.

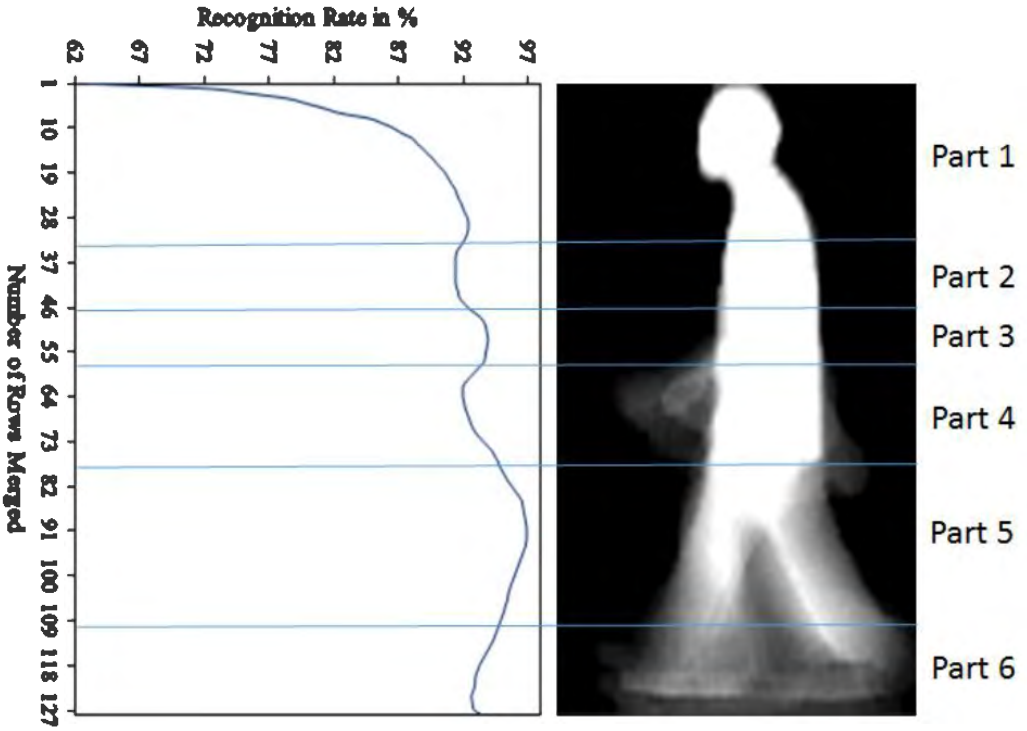

Figure 5.2 Human gait unequal parts division [93].

We examine the curve in Figure 5.2, from top row (here local minima) until local maxima is obtained. After the first local maxima, we again traverse for next local minima, calculate the average among the initial local maxima and local minima and find out the position of the average value to divide the body there. Again, search for another local maxima, compute the average value with the previous local minima, find out the position as before and divide the body there. We will continue this process until we reach the bottom of the GEI. After completing the procedure, the human gait is unequally partitioned into six different parts (Figure 5.2). The steps of implementation are presented in **Algorithm 1**.

Table 5.2 Different combination of parts (1-6) with cross speed recognition rate within bracket (%) [93].

Probe / Gallery	2km/h	3 km/h	4 km/h	5 km/h	6 km/h	7 km/h
2 km/h	1, 2, 3, 4, 5, 6 (100%) 1, 2, 3 (100%)	1, 2, 3, 5, 6 (100%) 1, 2 (100%)	1, 2, 3 (94.4%) 1, 2 (94.4%)	1 (94.4%)	1 (83.3%)	1 (72.2%)
3 km/h	1, 2, 3, 5 (100%) 1, 2, 3 (100%) 1, 2 (100%)	1, 2, 3, 4, 5, 6 (100%) 1, 2 (100%)	1, 2, 3, 4, 5, 6 (94.4%) 1, 2, 3 (94.4%) 1, 3, 6 (94.4%) 1, 2 (94.4%)	1, 2, 5 (83.3%) 1, 2 (83.3%)	1 (83.3%)	1 (72.2%)
4 km/h	1, 2, 3, 6 (94.4%) 1, 2, 3 (94.4%) 1, 2 (94.4%)	1, 3, 6 (83.3%) 1, 3 (83.3%)	1, 3, 4, 5, 6 (94.4%) 1, 3, 4, 5 (94.4%) 1, 3, 4 (94.4%) 1, 3 (94.4%)	1, 2, 3 (94.4%)	1 (77.8%)	1 (77.8%)
5 km/h	1, 2 (88.9%)	1, 2, 6 (83.3%) 1, 2 (83.3%)	1, 2, 3 (100%)	1, 3, 4, 5, 6 (100%) 1, 3, 4, 5 (100%) 1, 3, 4 (100%)	1 (88.9%) 1, 6 (88.9%)	1 (88.9%)
6 km/h	1 (88.9%)	1, 2 (94.4%)	1, 2 (72.2%) 1 (72.2%)	1 (100%)	1, 2, 3, 4, 5, 6 (100%) 1, 2, 3, 4, 5 (100%) 1, 2, 3, 4 (100%)	1, 6 (94.4%) 1 (94.4%)
7 km/h	1 (72.2%)	1, 2, 6 (55.6%) 1, 2 (55.6%) 1 (55.6%)	1 (77.8%)	1 (88.9%)	1, 3, 4 (94.4%) 1, 3 (94.4%) 1, 4 (94.4%) 1(94.4%)	1, 3, 4 (94.4%) 1, 3 (94.4%) 1, 4 (94.4%) 1 (94.4%)

Table 5.3 Parts (1-6) selection lookup table for cross speed gait recognition [93].

Probe / Gallery	2 km/h	3 km/h	4 km/h	5 km/h	6 km/h	7 km/h
2 km/h	1, 2, 3, 4, 5, 6	1, 2, 3, 5	1, 2, 3	1	1	1
3 km/h	1, 2, 3, 5	1, 2, 3, 4, 5, 6	1, 3, 6	1, 2	1	1
4 km/h	1, 2, 3	1, 3, 6	1, 3, 4, 5, 6	1, 2, 3	1	1
5 km/h	1	1, 2	1, 2, 3	1, 3, 4, 5, 6	1	1
6 km/h	1	1	1	1	1, 2, 3, 4, 5, 6	1
7 km/h	1	1	1	1	1	1, 3, 4

5.4.2 Effective Parts Selection

In the previous sub-section describes, the human gait is experimentally segmented into six unequal sections depending on the states of contributions of single row. For determining the effectiveness of parts in walking speed changes, these partitions are used for cross speed recognition on training set. The recognition rate in percentages are measured by combining of six parts. From the experiment, we noted that for some combinations the recognition rate decreased and increased for some combinations. The combinations that shows high recognition rate are listed with percentages of rate within bracket in Table 5.2. For some cell in the Table 5.2, the same recognition rate is found for several combinations of parts. It is also found that, for cross speed (like gallery 2 km/h, probe 3 km/h, and gallery 3 km/h, probe 2 km/h) different combinations are highest recognition rate i.e. more effective. So, we could select more effective sections out of the six, only the common parts of the combinations are kept for the cross-speed gait recognition task (Table 5.3) by discarding the remaining parts as less effective. The implementation steps of parts definition are presented in **Algorithm 1**.

5.5 Experiments

In our experiments, publicly available widely used benchmark datasets the OU-ISIR gait database A [29] and CASIA gait database C [30] are used. For human body division and selection procedure, huge walking speed variation treadmill OU-ISIR database A is used for training. The dataset is a collection of 34 subjects with 8 females and 26 males. It also contains a large scale of speed variation from two km/h to seven km/h. In training dataset to estimate get period elapsed time, gait parts division and effective part selection;

nine persons are selected from the database. The rest other twenty-five persons are used to evaluate performance of gait recognition [29]. In the database, for each walking speed two video sequences has recorded of each person. The training set of 108 video sequences of nine persons with six different speed are utilized from the OU-ISIR database A.

For the proposed method's performance evaluation is carried out by 25 subjects with a known walking speed as gallery set and for probe set 300 sequences of these 25 subjects with six different walking speed are used excluding the nine training subjects.

Table 5.4 Cross speed recognition rate (%) of the proposed method with GEI on the OU-ISIR gait database A.

Probe / Gallery	**2 km/h**	**3 km/h**	**4 km/h**	**5 km/h**	**6 km/h**	**7 km/h**
2 km/h	100	92	94	88	84	74
3 km/h	92	100	88	92	84	74
4 km/h	78	100	100	98	94	88
5 km/h	86	100	96	100	86	84
6 km/h	74	80	86	94	100	90
7 km/h	76	72	82	88	94	100

Table 5.5 Cross speed recognition rate (%) of the proposed method with DFT on the OU-ISIR gait database A.

Probe / Gallery	**2 km/h**	**3 km/h**	**4 km/h**	**5 km/h**	**6 km/h**	**7 km/h**
2 km/h	100	94	92	88	86	72
3 km/h	92	100	90	94	88	72
4 km/h	88	98	98	98	94	84
5 km/h	84	96	94	100	94	90
6 km/h	72	78	86	96	100	90
7 km/h	72	70	80	90	92	100

Table 5.6 Cross speed recognition rate (%) of the proposed method with GEI+PCA on the OU-ISIR gait database A.

Probe / Gallery	2 km/h	3 km/h	4 km/h	5 km/h	6 km/h	7 km/h
2 km/h	100	92	94	88	84	74
3 km/h	94	100	88	92	86	74
4 km/h	80	100	100	98	96	88
5 km/h	84	98	96	100	88	84
6 km/h	76	80	86	94	100	90
7 km/h	76	72	82	86	92	100

Table 5.7 Cross speed recognition rate (%) of the proposed method with DFT+PCA on the OU-ISIR gait database A.

Probe / Gallery	2 km/h	3 km/h	4 km/h	5 km/h	6 km/h	7 km/h
2 km/h	100	92	92	92	84	72
3 km/h	94	100	92	96	86	76
4 km/h	90	100	100	98	94	88
5 km/h	84	96	96	100	92	86
6 km/h	78	82	88	98	100	90
7 km/h	74	72	84	92	94	100

Table 5.8 Cross speed recognition rate (%) of the proposed method with GEI+PCA+LDA on the OU-ISIR gait database A.

Probe / Gallery	2 km/h	3 km/h	4 km/h	5 km/h	6 km/h	7 km/h	Average
2 km/h	100	98	98	92	90	82	**93.99**
3 km/h	98	100	98	98	92	86	**95.33**
4 km/h	90	100	100	96	90	82	**93**
5 km/h	90	100	94	100	96	96	96
6 km/h	88	90	96	96	100	90	**93.33**
7 km/h	88	82	90	94	100	100	**92.33**

Table 5.9 Cross speed recognition rate (%) of the proposed method with DFT+PCA+LDA on the OU-ISIR gait database A.

Probe / Gallery	2 km/h	3 km/h	4 km/h	5 km/h	6 km/h	7 km/h
2 km/h	100	98	98	90	82	74
3 km/h	100	100	98	92	94	84
4 km/h	80	98	100	96	94	84
5 km/h	88	96	94	100	100	98
6 km/h	74	82	94	96	98	90
7 km/h	80	84	84	90	98	100

Table 5.10 Cross speed recognition rate (%) without DCM method [74] on the OU-ISIR gait database A.

Probe / Gallery	2 km/h	3 km/h	4 km/h	5 km/h	6 km/h	7 km/h
2 km/h	100	96	84	72	72	72
3 km/h	100	100	96	80	76	60
4 km/h	76	96	96	92	92	80
5 km/h	76	76	96	96	100	96
6 km/h	64	68	80	96	100	96
7 km/h	56	68	80	96	100	100

Table 5.11 Cross speed recognition rate (%) with DCM method [74] on the OU-ISIR gait database A.

Probe / Gallery	2 km/h	3 km/h	4 km/h	5 km/h	6 km/h	7 km/h	Average
2 km/h	100	100	88	80	80	84	88.67
3 km/h	100	100	100	88	84	80	92
4 km/h	88	96	100	92	92	84	92
5 km/h	96	96	96	96	100	96	**96.67**
6 km/h	84	84	96	96	100	100	**93.33**
7 km/h	84	88	84	96	100	100	92

We also evaluate the proposed method with CASIA gait database C [30] that contains three different walking speeds, namely slow (fs), normal (fn) and quick (fq) of 153 subjects. Out of the 153 subjects, 33 subjects are used for absolute speed estimation as training and 120 subjects are for testing. We used the same parts division and selection procedure of OU-ISIR database A for the CASIA database C to validate our proposed method. All the experimental results of different gait representations and methods are listed in Table 5.4 to Table 5.11. The recognition rate shows in all the tables are at rank 1.

5.6 Result and Discussion

5.6.1 Treadmill OU-ISIR dataset A

The recognition rate of the proposed part definition and selection method achieves promising performance at rank-1 for cross speed gait recognition of OU-ISIR dataset, which are listed in Table 5.4 to Table 5.9, and compared with the method without and with DCM [82] that are given in Table 5.10 and Table 5.11.

It is clearly comparable that Table 5.8 (proposed method with GEI+PCA+LDA) shows better cross-speed recognition rate than Table 5.11 (with DCM [82]). The minimum average recognition rate of the proposed method is 92.33% whereas it is 82.67% with DCM [82]. So, the minimum average recognition rate is about 10% more with proposed method. The maximum average rate is 96% for proposed methods which is slightly (0.67%) lower than with DCM methods.

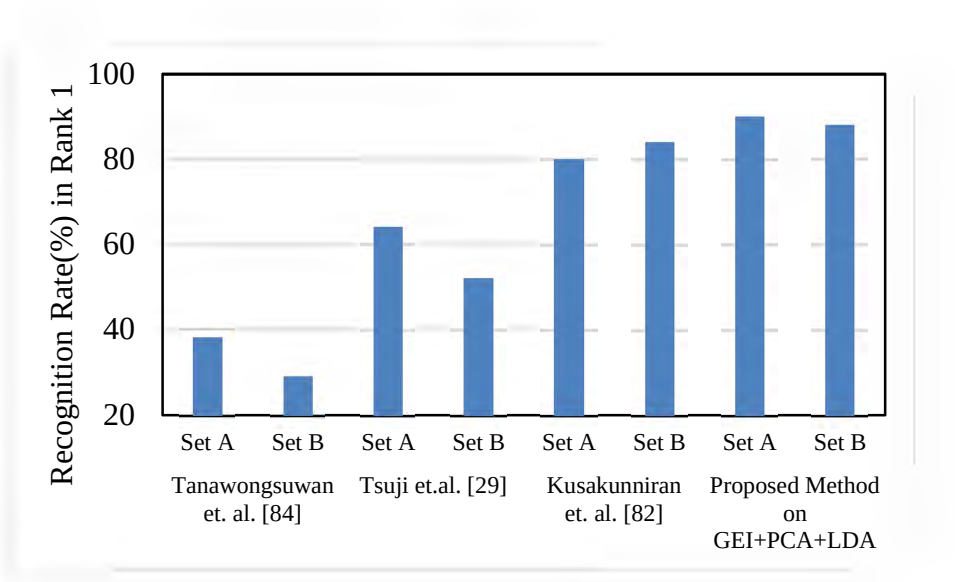

Figure 5.3 Recognition rate in % of different methods with large speed variation of OU-ISIR set A.

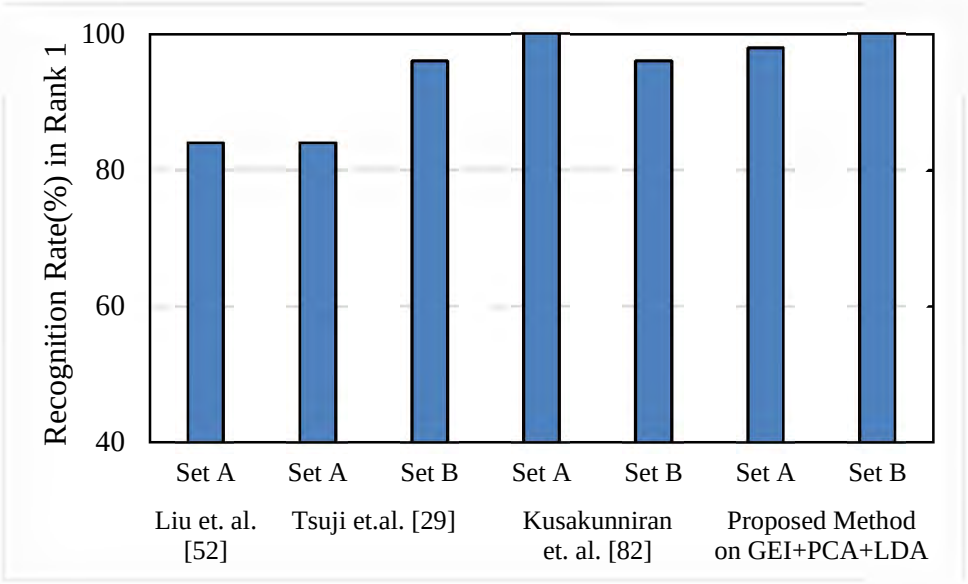

Figure 5.4 Recognition rate in % of different methods with small speed variation of OU-ISIR set A.

The proposed part-based intra-class variation reduction method are also compared with Tsuji et al. [29], and Tanwongsuwan et al. [84] for small and large speed variation dataset. The comparative performance evaluations are presented in Figure 5.3 and Figure 5.4. In dataset A slower walkers are selected as gallery and vice versa in Set B. For large

speed variation Tanwongsuwan et al. [84] are used 2.5 km/h and 5.8 km/h, and Tsuji et al. [29], DCM method [82] and our proposed method are used 2 km/h and 6 km/h as gallery and probe. In Figure 5.3, for large speed variations the proposed method's performance is much better than [82], but significantly greater than [29] and [84].

For small speed variations, Liu et. Al. [52] proposed time normalization method and used approximately 1 km/h speed difference with a combination of 3.3 km/h and 4.5 km/h speed variation. Similarly, Kusakunniran et al. [82] the DCM method, Tsuji et al. [29] the speed transformation model and our proposed part-based method match between 3 km/h and 4 km/h. The comparative results are presented in Figure 5.4 and our proposed method achieved 100% recognition rate for Set B but for set A it is slightly less than [82]. As a whole, the evaluation of performance of our proposed part-based method that reduce intra-class variation is effective and gives better recognition rate.

5.6.2 The CASIA gait database C

The CASIA gait database C [30] is used to validate the proposed method in this research. Table 5.12 shows the comparison of gait recognition performance on the CASIA gait database C with other existing methods and our proposed part-based method at rank-1. For gallery normal and slow walking speed to probe normal and slow walking speed, our proposed method performs 100% recognition rate.

Table 5.12 Comparison of cross speed recognition rate (%) on the CASIA gait database C using different methods with GEI representation.

Gallery, Probe		fn, fn	fn, fs	fn, fq	fs, fs	fq, fq
Methods	Unprojective [54]	97	84	88	-	-
	WBP [106]	99	86	90	-	-
	AEI [58]	88	89	90	-	-
	Pseudoshape [107]	98	82	92	-	-
	Wavelet packet [108]	93	83	85	-	-
	Orthogonal Projections [109]	98	80	80	-	-
	NDDP [110]	97	85	74	-	-
	Gait curves [111]	91	78	80	-	-
	Without DCM [82]	96	87	89	95	91
	With DCM [82]	97	92	**93**		
	The proposed method	**100**	**97**	88	**100**	**98**

For cross speed, gallery normal to probe slow walking speed, proposed method gives highest 97% correct recognition rate. However, our proposed method shows comparatively lower recognition rate for gallery normal and probe quick walking speed. Nevertheless, the proposed method achieves comparable performance and some gallery-probe it shows much better recognition rate over existing methods.

5.7 Conclusion

The proposed part-based speed invariant gait recognition system could manage the situation of large intra-class variations created to the huge changes of walking speed. The body parts containing dynamic features are greatly affected with speed changes while the parts cover static features are less or not affected. The proposed method increases the discriminating features by selecting less affected parts (static area) dynamically (using lookup table) by discarding more affected body parts (dynamic area) for walking speed changes. We can infer from our experimental result that for cross-speed gait recognition, the correct recognition rate is higher when the speed changes are smaller in gallery and probe, but the recognition rate shrinks gradually with the increasing of walking speed

difference. The experimental results are reported in different tables and figures on two benchmark databases OU-ISIR treadmill A and CASIA dataset B.

CHAPTER 6. ADAPTIVE PARTS SELECTION FOR PART-BASED HUMAN IDENTIFICATION CONSIDERING CLOTHING AND CARRYING CONDITIONS AND SPEED CHANGES

6.1 Introduction

Part-based methods primarily define the parts of human gait manually, experimentally [21, 95, 104], into components [17] or based on anatomical statistics [25]. After defining the parts, significant features are extracted from the early defined parts or select the most effective parts statically or dynamically for gait recognition. The reason to select the most effective parts and reject the redundant part to overcome the complications arises due to various covariate conditions. Cofactors like, clothing and carrying conditions speed changes also affect some region of the body. So, the rejection of the more affected body parts can contribute to performance enhancement.

The main contribution of the proposed system in this chapter is to investigate the selection procedure of body parts adaptively and independently for each subject on the impacts to the covariate condition on each part. Legendre and Zernike moments based adaptive parts selection methods are used in the proposed system. A common framework for clothing and carrying condition and speed changes is evaluated with four benchmarking gait datasets. The experimental results of the proposed system show comparatively better or very similar performance with some previous methods.

6.2 Pre-processing and Feature Representation

The pre-processing including gait cycle estimation for the standard gait recognition is explained in Preprocessing section 2.1. The details of different gait feature representation techniques GEI, GEnI, DFT and EnDFT, and example images are presented in section 2.2.

6.3 Part Definition and Adaptive part selection

6.3.1 Parts definition

The whole procedure of part definition for clothing and carrying condition is discussed in section 3.4. Based on the recognition accuracy of each row of GEI gait representation, Rokanujjaman et al. [104] defined the human gait into five unequal parts.

Similarly, for speed changes the human body is divided into six unequal parts and the procedure is discussed in section 5.4 and this is reported in [93].

6.3.2 Adaptive parts selection

In this research, Legendre moments and Zernike moments has been used for selecting effective human body part adaptively in the presence of covariate conditions such as clothing and carrying and speed changes gait recognition. The details of Legendre and Zernike moments is presented in section 2.4. The whole procedure to adaptively select effective parts is presented in **Algorithm 2**. Legendre moments and Zernike moments are invariant to geometric transformations. However, they are not invariant to the covariate conditions.

Algorithm 2

Based on Legendre moments and Zernike moments an algorithm WEIGHT-CALCULATION is written to compute the weight of different sub-parts of probe image. Algorithm WEIGHT-CALCULATION takes two sets of images, G = ($G_1, G_2, \ldots . G_n$) for gallery images and P=(P_1) for probe image as inputs. k sub-parts of gallery and probe images are used in the algorithm. Parts definition is described in section 3.4 and 5.4.

The algorithm requires GL[] and GZ[] arrays to hold the Legendre moments and Zernike moments for gallery, PL[] and PZ[] arrays to hold the Legendre moments and Zernike moments for probe. Each part gallery to gallery Euclidean distances are calculated and inserted into EL[] and EZ[] arrays based on Legendre moments and Zernike moments. Similarly, Each part probe to gallery Euclidean distances are calculated and inserted into DL[] and DZ[] arrays based on Legendre moments and Zernike moments. The procedure EUCLIDEAN-DISTANCE returns ordinary Euclidean distance.

The algorithm maintains AL[] and AZ[] arrays to store average of Euclidean distances. It also maintains ML[] and MZ[] arrays to store minimum of Euclidean distances. The weight of the probe parts are returned as WL[] and WZ[] arrays from the algorithm. The parts with weight 1 are used in probe gait recognition and parts with weight 0 are rejected as redundant. The following algorithm uses two auxiliary procedures LEGENDRE-MOMENTS() and ZERNIKE-MOMENTS(), whose pseudo-codes are given in section 2.4.1 and 2.4.2.

WEIGHT-CALCULATION(G, P)

1. n=G.length
2. For i= 1 to k
3. GL[n, i] = LEGENDRE-MOMENTS (p, q, G, n, i)
4. GZ[n, i]= ZERNIKE-MOMENTS (p, q, G, n, i)

► p+q is the order of Legendre moments

► p is the order and q is the repetition of Zernike moments

5. End of for loop
6. c=0
7. For j=1 to n
8. For l = 1 to n
9. If j==l
10. continue
11. c=c+1

► distance for Legendre moments

12. EL[c, k]= EUCLIDEAN-DISTANCE (GL[j,k], GL[l, k])

► distance for Zernike moments

13. EZ[c, k]= EUCLIDEAN-DISTANCE (GZ[j,k], GZ[l,k])
14. End of inner loop
15. End of outer loop
16. AL[k]=MEAN(EL[c,k])
17. AZ[k]=MEAN(EZ[c,k])
18. For i= 1 to k
19. PL[i] = LEGENDRE-MOMENTS (p, q, P, i)
20. PZ[i]= ZERNIKE-MOMENTS (p, q, P, i])
21. End of for loop
22. For j=1 to n
23. DL[j, k]= EUCLIDEAN-DISTANCE(PL[k], GL[j,k])
24. DZ[j, k]= EUCLIDEAN-DISTANCE (PZ[k], GZ[j,k])
25. End of for loop
26. ML[k]=MIN(DL[n,k])
27. MZ[k]=MIN(DZ[n,k])
28. For j=1 to k
29. If ML[j] <= AL[j]
30. WL[j]=1

```
31.    Else
32.        WL[j]=0
33.    If MZ[j] <= AZ[j]
34.        WZ[j]=1
35.    Else
36.        WZ[j]=0
37. End of for loop
38. Return WL and WZ
```

6.4 Matching Measure

The method of matching measure used for experiments section in this chapter is described in section 4.4.2 and section 5.3.

6.5 Experiments

This section shows experimental results using different datasets. The experiments carried out in this work to show the effectiveness of the adaptive parts selection for human gait recognition using GEI, GEnI, DFT and EnDFT features.

6.5.1 Datasets

The details of the datasets used in this study are discussed in this section. The following four benchmarking gait datasets with most of the challenging cofactors are used in our experiment.

(i) The OU-ISIR Gait Database, the treadmill dataset A [29]
(ii) The OU-ISIR Gait Database, the treadmill dataset B [23]
(iii) The CASIA Gait Database, dataset B [24]
(iv) The CASIA Gait Database, dataset C [30]

6.5.1.1 The datasets containing clothing and carrying cofactors

The OU-ISIR Gait Database, the Treadmill Dataset B [23] is chosen due to its massive variation in clothing cofactors which is one of the most challenging artifacts. The dataset is a collection of 68 subjects with at most 32 combinations of different types of clothing such as skirt, raincoat, down jacket, long coat, hat, parker, muffler, short pants, casual wears, regular pants, half shirt, full shirt etc. This whole dataset is divided into three subsets: training set, gallery set and probe set. This training set holding 446 video sequences of 20 subjects (10 males and 10 females) with the range of 15 to 28 different clothing combinations are used for part definition in training phase. The training dataset is not used in validation phase. Other two subsets (gallery and probe) of OU-ISIR dataset B are used in testing phase. Gallery set contains only standard clothing type, i.e., regular pant and full shirt of 48 subjects. Probe set contains 856 sequences of these 48 subjects considering all types of different clothing combinations excluding the standard one.

The CASIA Gait Database, Dataset B [24] is chosen due to its subject diversity with multiple sequences and multiple cofactors. The dataset contains normal walking sequences, carrying objects (i.e., carrying a bag) and only one clothing type (i.e., wear a bulky coat). The total 124 subjects contributed to the dataset. There are 10 walking sequences with the cofactors are captured from each of the subjects. This dataset is used only for validation of the proposed method.

6.5.1.2 The datasets containing speed changes

The treadmill OU-ISIR database A [29] with a large scale of walking speed variations ranging from two km/h to seven km/h is used in this work. This dataset comprises of 34

subjects with 8 females and 26 males. In the dataset, considering each walking speed two video sequences is captured for each person. In case of OU-ISIR dataset A, 108 video sequences of nine persons with six different speeds are used for part division during training. The OU-ISIR dataset A containing video sequences of other 25 persons (out of 34 persons) are used to evaluate the performance of the proposed approach.

The CASIA Gait Database, Dataset C [30] is developed on the basis of three different walking speeds, namely slow (fs), normal (fn) and quick (fq). The dataset contains 153 subjects where each subject has 4 normal, 2 slow and 2 quick walking sequences. This dataset is used only for validation of our proposed method.

6.5.2 Result and discussion

Extensive experiments are carried out on CASIA B and OU-ISIR B database on our defined partition system. We have selected body parts adaptively using Legendre and Zernike moments-based weight calculation. The results are shown in Figure 6.1 to Figure 6.8 as a cumulative matching curve (CMC) on different gait representation technique without and with linear discriminant analysis (LDA).

Figure 6.1 shows that GEI in combination with LDA perform better than other combinations and achieved 83.02% recognition rate at rank-1. Another combination DFT+LDA presents almost similar recognition rate. However, GEI representation shows poor recognition rate. In this case, for Dataset CASIA B with clothing and carrying cofactors, Legendre moments is used for adaptive parts selection.

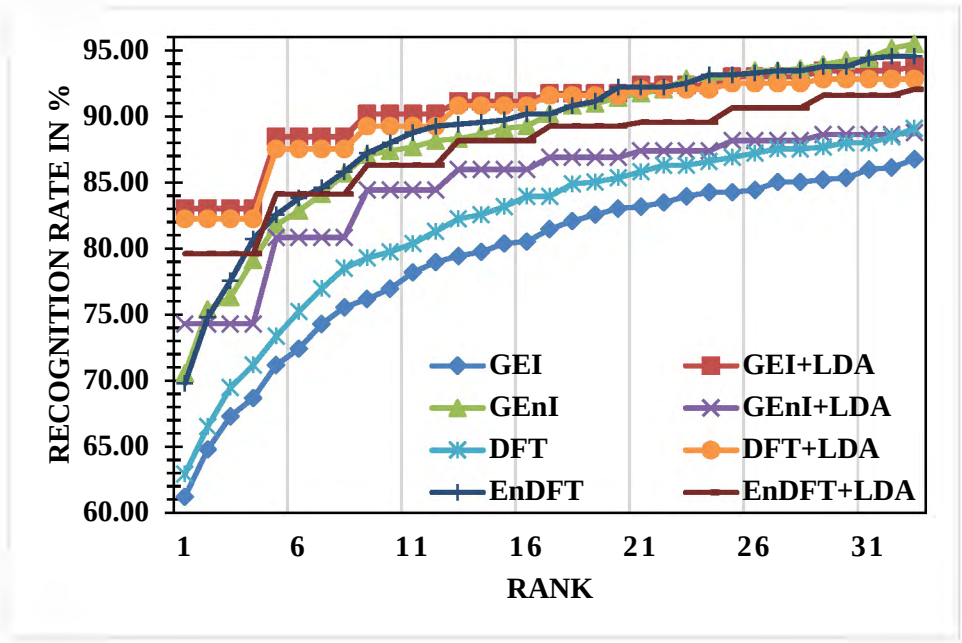

Figure 6.1 The CMC on CASIA B with clothing and carrying condition for adaptive parts selection using Legendre Moments.

The highest recognition rate 74.3% is achieved in Figure 6.2 for EnDFT+LDA. On the other hand, the recognition rate of other representation techniques is found decreasing gradually. In this case, for Dataset OUISIR B with bulk clothing variations, Legendre moments is used for adaptive parts selection.

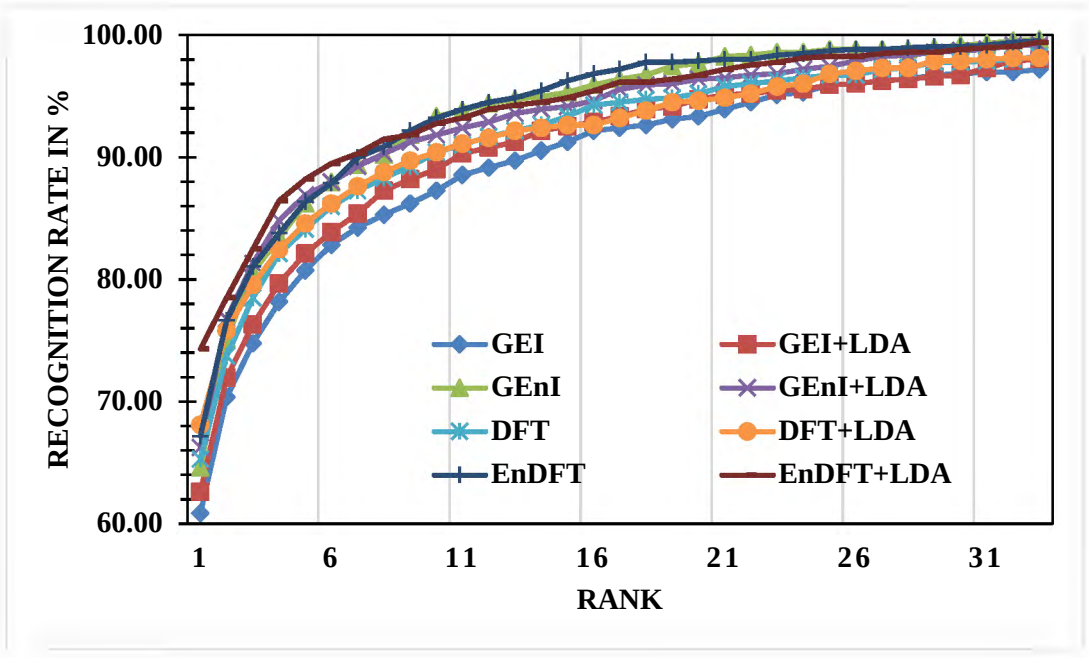

Figure 6.2 The CMC on OUISIR B with clothing and carrying condition for adaptive parts selection using Legendre Moments.

Figure 6.3 shows that GEI+LDA perform better than other single and combined representations and obtained on average 80.69% recognition rate. Next very close recognition rate is provided by DFT+LDA and EnDFT+LDA. However, GEI representation shows poor recognition rate. In this case, for Dataset CASIA B with clothing and carrying cofactors, Zernike moments is used for adaptive parts selection.

Figure 6.4 shows that EnDFT+LDA perform better than other single and combined representations and obtained on average 71.85% correct recognition rate. However, GEI representation shows unfortunate recognition rate. In this case, for Dataset OUISIR B with huge clothing variation, Zernike moments is used for adaptive parts selection.

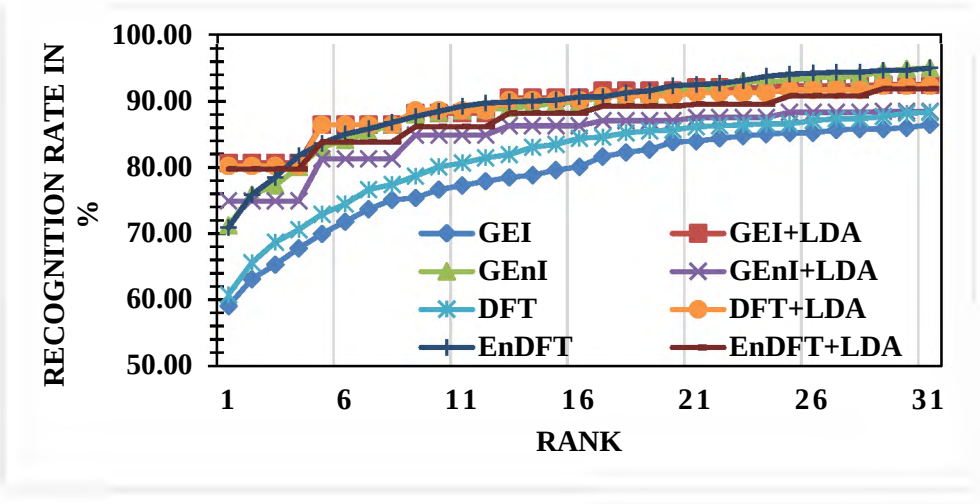

Figure 6.3 The CMC on CASIA B with clothing and carrying condition for adaptive parts selection using Zernike Moments.

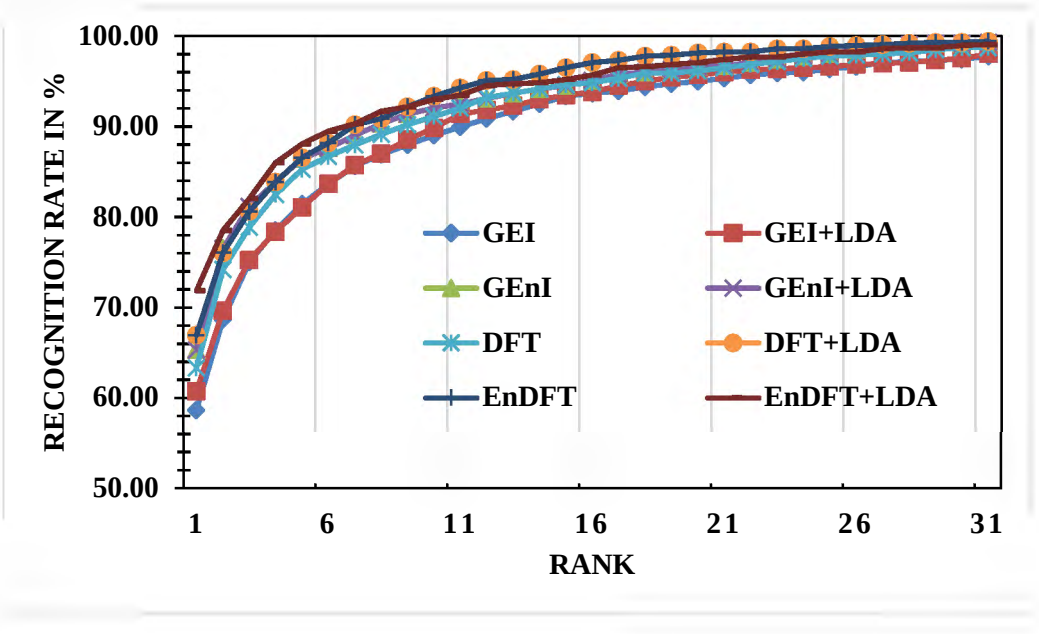

Figure 6.4 The CMC on OUISIR with clothing and carrying condition for adaptive parts selection using Zernike Moments.

In Figure 6.5, CMC curve is plotted for different speeds as gallery and all speeds as probe. 3km and 4km gallery shows the highest recognition rate and other decreases due to

increasing speed difference from gallery to probe. In this case, for Dataset OUISIR A with speed changes, Legendre moments is used for adaptive part selection. GEI representation with LDA is used for gait recognition.

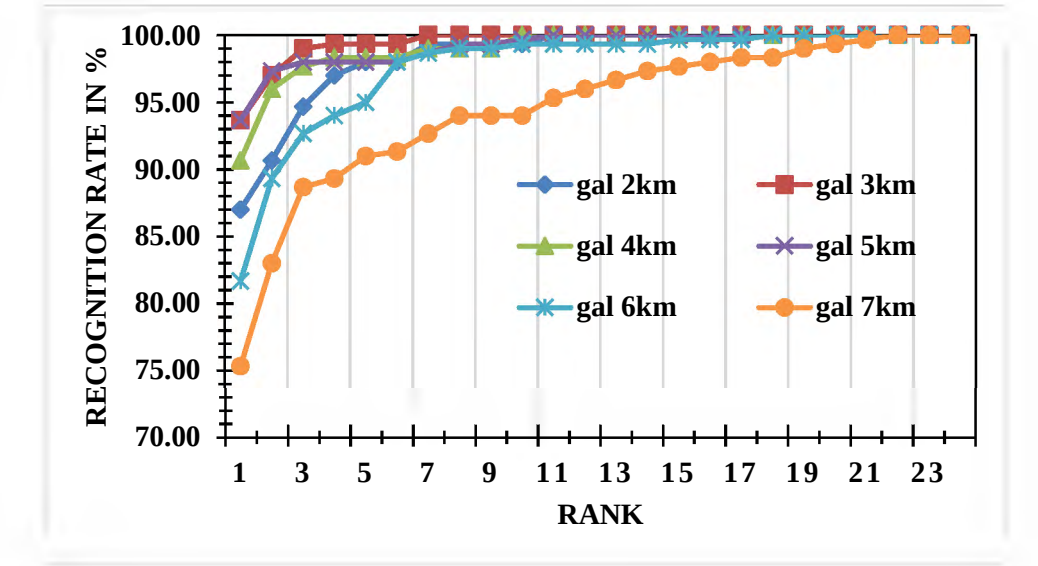

Figure 6.5 The CMC on OUISIR A with speed changes condition for adaptive parts selection using Legendre Moments.

Similarly, for Dataset OUISIR A, Figure 6.6 shows for different speeds as gallery and all speeds as probe. 4km and 5km gallery shows the highest recognition rate. GEI representation with LDA is used for gait recognition and Zernike moments for adaptive part selection.

Figure 6.7 shows the CMC curve for Dataset CASIA C where Legendre moments is used for adaptive part selection. GEI representation with LDA is used for recognition. The recognition rate is lowest for gallery slow to probe quick speed and vice versa. The other speed combination shows better results.

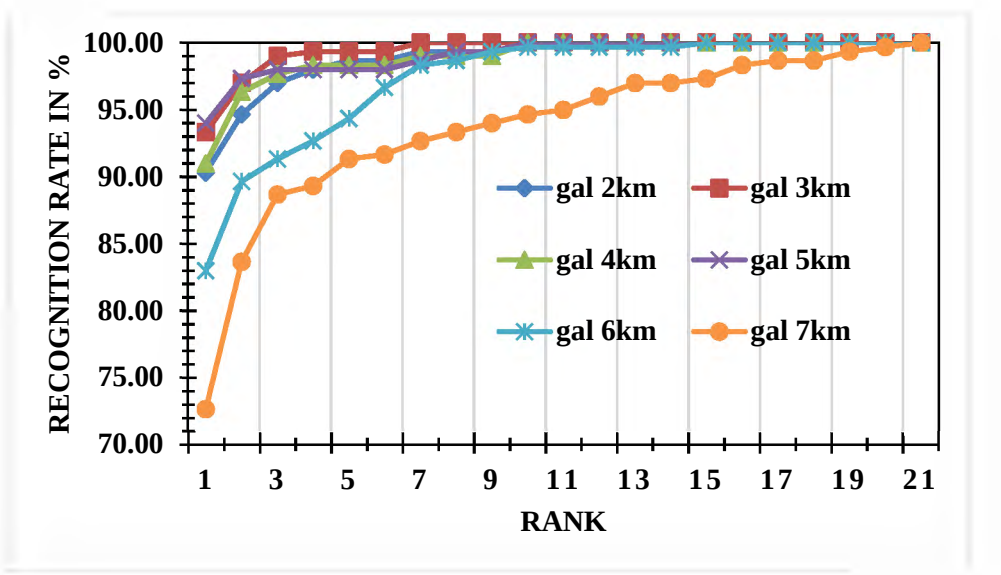

Figure 6.6 The CMC on OUISIR A with speed changes condition for adaptive parts selection using Zernike Moments.

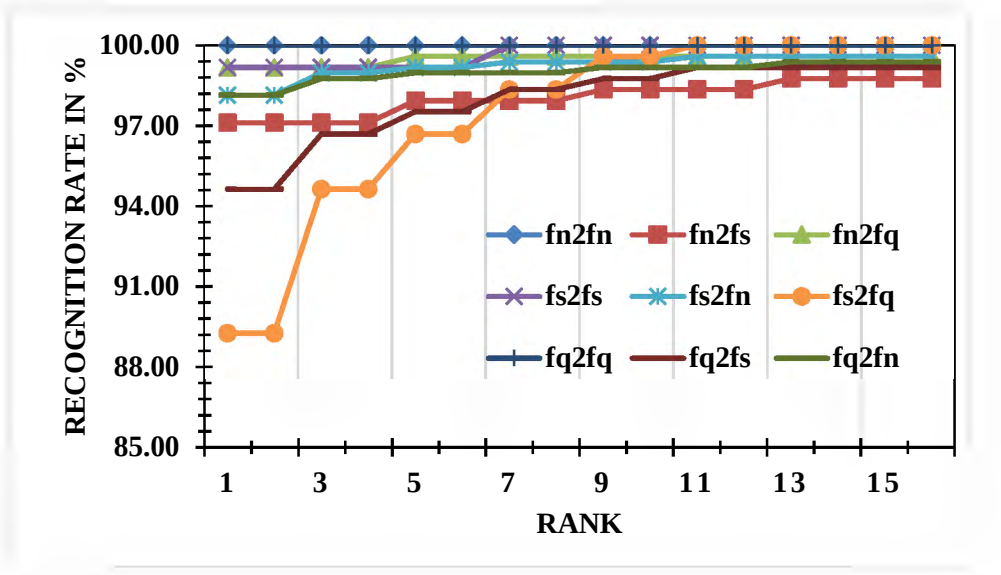

Figure 6.7 The CMC on CASIA C with speed changes condition for adaptive parts selection using Legendre Moments.

The CMC curve for Dataset CASIA C with GEI representation is shown in Figure 6.8. Zernike moments is used for adaptive part selection and LDA is used dimensionality

reduction. For fq2fq the recognition rate is 100% and for all other combination, the recognition rate is similarly changed as in Figure 6.7.

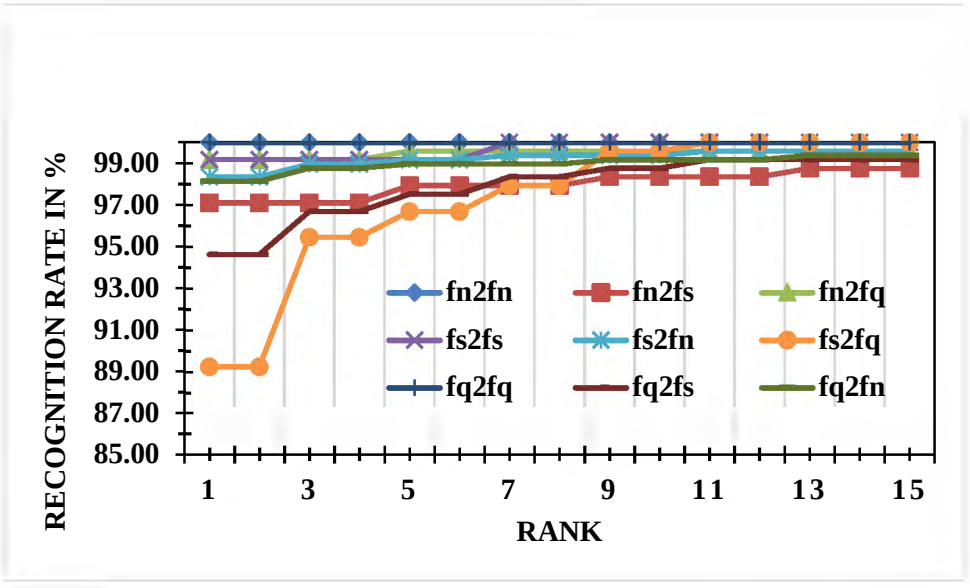

Figure 6.8 The CMC on CASIA C with speed changes condition for adaptive parts selection using Zernike Moments.

The proposed methods are evaluated over four datasets under different covariate cofactors. Table 6.1 shows the results for the OUISIR B and CASIA B dataset. The results achieved by our method and most of the existing methods are outlined in Table 6.1. The comparison is carried out on the basis of different feature extraction methods and part selection methods. The method used in [80] performs better than our proposed method. However, the proposed method outperforms all the other compared methods achieving highest 83.02% recognition rate based on GEI+LDA and Legendre moments for CASIA B dataset and 82.24% recognition rate based on DFT+LDA and Legendre moments for the

same dataset. In case of another dataset (OUISIR B), best performance (74.30%) is obtained so far with respect to the performance of the other existing methods.

Table 6.1 Comparative results for the OUISIR B and CASIA B dataset.

Method	**Part selection (Moment-based)**	**Dataset**	**CCR (%)**	**Method**	**Part selection**	**Dataset**	**CCR (%)**
EnDFT+LDA (proposed)	Legendre	OUISIR B	**74.30**	Hawas, A.R. [116]	-	CASIA B	64.1
DFT+LDA (proposed)	Legendre	OUISIR B	68.11	L. Yao et al. [117]	-	CASIA B	68.01
EnDFT+LDA (proposed)	Zernike	OUISIR B	**71.85**	Jingran Su et al. [118]	-	CASIA B	75.03
EnDFT (proposed)	Zernike	OUISIR B	66.94	Guoheng Huang et al. [119]	-	CASIA B	**81.50**
GEI+LDA (proposed)	Legendre	CASIA B	**83.02**	Maryam Bukhari et al. [120]	-	CASIA B	**90.32**
DFT+LDA (proposed)	Legendre	CASIA B	**82.24**	PCA+LDA+GEI [51]		OUISIR B	54.32
GEI+LDA (proposed)	Zernike	CASIA B	**80.69**	Baseline+GEI [72]		OUISIR B	55.26
DFT+LDA (proposed)	Zernike	CASIA B	**80.22**	PCA+LDA+GEnI [73]		OUISIR B	57.36
Bashir et al. [65]	-	CASIA B	74.2	Whole DFT [23]		OUISIR B	58.06
Rokanujjaman, M. [21]	Local maxima and minima	CASIA B	77.69	Part-based [25] Without weight		OUISIR B	58.06
Gupta, S.K. [115]	-	CASIA B	73.8	Part based EnDFT [21]	Local maxima and minima	OUISIR B	**72.78**

Table 6.2 shows the comparison of gait recognition performance on the CASIA C gait database with other existing methods and our proposed methods. The results reveal that the proposed methods outperform all the competing methods in terms of all the speed combinations, except in fn2fs and fn2fq where the methods in [114] perform slightly better than the proposed methods. However, the recognition rate for fs2fs, fq2fq, fs2fn, fs2fq, fq2fn and fq2fs is not found in [114]. The recognition rate of the proposed method turns to

the highest 100% for fn2fn and fq2fq. On the other hand, recognition rate 89.3% and 94.6 is found for large speed variation (fs2fq and fq2fs). The recognition rate for other speed combinations are also shown in Table 6.2. It should be noted that both Legendre moments and Zernike moments based adaptive parts selection approaches show very similar performance.

Table 6.2 Comparison of cross speed recognition rate (%) on the CASIA C gait database using different methods.

Gallery, Probe / **Methods**	**fn2fn**	**fn2fs**	**fn2fq**	**fs2fs**	**fq2fq**	**fs2fn**	**fs2fq**	**fq2fn**	**fq2fs**
Unprojective [54]	97	84	88	-	-				
Orthogonal projections [109]	98	80	80	-	-				
NDDP [110]	97	85	74	-	-				
Gait curves [111]	91	78	80	-	-				
Without DCM [82]	96	87	89	95	91				
With DCM [82]	97	92	93						
M. Rokanujjaman et al. [112]	100	97	88	100	98				
AEI+2DLPP [58]	88.9	89.2	90.2						
WBP [106]	99	86.4	89.6						
Orthogonal projection [109]	98	80	80						
HSD [12]	97	86	89						
Wavelet packet [108]	93	83	85						
Pseudo shape [107]	98.4	91.3	93.7						
Gait curves [111]	91	65.4	69.9						
HTI [30]	94	85	88						
SDL [113]	95.4	91.2	92.5						
M. H. Khan et al. [114]	100	99	100						
Proposed GEI+LDA with Legendre Moments	100	97.1	99.2	99.2	100	98.1	89.3	98.1	94.6
Proposed GEI+LDA with Zernike Moments	100	97.1	99.2	99.2	100	98.4	89.3	98.1	94.6

Table 6.3 shows the gait recognition performance comparison between our proposed method and other existing methods over OUISIR A gait database. All the methods are evaluated for 6 different walking speeds. In our previous work [112], highest recognition rate 96% is obtained for 5km gallery and for DCM [82] it is 96.67% for 5km gallery. In

our proposed methods, the correct recognition rate is 93.67% and 94% with Legendre moment and Zernike moment-based parts selection respectively for 5km gallery. It is realized from the table that recognition rate is decreasing for large speed variations from gallery to probe and increasing for small speed differences.

Table 6.3 Average gait recognition performance comparison between our proposed method and other existing methods over OUISIR A gait database.

Methods	Gallery	Average recognition rate (%)
Effective part selection [112]	2km	**93.99**
	3km	**95.33**
	4km	**93**
	5km	96
	6km	**93.33**
	7km	**92.33**
Without DCM [82]	2km	82.67
	3km	85.33
	4km	88.67
	5km	90
	6km	84
	7km	83.33
With DCM [82]	2km	88.67
	3km	92
	4km	92
	5km	**96.67**
	6km	**93.33**
	7km	92
Proposed method with Legendre moments	2km	87
	3km	93.67
	4km	90.67
	5km	93.67
	6km	81.67
	7km	75.33
Proposed method with Zernike moments	2km	90.33
	3km	93.33
	4km	91
	5km	94
	6km	83
	7km	72.67

6.6 Conclusion

In this thesis human body parts are defined experimentally and selected adaptively using Legendre and Zernike moments for the purpose of gait recognition. Having obtained different number of body parts, GEI, GEnI, DFT and EnDFT representation is computed and exploited as gait features. For speed changes the dynamic parts are responsible for intra-class variation and static parts are useful as an invariant feature. So, only the GEI representation is used for speed changes dataset because the other representation highlights the dynamic body parts and lessen the static parts.

The proposed parts selection methods are compared with previously published methods. The recognition rates of our proposed methods confirm the effectiveness and validity over the four comprehensive benchmarking gait datasets under the clothing and carrying conditions and speed changes. The proposed methods perform better in most of the cases compared with the results of the other recognition methods verified on the OUISIR A, OUISIR B, CASIA B and CASIA C gait database.

CHAPTER 7. CONCLUSIONS AND FUTURE WORKS

7.1 Conclusions

In this research, the goal is to investigate the novel and robust methods of gait feature representation, humans body parts definition and effective body part selection to reduce the intra-class variations caused by different covariate conditions. In this thesis, we address the most challenging clothing and carrying covariate conditions and walking speed changes and have been studied their effects on human gait recognition.

First, in real life people can dress themselves with different clothing in different season and festival. Similarly, they can carry different types of bag for their needs. So, human gait can be altered by different clothing and carrying bag these made gait recognition more complicated and challenging.

Second, in practice, people can walk freely in any speed in many situations. So, walking speed is a factor to contaminate human gait and affect the recognition rate. Walking speed changes can affect different body parts, when speed increases, legs lift up higher, stride length becomes lengthier, arms swing faster, and gait cycle is reduced. The possible solutions are i) modeling or projecting gaits across different walking speeds; ii) finding speed invariant gait features; iii) discarding contaminated body part/parts.

This thesis has proposed novel and robust gait parts definition and parts selection methods and a novel gait representation technique. The summaries and benefits of proposed methods are presented in each chapter's conclusion section. This section summarizes them as key concept in brief.

The method in CHAPTER 3 is proposed for human gait identification considering clothing conditions. Here, we proposed the gait partition and parts selection methods. The whole gait is partitioned into five unequal parts based on local maxima and local minima considering the contribution of each row of GEI as recognition rate. The three parts are selected among five parts for gait recognition by rejecting two most affected parts due to clothing cofactor. The procedure is described in section 3.4.

In CHAPTER 4, a novel gait representation technique entropy based DFT (EnDFT) is proposed. This feature representation technique is evaluated with two widely used database with clothing and carrying conditions. The validation of parts definition and parts selection (previous chapter) is done in section 4.5.2.

The parts definition and look-up table-based parts selection procedure for speed changes is proposed in CHAPTER 5. The whole human body is partitioned into six unequal parts based on local maxima and local minima considering the contribution of each row of GEI as recognition rate. The benefits of look-up table for parts selection are to select different body parts with speed changes.

A common frame work for clothing and carrying conditions and speed changes is proposed in CHAPTER 6. For selecting body parts adaptively, we proposed Legendre moments and Zernike moments to calculate the weights of each part. The next step is to measure the distances for all gallery using the weights and compute the average for each part and used as threshold for parts selection. If the weight of certain part of a probe is greater than the threshold value, discard that part otherwise accept for gait recognition.

7.2 Future works

We will further investigate on the combination of our effective part selection methods and state-of-the-art gait features in future work. Moreover, adaptive fusion of all the methods on feature level, score level and decision level will be another future extension of this work. In CHAPTER 6, we consider clothing conditions and walking speed changes as different datasets with different subjects. So, we have partitioned the gait of the two covariate conditions separately but the effective parts are selected adaptively with the same algorithm. In real situation these covariate conditions may happen together. To overcome the situations and for actual applications it is necessary to consider the covariate conditions jointly and it may be another future work.

REFERENCES

[1] Jain, A.K., Ross A. & Nandakumar, K. Introduction to Biometrics. Springer Science and Business Media LLC, ISBN 978-0-387-77325-4, 2011.

[2] Connor, P. & Ross, A. Biometric recognition by gait: A survey of modalities and features. Computer Vision and Image Understanding, 167, p.1–27, 2018.

[3] Wang, L., Zhao, G., Rajpoot, N. & Nixon, M. S. Special issue on new advances in video-based gait analysis and applications: challenges and solutions. IEEE Tran. on Systems, Man, and Cybernetics, Part B: Cybernetics, 40(4), p.982–985, August 2010.

[4] Grabiner, P. C., Biswas, S. T. & Grabiner, M. D. Age-related changes in spatial and temporal gait variables. Arch Phys Med Rehabil 82: 5-31, 2001.

[5] Mather, G. & Murdoch, L. Gender discrimination in biological motion displays based on dynamic cues. the Royal Society: Biological Sciences 258(1353), p.273-279, 1994.

[6] Menant, J. C., Steele, J. R., Menz, H. B., Munro, B. J. & Lord, S. R. Effects of walking surfaces and footwear on temporo-spatial gait parameters in young and older people. Gait & Posture 29(3), p.392-397, 2009.

[7] Nigg, B. M., Fisher, V. & Ronsky, J. L. Gait characteristics as a function of age and gender. Gait & Posture 2(4), p.213-220, 1994.

[8] Powers, C. M. & Perry, J. Gait characteristics in subjects with patellofemoral pain: The influence of pain and quadriceps strength. Gait & Posture 5(2), p.183-184, 1997.

[9] Troje, N. F. The little difference: Fourier-based gender classification from biological motion. Dynamic Perception Eds R P Würtz, M Lappe (Berlin: Aka Verlag), p.115-120, 2002.

[10] Zhang, B., Zhang, Y. & Begg, R. K. Gait classification in children with cerebral palsy by Bayesian approach. Pattern Recognition 42(4), p.581-586, 2009.

[11] Foster, J. P., Nixon, M. S. & Prel-Bennett, A. Automatic gait recognition using area-based metrics. Pattern Recognition Letters 24(14), p.2489-2497, 2003.

[12] Kusakunniran W. Attribute-based learning for gait recognition using spatio-temporal interest points. Image and Vision Computing, 32(12), p.1117–1126, 2014.

[13] Chellappa, R., Roy-Chowdhury, Jain A.K. & Kale, A. Human Identification using Gait and Face. IEEE Conference on Computer Vision and Pattern Recognition, CVPR, 2007.

[14] Han, J. & Bhanu, B. Performance prediction for individual recognition by gait. Pattern Recognition Letters 26(5), p.615-624, 2005.

[15] Sarkar, S., Phillips, P. J., Liu, Z., Vega, I. R., Grother, P. & Bowyer, K. W. The humanID gait challenge problem: data sets, performance, and analysis. Pattern Analysis and Machine Intelligence, IEEE Transactions on 27(2), p.162-177, 2005.

[16] Wang, J. J. & Singh, S. Video analysis of human dynamics - a survey. Real-Time Imaging 9(5), p.321-346, 2003.

[17] Lee, L. & Grimson, W. Gait analysis for recognition and classification. In: Proceedings of the fifth IEEE conference on face and gesture recognition. Washington DC, p.148–155, 2002

[18] Boulgouris, N.V., Hatzinakos, D. & Plataniotis K.N. Gait recognition: a challenging signal processing technology for biometric identification. IEEE Signal Proc Mag 22, p.78–90, 2005.

[19] Lu, H., Plataniotis, K. & Venetsanopoulos A. Uncorrelated multilinear discriminant analysiswith regularization for gait recognition. In: Proceedings of biometrics symposium. Baltimore, p.1–6, 2007.

[20] Rogers E. Gait recognition. In: Bell Canada chair in multimedia IPSI: Identity, Privacy and Security Initiative. Department of Electrical and Computer Engineering, University of Toronto.

[21] Rokanujjaman, M., Islam, M.S., Hossain, M.A., Islam, M.R., Makihara, Y. & Yagi, Y. Effective part-based gait identification using frequency-domain gait entropy features. Multimedia Tools and Applications 74 (9), p.3099-3120, 2015.

[22] Li, X., Makihara, Y., Xu, C., Yagi, Y. & Ren, M. Joint Intensity Transformer Network for Gait Recognition Robust against Clothing and Carrying Status. IEEE Transactions on Information Forensics and Security, p.1-13, April 2019.

[23] Makihara, Y., Mannami, H., Tsuji, A., Hossain, M., Sugiura, K., Mori, A. & Yagi, Y. The ou-isir gait database comprising the treadmill dataset. IPSJ Trans Comput Vis Appl 4:53–62, 2012.

[24] Yu, S., Tan, D. & Tan, T. A framework for evaluating the effect of view angle, clothing and carrying condition on gait recognition. in Pattern Recognition, 2006. ICPR 2006. 18th International Conference on, IEEE, vol. 4, p.441–444, 2006.

[25] Hossain, M, Makihara, Y., Wang, J. & Yagi, Y. Clothing-invariant gait identification using part-based clothing categorization and adaptive weight control. Pattern Recognition, vol. 43, no. 6, p. 2281–2291, 2010.

[26] Matovski, D. S., Nixon M. S., Mahmoodi, S. & Carter, J. N. The effect of time on gait recognition performance, Information Forensics and Security. IEEE Transactions on, vol. 7, no. 2, p.543–552, 2012.

[27] Boulgouris, N. & Chi, Z. Human gait recognition based on matching of body components. Pattern Recogn, 40, p.1763–1770, 2007.

[28] Li, X., Maybank, S., Yan, S., Tao, D. & Xu, D. Gait components and their application to gender recognition. IEEE Trans Syst Man Cybern., 38, p.145–155, 2008.

[29] Tsuji, A., Makihara, Y. & Yagi, Y. Silhouette transformation based on walking speed for gait identification. IEEE Conf. on Computer Vision and Pattern Recognition, United States, p.717-722, June 2010.

[30] Tan, D., Huang, K., Yu, S. & Tan, T. Efficient night gait recognition based on template matching. in Pattern Recognition, ICPR 2006, 18th International Conference on, IEEE, vol. 3, p.1000–1003, 2006.

[31] Rose, D. A comprehensive balance and mobility training program. Human Kinetics, United States, edition 2, 2010.

[32] Bouchrika, I. & Nixon, M.S. Exploratory factor analysis of gait recognition. Proceedings of the 8th IEEE International Conference on Automatic Face & Gesture Recognition (FG'08). p.1–6, 2008.

[33] Kusakunniran, W., Wu, Q., Zhang, J. & Li, H. Speed-invariant gait recognition based on Procrustes shape analysis using higher-order shape configuration. Proceedings of the 18th IEEE International Conference on Image Processing (ICIP), p.545–548, 2001.

[34] Guan, Y. & Li, C-T. A Robust Speed-Invariant Gait Recognition System for Walker and Runner Identification. International Conference on Biometrics, Madrid, p.1-8, 2013.

[35] Abdelkader, C. B., Culter, R. & Davis, L. Stride and cadence as a biometric in automatic person identification and verification. Int. Conf. on Automatic Face and Gesture Recognition, United States, p.372-377, May 2002.

[36] Bobick, A. & Johnson, A. Gait recognition using static, activity-specific parameters. IEEE Int. Conf. on Computer Vision and Pattern recognition, United States, p.423-430, December 2001.

[37] Bouchrika, I. & Nixon, M. S. Model-based feature extraction for gait analysis and recognition. Int. Conf. On Computer Vision/Computer Graphics Collaboration Techniques and Applications, France, p.150-160, March 2007.

[38] Cunado, D., Nixon, M. S. & Carter, J. N. Using gait as a biometric, via phase-weighted magnitude spectra. Int. Conf. on Audio- and Video-Based Biometric Person Authentication, Switzerland, p.95-102, March 1997.

[39] Huazhong, N., Tieniu, T., Liang, W. & Weiming, H. Kinematics-based tracking of human walking in monocular video sequences. Journal of Image and Vision Computing, 22(5), p,429-441, May 2004.

[40] Johnson, A. & Bobick, A. A multi-view method for gait recognition using static body parameters. Int. Conf. on Audio- and Video-Based Biometric Person Authentication, Sweden, p.301-311, June 2001.

[41] Lee, C. S. & Elgammal, A. Gait tracking and recognition using person dependent dynamic shape model. Int. Conf. on Automatic Face and Gesture Recognition, United Kingdom, p.553-559, April 2006.

[42] Wang, L., Tan, T., Ning, H. & Hu, W. Fusion of static and dynamic body biometrics for gait recognition. IEEE Tran. on Circuits and Systems for Video Technology, 14(2), p.149-158, February 2004.

[43] Yam, C. Y. & Nixon, M. S. Model-based gait recognition. Encyclopedia of Biometrics. Springer, 2009.

[44] Yam, C. Y., Nixon, M. S. & Carter, J. N. Gait recognition by walking and running: A model-based approach. Asian Conf. on Computer Vision, Australia, p.1-6, 2002.

[45] Wagg, D. & Nixon, M. On automated model-based extraction and analysis of gait. In: Proceedings of the 6th IEEE international conference on automatic face and gesture recognition. Seoul, p.11–16, 2004.

[46] Urtasun, R. & Fua, P. 3d tracking for gait characterization and recognition. In: Proceedings of the 6th IEEE international conference on automatic face and gesture recognition. Seoul, p.17–22, 2004.

[47] Jang-Hee, Y., Doosung, H., Ki-Young, M. & Nixon, M. S. Automated human recognition by gait using neural network. In: Proceedings of first workshops on image processing theory, tools and applications. Sousse, p.1–6, 2008.

[48] Ariyanto, G. & Nixon, M. S. Marionette mass-spring model for 3d gait biometrics. In: Proceedings of the 5th IAPR international conference on biometrics. New Delhi, p.354–359, 2012.

[49] Chen, C., Liang, J., Zhao, H., Hu, H. & Tian, J. Frame difference energy image for gait recognition with incomplete silhouettes. Pattern Recognition Letters, 30(11), p.977-984, August 2009.

[50] Choudhury, S. D. & Tjahjadi, T. Silhouette-based gait recognition using procrustes shape analysis and elliptic Fourier descriptors. Pattern Recognition, 45(9), p.3414-3426, September 2012.

[51] Han, J. & Bhanu, B. Individual recognition using gait energy image. IEEE Tran. on Pattern Analysis and Machine Intelligence, 28(2), p.316-322, February 2006.

[52] Liu, Z. & Sarkar, S. Improved gait recognition by gait dynamics normalization. IEEE Tran. on Pattern Analysis and Machine Intelligence, 28(6), p.863-876, 2006.

[53] Roy, A., Sural, S. & Mukherjee, J. Gait recognition using pose kinematics and pose energy image. Signal Processing, 92(3), March 2012.

[54] Tan, D., Huang, K., Yu, S. & Tan, T. Uniprojective features for gait recognition. Int. Conf. on Biometrics, Korea, p.673-682, August 2007.

[55] Venkat, I. & Wilde, P. D. Robust gait recognition by learning and exploiting sub-gait characteristics. Int. Journal of Computer Vision, 91(1), p.7-23, 2011.

[56] Wang, C., Zhang, J., Wang, L., Pu, J. & Yuan, X. Human identification using temporal information preserving gait template. IEEE Tran. on Pattern Analysis and Machine Intelligence, vol. 34, no. 11, p. 2164-2176, Nov 2012.

[57] Xue., Ming, D., Song, W., Wan, B. & Jin, S. Infrared gait recognition based on wavelet transform and support vector machine. Pattern Recognition, 43(8), p.2904-2910, August 2010.

[58] Zhang, E, Zhao, Y. & Xiong, W. Active energy image plus 2dlpp for gait recognition. Signal Processing. 90(7), p.2295-2302, July 2010.

[59] Dawson, M. Gait recognition final report. Department of Computing, Imperial College of Science, Technology and Medicine, London, 2002

[60] Nixon, M. S. & Carter, J. Automatic recognition by gait. In: Proceedings of the IEEE, p.2013–2024, 2006.

[61] Nixon, M. S., Tan, T. & Chellappa, R. Human identification based on gait. Springer, Berlin, 2010.

[62] Dempster, W. & Gaughran, G. Properties of body segments based on size and weight. American Journal of Anatomy, 120, p.33–54, 1967.

[63] Zhang, R., Vogler, C. & Metaxas, D. Human gait recognition at sagittal plane. Image and vision computing, vol. 25, no. 3, p.321–330, 2007.

[64] Wang, L., Tan, T., Hu, W. & Ning, H. Automatic gait recognition based on statistical shape analysis. IEEE transactions on image processing, vol. 12, no. 9, p.1120–1131, 2003.

[65] Bashir, K., Xiang, T. & Gong, S. Gait recognition without subject cooperation. Pattern Recognition Letter 31, p.2052–2060, 2010.

[66] Wang, L., Tan, T., Ning, H. & Hu, W. Silhouette analysis based gait recognition for human identification. IEEE Trans Pattern Anal Mach Intell 25, p.1505–1518, 2003.

[67] BenAbdelkader, C., Culter, R., Nanda, H. & Davis, L. Eigengait: motion based recognition of people using image self-similarity. Int. Conf. on Audio- and Video-Based Biometric Person Authentication, Sweden, p.284-294, June 2001.

[68] BenAbdelkader, C., Culter, R. & Davis, L. Motion-based recognition of people in eigengait space. Int. Conf. on Automatic Face and Gesture Recognition, United States, 7, 53, p.267-272, May 2002.

[69] Cuntoor, N., Kale, A. & Chellappa, R. Combining multiple evidences for gait recognition. In: Proceedings of IEEE international conference on acoustics, speech, and signal processing. Hong Kong, p.33–36, 2003.

[70] Liu, Y., Collins, R. & Tsin, Y. Gait sequence analysis using frieze patterns. In: Proceedings of the 7th European conference on computer vision. Copenhagen, p.657–671, 2002.

[71] Makihara, Y., Sagawa, R., Mukaigawa, Y., Echigo, T. & Yagi, Y. Gait recognition using a view transformation model in the frequency domain. In: Proceedings of the ninth European conference on computer vision. Graz, p.151–163, 2006.

[72] Liu, Z. & Sarkar, S. Simplest representation yet for gait recognition: averaged silhouette. In. Proceedings of international conference on pattern recognition (ICPR). Cambridge, p.211–214, 2004.

[73] Bashir, K., Xiang, T. & Gong, S. Gait recognition using gait entropy image. In: Proceedings of 3rd international conference on crime detection and prevention. London, p.1–6, 2009.

[74] Lam, T., Cheung, K. & Liu, J. Gait flow image: a silhouette-based gait representation for human identification. Pattern Recognition, 44, p.973–987, 2011.

[75] Guan, Y., Li, C-T. & Hu, Y. Robust clothing-invariant gait recognition. In: Proceedings of eighth international conference on intelligent information hiding and multimedia signal processing. PiraeusAthens, p.321–3324, 2012.

[76] Kuncheva. L. I., Roli, F., Marcialis, G. & Shipp, C. Complexity of data subsets generated by random subspace method: an experimental investigation, multiple classifier systems. In: Proceedings of 2nd international workshop on multiple classifier systems, vol 2096, P.349–358, 2001.

[77] Islam, M. S., Islam, M. R., Akter, M. S., Hossain, M. A. & Molla, M. K. I. Window based clothing invariant gait recognition. Proceedings of the 2013 International Conference on Advances in Electrical Engineering (ICAEE). pp. 411–414, 2013.

[78] Yeoh, T., Aguirre, H. E. & Tanaka, K. Clothing-invariant gait recognition using convolutional neural network. 2016 International Symposium on Intelligent Signal Processing and Communication Systems (ISPACS), Phuket, p.1-5, 2016.

[79] Han, S. The influence of walking speed on gait patterns during upslope walking. J. Med. Imaging Health Inform. 5 (1), p.89–92, 2015.

[80] Tanawongsuwan, R. & Bobick, A. A Study of Human Gaits Across Different Speeds. Technical Report. Georgia Tech, 2003

[81] Mason, J. E., Traoré, I. & Woungang, I. Machine Learning Techniques for Gait Biometric Recognition. Springer. 2016.

[82] Kusakunniran, W., Wu, Q., Zhang, J. & Li, H. Gait recognition across various walking speeds using higher order shape configuration based on a differential composition model. IEEE Transactions on Systems, Man, and Cybernetics, PartB: Cybernetics, 42(6), p.1654–1668, 2012.

[83] Tsuji, A., Makihara, Y. & Yagi, Y. Silhouette transformation based on walking speed for gait identification. United States, IEEE Conf. on Computer Vision and Pattern Recognition, p.717-722, June 2010.

[84] Tanawongsuwan, R. & Bobick, A. Modelling the effects of walking speed on appearance-based gait recognition. In: Proceedings of the 17th IEEE Computer Society Conference on Computer Vision and Pattern Recognition, vol 2, p.783–790, 2004.

[85] Xu, C., Makihara, Y., Li, X., Yagi, Y. & Lu, J. Speed-Invariant Gait Recognition Using Single-Support Gait Energy Image. Multimedia Tools and Applications, Volume 78, Issue 18, p.26509–26536, September 2019.

[86] Wang, L., Tan, T., Ning, H. & Hu, W. Silhouette analysis-based gait recognition for human identification. Pattern Analysis and Machine Intelligence, IEEE Transactions on, vol. 25, no. 12, p.1505–1518, 2003.

[87] Gross, R & Shi, J. The cmu motion of body (mobo) database technical report. CMU-RI-TR-01-18, Robotic Institute, Carnegie Mellon University, 2001.

[88] Sarkar, S., Phillips, P. J., Liu, Z., Vega, I. R., Grother, P. & Bowyer, K. W. The humanid gait challenge problem: Data sets, performance, and analysis. Pattern Analysis and Machine Intelligence, IEEE Transactions on, vol. 27, no. 2, p.162–177, 2005.

[89] Shutler, J. D., Grant, M. G., Nixon, M. S. & Carter J. N. On a large sequence-based human gait database. in Applications and Science in Soft Computing, Springer, p.339–346, 2004.

[90] Kale, A., Sundaresan, A., Rajagopalan, A., Cuntoor, N. P., Roy-Chowdhury, A. K., Kruger, V. & Chellappa, R. dentification of humans using gait. Image Processing, IEEE Transactions on, vol. 13, no. 9, p.1163–1173, 2004.

[91] Lee, L. & Grimson, W. E. L. Gait analysis for recognition and classification," in Automatic Face and Gesture Recognition. Proceedings. Fifth IEEE International Conference on, IEEE, p.148–155, 2002.

[92] Makihara, Y. & Yagi, Y. Silhouette Extraction based on Iterative Spatio-temporal Local Color Transformation and Graph-Cut Segmentation. Proc. of the 19th Int. Conf. on Pattern Recognition (ICPR 2008), Paper ThAT1.4, Tampa, USA, p.1-4, Dec. 2008.

[93] Rokanujjaman, M, Hossain, M. A., Islam, M. R., Hossain, A. A. & Ferworn, A. Part definition and selection for part-based speed invariant gait recognition, 9th International Conference on Electrical and Computer Engineering (ICECE), Dhaka, 2016, p. 218-221, 2016.

[94] Liu, Z. & Sarkar, S. Outdoor recognition at a distance by fusing gait and face. Image Vision Comput., 25(6), p.817–832, 2007.

[95] Huang, P. S., Harris, C. J. & Nixon, M. S. Recognizing humans by gait via parametric canonical space. Artificial Intelligence in Eng., 13(4), p.359-366, Oct 1999.

[96] Teague, M. R. Image Analysis via the General Theory of Moments. Journal of the Optical Society of America, 70, p.920-930, 1980.

[97] Chong, C. W., Raveendran, P. & Mukundan, R. Translation and scale invariants of Legendre moments. Pattern Recognition, 37(1), p.119-129, 2004.

[98] Oujaoura, M., Minaoui, B. & Fakir, M. Moments and Moment invariants - theory and applications. Edition: GCSR Volume 1, Chapter 10: Image Annotation by Moments, Publisher: Gate to Computer Science and Research (GCSR), Science gate publishing, p.227 – 252, 2014.

[99] Hosny, K. M. Exact Legendre moment computation for gray level images. Pattern Recognition, 40(12), p.3597-3605, 2007.

[100] Hwang, S. K. & Kim, W. Y. A novel approach to the fast computation of Zernike moments. Pattern Recognition, 39(11), p.2065-2076, 2006.

[101] Tumen, R. S., Acer, M. E. & Sezgin, T. M. Feature extraction and classier combination for image-based sketch recognition. In Sketch-Based Interfaces and Modeling Symposium (SBIM), p.63-70, 2010.

[102] Veres, G. V., Gordon, L., Carter, J. N. & Nixon M. S. What image information is important in silhouette-based gait recognition? IEEE Computer Vision and Pat. Recog. Conf., p. II-II, 2004.

[103] Ng, H., Tong, H. L., Tan, W. H. & Abdullah, J. Classification of human gait features with different apparel and walking speed, 10th International Conference on Information Science, Signal Processing and their Applications, p.662-665, 2010.

[104] Rokanujjaman, M., Hossain, M. A., Islam, M. R. Effective part selection for part-based gait identification. In: Proceedings of the 7th international conference on electrical and computer engineering. BUET, p.17–19, 2012.

[105] Belhumeur, P. N., Hespanha, J. P. & Kriegman, D. J. Eigenfaces vs. fisherfaces: recognition using class specific linear projection. IEEE Trans Pattern Anal Mach Intell 19:711–720, 1997.

[106] Kusakunniran, W., Wu, Q., Li, H. & Zhang, J. Automatic gait recognition using weighted binary pattern on video in IEEE Conf. on Advanced Video and Signal Based Surveillance, Italy, p.49–54, Sep 2009.

[107] Tan, D., Huang, K., Yu, S. & Tan, T. Recognizing night walkers based on one pseudo-shape representation of gait. in IEEE Conf. on Computer Vision and Pattern Recognition, p.1–8, 2007.

[108] Dadashi, F, Araabi, B. N. & Soltanian-Zadeh, H. Gait recognition using wavelet packet silhouette representation and transductive support vector machines. in Int. Cong. on Image and Signal Processing, p.1–5, October 2009.

[109] Tan, D., Huang, K., Yu, S. & Tan, T. Orthogonal diagonal projections for gait recognition. in IEEE Int. Conf. on Image Processing, p.337–340, November2007.

[110] Tan, D., Huang, K., Yu, S. & Tan, T. Walker recognition without gait cycle estimation. in Int. Conf. on Biometrics, p. 222 – 231, 2007.

[111] DeCann, B. & Ross, A. Gait curves for human recognition, backpack detection and silhouette correction in a nighttime environment. in SPIE Conf. on Biometric Technology for Human Identification, United States, April 2010.

[112] Rokanujjaman, M., Hossain, M. A., Islam, M. R. & Hossain, A. A. Part-Based Speed Invariant Human Gait Identification, Rajshahi University journal of science and engineering, vol.45, p.1-12, 2017.

[113] Zeng, W., Wang, C. & Yang, F. Silhouette-based gait recognition via deterministic learning. Pattern Recognition, 47(11), p.3568–3584, 2014.

[114] Khan, M. H., Farid, M. S. & Grzegorzek, M. A generic codebook based approach for gait recognition. Multimedia Tools and Applications, 78, p.35689–35712, 2019.

[115] Gupta, S. K., Sultaniya, G. M. & Chattopadhyay, P. An Efficient Descriptor for Gait Recognition Using Spatio-Temporal cues. in Emerging Technology in Modelling and Graphics, Springer. p.85-97, 2020.

[116] Hawas, A. R., El-Khobby, H., Elnaby, M. M. A. & El-Samie, F. E. A. Gait identification by convolutional neural networks and optical flow. Multimedia Tools and Applications, 78(18), p.25873-25888, 2019.

[117] Yao, L., Kusakunniran, W., Wu, Q., Zhang, J., Tang, Z. & Yang, W. Robust gait recognition using hybrid descriptors based on Skeleton Gait Energy Image. Pattern Recognition Letters, 2019.

[118] Su, J., Zhao, & X. Li. Deep Metric Learning Based On Center-Ranked Loss for Gait Recognition. In IEEE International Conference on Acoustics, Speech and Signal Processing (ICASSP), p.4077-4081, 2020.

[119] Huang, G., Lu, Z., Pun, C. & Cheng, L. Flexible Gait Recognition Based on Flow Regulation of Local Features Between Key Frames. IEEE Access, 8, p.75381-75392, 2020.

[120] Bukhari, M., Bajwa, K. B., Gillani, S., Maqsood, M., Durrani, M. Y., Mehmood, I., Ugail, H & Rho, S. An Efficient Gait Recognition Method for Known and Unknown Covariate Conditions. IEEE Access,9, p.6465-6477, 2021.

LIST OF PUBLICATIONS BASED ON THESIS

Journal

1. Md Rokanujjaman, Md Altab Hossain, Md Rezaul Islam, AKM Akhtar Hossain "Part-Based Speed Invariant Human Gait Identification" Rajshahi University Journal of Science and Engineering, Vol 45, PP. 1-12,2017
2. M Rokanujjaman, MS Islam, MA Hossain, MR Islam, Y Makihara, Y Yagi "Effective part-based gait identification using frequency-domain gait entropy features" Multimedia Tools and Applications Vol 74 Issue9, pp 3099-3120, 2015

Conference

1. M Rokanujjaman, MA Hossain, MR Islam, AKMA Hossain, A Ferworn "Part definition and selection for part-based speed invariant gait recognition" Electrical and Computer Engineering (ICECE), 2016 9th International Conference, BUET, Dhaka
2. MS Islam, A Matin, J Paul, M Rokanujjaman, MA Hossain "A new effective part selection approach for part-based gait recognition" Computer and Information Technology (ICCIT), 2013 16th International Conference, Khulna, Bangladesh
3. M Rokanujjaman, MA Hossain, MR Islam, MS Islam "Effective part definition for gait identification using gait entropy image" Informatics, Electronics & Vision (ICIEV), 2013 International Conference on, 1-4
4. M Rokanujjaman, MA Hossain, MR Islam "Effective part selection for part-based gait identification" Electrical & Computer Engineering (ICECE), 2012 7th International Conference, BUET, Dhaka